ABSTRACT

Title of Document:	THE SPATIAL DISTRIBUTION OF IMPERVIOUSNESS IN WATERSHED HYDROLOGY
	Alfonso I. Mejía, Doctor of Philosophy, 2009
Directed By:	Dr. Glenn E. Moglen, Department of Civil and Environmental Engineering

Urbanization affects the hydrology of watersheds often leading to increases in runoff volumes and peak flows. These impacts are mainly attributed to the presence of imperviousness on the landscape which inhibits the soil infiltration process. Normally, these impacts are studied at the hillslope scale and under lumped watershed conditions. The impacts at the watershed scale under more spatially distributed conditions have been studied less. Advancements in spatial observations and techniques, distributed hydrologic modeling, and greater understanding of the importance of scale in hydrology have increased the feasibility and need for including spatial data sets and methods into hydrologic investigations.

This dissertation focuses on understanding the role and importance of the spatial distribution of imperviousness in watershed hydrology. The spatial distribution of imperviousness is investigated by incorporating various spatial datasets, techniques, and modeling approaches that are used routinely for the hydrology of natural watersheds but

less frequently for urbanized conditions. The distribution of imperviousness is investigated based on three approaches. The first approach uses optimization concepts to study where imperviousness can be placed in the watershed to reduce negative impacts on flooding. The second approach develops, implements, and tests a hydrologic event-based model to study the influence of the spatial distribution of imperviousness on the hydrologic response. The last approach relates analytically the space-time variability of rainfall, runoff, and the routing process to the imperviousness pattern, and synthesizes the complex space-time variations into a simpler framework.

From the first approach distinct patterns of imperviousness were obtained that embodied water resources objectives. For example, the clustering of imperviousness along the main channel was found to globally reduce peak flows along the stream network. The second approach indicated that the overall imperviousness pattern can have a considerable impact on the hydrologic response. The last approach showed that the spatial patterns of rainfall and imperviousness can interact to increase or decrease the average amount of rainfall excess. The main contribution from this research is a larger understanding of the role of the spatial distribution of imperviousness in watershed hydrology. It also demonstrates the usefulness of applying hydrologic knowledge of natural watersheds to anthropogenically-altered watersheds.

THE SPATIAL DISTRIBUTION OF IMPERVIOUSNESS IN WATERSHED HYDROLOGY

By

Alfonso I. Mejía

Dissertation submitted to the Faculty of the Graduate School of the
University of Maryland, College Park, in partial fulfillment
of the requirements for the degree of
Doctor of Philosophy
2009

Advisory Committee:
Professor Glenn E. Moglen, Chair
Associate Professor Kaye L. Brubaker
Professor Richard H. McCuen
Associate Professor Hubert J. Montas
Professor Adel Shirmohammadi

DEDICATION

Quisiera dedicar, de modo primordial, este esfuerzo y trabajo de investigación a Saka. Sin ella no hubiera sido posible. Por la paciencia que tuvo ante mis aciertos y desaciertos; por el amor, amistad, y apoyo que me supo brindar a lo largo del trayecto. Le dedico este trabajo con ilusión y honda admiración.

Quisiera también dedicar este trabajo a mi familia como gesto de agradecimiento. A mi viejo, por el ejemplo constante en el valor del aprendizaje y el estudio como camino cierto hacia el entendimiento de uno, los demás, y el mundo. A mi vieja, por su constante dedicación a la familia y a las exigencias del amor.

"We shall not cease from exploration
And the end of all our exploring
Will be to arrive where we started
And know the place for the first time.
Through the unknown, unremembered gate…"
[*T.S. Elliot*, 1967, p. 138]

ACKNOWLEDGEMENTS

I would like to acknowledge first and foremost the support, patience, guidance, and motivation provided by my advisor, Dr. Glenn Moglen, throughout this research. I am truly grateful to him for letting me take the time to understand hydrology. I would also like to acknowledge the support and patience provided by my committee: Drs. Kaye Brubaker, Richard McCuen, Hubert Montas, and Adel Shirmohammadi. I am grateful for their insightful questions and suggestions regarding this research.

I would like to extent the acknowledgement to the following professors and researchers who kindly responded to my questions, offered suggestions and clarifications: Drs. Keith Beven, Claire Jantz, Michael Koterba, Francisco Olivera, Jeff Raffensperger, Ignacio Rodríguez-Iturbe, Renata Romanowicz, Jozsef Szilagy, Jasper Vrugt, and Yu Zhang.

The financial support of the U.S. Environmental Protection Agency through grant number RD83334601 is also gratefully acknowledged.

TABLE OF CONTENTS

LIST OF TABLES

LIST OF FIGURES

CHAPTER 1 - INTRODUCTION

1.1 Introduction

There is growing and renewed interest in the hydrology of urbanizing watersheds [*Delleur*, 2003; *McCuen*, 2003; *Andrieu and Chocat*, 2004; *DeFries and Eshleman*, 2004; *Moglen*, 2009]. Traditionally, urban hydrology focused on the hydraulic representation of floods on streets and pipes, and the design of water distribution and sewer systems [*Delleur*, 2003]. Later, knowledge about the impacts of urbanization on the environment led to the analysis and modeling of pollutants in urban systems, and to the implementation of design techniques (often collectively referred to as best management practices and more recently low impact development) for reducing some of the effects of urban growth on water resources [*Delleur*, 2003]. Today, along with sustainability concerns and requirements for integrative water resources designs, there are pressing scientific and practical needs to better understand the relation between local and large scale land use changes from urbanization [*Vörösmarty et al.*, 2000; *Pielke*, 2005]. Scientific needs are clear in the context of climate change studies and in land surface modeling where the effects of urbanization on land processes can be an important control [*Pielke*, 2005; *Oleson et al.*, 2008]. Practical needs arise from the increasing relevance of watershed-wide planning and the broader recognition of the connections between local and global natural processes [*Vörösmarty et al.*, 2000]. A good example of these practical needs are large scale restoration projects where the ability to understand present

and future urban growth can be as important as predicting climatic, hydrologic, and other natural variability [*Claggett et al.*, 2005]. This need has been accentuated by the ubiquitous presence of suburban growth or sprawl, which has reduced the land area assumed to be in natural conditions [*Vörösmarty et al.*, 2000]. In addition, progress made in other disciplines is facilitating the treatment of urbanization at a larger scale. One example is the development of large scale urban growth and land use change models used to predict future growth scenarios [*Claggett et al.*, 2005].

In order to meet these needs, and for research and design considerations as well, the application of knowledge about hydrological processes and analytical methods used routinely in hydrology, is slowly expanding to include the effects of land use change from urbanization. Some of these applications include, in addition to the well established stormwater and sewer design models (e.g. SWMM5, InfoWorks, and MIKE URBAN), conceptual rainfall-runoff models for urbanized watersheds [*Grimmond et al.*, 1986; *Burges et al.*, 1998], variable source area-based concepts [*Valeo and Moin*, 2001; *Easton et al.*, 2007], physically-based distributed modeling [*Cuo et al.*, 2008], derived distribution methods [*Guo and Adams*, 1998], GIS-based modeling [*Smith*, 1993; *Moglen and Beighley*, 2002], and unit hydrograph and routing-based methods [*Olivera and Maidment*, 1999; *Moramarco et al.*, 2005; *Rodriguez et al.*, 2005]. Besides investigating and recognizing the applicability of hydrologic concepts and methods to urbanizing watersheds, these applications emphasize the need for analytical and modeling studies at a range of watershed scales, and the increasing importance of the mixed pervious-impervious land use condition.

Physical changes to the natural landscape brought about by urbanization alter the way in which hydrologic processes respond to climatic forcings and interact with each other [*Leopold*, 1968; *DeFries and Eshleman*, 2004]. These alterations cause changes in streamflow, stream morphology, stream water quality, and stream ecosystems [*Carter*, 1961; *Leopold*, 1968; *Anderson*, 1970; *Hammer*, 1972; *Hollis*, 1975; *Schueler*, 1994; *Arnold and Gibbons*, 1996; *Poff et al.*, 1997; *Center for Watershed Protection*, 2003; *Booth et al.*, 2004; *DeFries and Eshleman*, 2004; *Shuster et al.*, 2005; *Walsh et al.*, 2005; *Reed et al.*, 2006]. Common changes in streamflow are increases in flow volumes and in the magnitude and frequency of flood flows, and decreases in the time for flood flows to peak [*Hollis*, 1975; *Dunne and Leopold*, 1978; *Shuster et al.*, 2005; *Walsh et al.*, 2005]. Stream morphology affected by urbanization can result in unstable and eroding channels characterized by wider and deeper cross sectional areas [*Hammer*, 1972; *Hollis*, 1975; *Dunne and Leopold*, 1978]. Water quality in streams draining urban areas typically shows increases in the concentrations and loads of several pollutants [*Booth et al.*, 2004; *Hatt et al.*, 2004]. Changes in streamflow, channel morphology, and water quality from urbanization can bring ecological degradation to streams [*Allan*, 2004]; for example, it can cause increases in algal biomass [*Hatt et al.*, 2004; *Walsh et al.*, 2005], and reduction or loss of sensitive macroinvertebrate and fish species [*Klein*, 1979; *Walsh et al.*, 2005].

Some of the effects and physical changes just described are consistently present in most urbanizing watersheds while others may be mitigated or dependent on local conditions such as the spatial distribution of urbanization, stormwater management standards, specific climatic, geologic and watershed conditions [*DeFries and Eshleman*, 2004; *Reed et al.*, 2006]. The magnitude of the effects of urbanization on streams and

their level of control varies greatly from watershed to watershed [*Hammer*, 1972; *Dunne and Leopold*, 1978; *Lee and Heaney*, 2003; *Poff et al.*, 2006]. Despite the variability in the effects of urbanization on hydrologic processes, a common and useful way of quantifying the effects is by means of imperviousness [*Carter*, 1961; *Anderson*, 1970; *Dunne and Leopold*, 1978; *Schueler*, 1994; *Arnold and Gibbons*, 1996; *Shuster et al.*, 2005; *Walsh et al.*, 2005]. Imperviousness is understood simply as the presence of impervious cover on the landform. Imperviousness has been used directly or as a surrogate measure to describe and explain changes in the quantification of hydrologic variables and processes, and to quantify impacts on stream ecosystems [*Schueler*, 1994; *Arnold and Gibbons*; 1996; *Shuster et al.*, 2005]. In fact, many studies have shown a high level of correlation between imperviousness and increased flooding, reduced stream water quality, and stream ecosystem degradation [*Carter*, 1961; *Anderson*, 1970; *Hammer*, 1972; *Dunne and Leopold*, 1978; *Sauer et al.*, 1983; *Schueler*, 1994; *Arnold and Gibbons*, 1996; *Shuster et al.*, 2005]. These studies have diagnosed many of the negative impacts of urbanization on water resources and stream ecosystems. However, not much attention has been given to the role played by the spatial distribution of imperviousness on impacts to watershed hydrology.

Taking into account the scientific and practical needs discussed, the importance of imperviousness as predictor of environmental impacts from urbanization, and the relatively sparse research on the spatial distribution of imperviousness in watersheds, the main objective of this dissertation is in studying and understanding the role of the spatial distribution of imperviousness in watershed hydrology. Although watershed hydrology includes all hydrologic processes, their interactions and feedbacks, in this dissertation the

emphasis is placed on surface processes at the watershed scale. The watershed scale is simply defined as the scale ranging from the drainage area or watershed size at which channel initiation begins [*Montgomery and Dietrich*, 1988] to larger drainage areas. The largest drainage area considered in this dissertation is 124 km^2 and this upper limit is set mostly for practical reasons.

1.2 Research Goals and Objectives

The main research goals and objectives of this dissertation are as follows:

1. To propose, develop, and implement an optimization algorithm for choosing where in the watershed to locate urbanization or imperviousness according to objective functions based on hydrologic variables. In addition the approach should meet the following conditions:
   1.1. Account for the nested structure of watersheds and their dendritic stream network.
   1.2. Lead to distinct patterns of imperviousness at the watershed scale that can be predicted and interpreted in terms of hydrologic behavior and watershed structure.
   1.3. Flexibility in the optimization algorithm to include objective functions and constraints of various mathematical forms.
2. To develop an event-based hydrologic model that accounts for the spatial distribution of imperviousness and use it to simulate the hydrologic response. In addition the modeling approach should meet the following conditions:

2.1. Account for actual hydrologic processes that rely as much as possible on physical parameters because their estimates and ranges are better known.

2.2. Use spatial data while maintaining modeling simplicity and parsimony in the parameters, and allow flexibility for predicting the hydrologic response at internal locations within the overall watershed.

2.3. Include a simple way for calibrating and evaluating the model, and estimating parameters.

2.4. Provide a way for understanding the uncertainty associated with the simulations so that the effects of land use change on the hydrologic response can be more properly identified.

3. To propose and develop a way to synthesize the complex relations between the imperviousness pattern and the space-time variation in rainfall, runoff generation, and routing at the watershed scale. In addition the synthesis should provide the following:

3.1. Help identify dominant processes across watershed scales.

3.2. Facilitate the analysis and understanding of relations between various data sets and processes to complement and guide more detail modeling undertakings.

3.3. Ability to obtain analytical relationships to quantify the relative influence of pervious and impervious areas on processes, as a way to gain insight on how the mixed pervious-impervious land use affects watershed hydrology.

Besides this dissertation having the spatial distribution of imperviousness as its central theme, other general conditions that defined and guided this investigation can be

summarized as follows: (1) the need to account for watershed size or scale when investigating imperviousness, (2) the usefulness of spatial data sets and techniques to account for heterogeneities, e.g. topography and land use, and facilitate the analysis across watershed scales, (3) the recognition of conceptual approaches that can simplify the representation and analysis of the spatially distributed impacts, and (4) the application of the analysis to suburban conditions where the landscape is viewed as a combination of pervious and impervious land uses. The first condition recognizes that urbanization can impact streams beyond the local scale, e.g. a single residential development or hillslope, and the impacts can vary along streams and across different watershed sizes. The second condition recognizes that spatial data sets can facilitate watershed studies and provide an invaluable source of information to hydrologic analysis. The third condition emphasizes the need for simplicity in studying watershed hydrology and the impacts from imperviousness. This is because the representation of the urban watershed in detail would require vast amounts of data which are rarely available, thus a need for simple approaches arises that can make good use of readily available data and offer elucidating insight despite the underlying complexity of the system. The fourth condition recognizes the increasing relevance of urban sprawl and the differences that can exist between a completely urbanized watershed and one that is only partially urbanized. The partially urbanized watershed introduces the challenge of distinguishing the impacts from urbanization when the impacts can potentially be magnified by complex interactions between impervious and pervious areas [*Burges et al.*, 1998; *Wong*, 2006; *Easton et al.*, 2007]. For example, *Easton et al.* [2007] found using a process-based model that some impervious areas in the watershed can augment the spatial extent of the soil saturated

areas by concentrating runoff in locations prone to saturation, this in turn can cause increases in rainfall excess. This type of increase is rarely recognized even though it can have important implications in the design of mitigation strategies.

Under these general conditions three methods or approaches are proposed and developed to investigate the role of the spatial distribution of imperviousness. The first method seeks to answer the question of, "Where in the watershed should new urban residential development be placed?" The purpose behind this question is to determine if there is a preferred way, in terms of water resources, to accommodate new residential development in a watershed. The method employs an optimization algorithm and objective functions based on hydrologic variables to investigate the question. The details and results from this method are presented in Chapter 3. As a natural complement to the first method, the second method investigates whether the imperviousness pattern has an impact on the hydrologic response at the watershed scale. To answer this question an event-based model is developed to simulate the hydrologic response while accounting for the imperviousness pattern. The modeling method used is explained and applied in Chapter 4. The third method proposes and develops an analytical framework to relate the imperviousness pattern to the variability in inputs, i.e. rainfall, and processes, i.e. runoff and routing. The third method tries to respond to the questions of, "Which source of variability is more dominant?" And, "How are these different variability related to each other?" The method is presented in Chapter 5. Before the three methods are described in detail, a brief review of the literature central to this dissertation is presented in Chapter 2. Chapter 6 summarizes the main conclusions and outlines the recommendations for future work.

CHAPTER 2 - LITERATURE REVIEW

2.1 Introduction

This chapter discusses the central ideas and research that stimulated and influenced each of the three proposed methods: (1) optimization approach for studying the spatial distribution of imperviousness, (2) hydrologic response under spatially distributed imperviousness, and (3) relating the imperviousness pattern to the space-time variation in rainfall, runoff, and routing. For convenience the literature review is grouped according to the three proposed methods.

2.2 Optimization Approach for Studying the Spatial Distribution of Imperviousness

There are relatively few studies that have proposed and developed ways for optimizing land use changes from urbanization based on hydrologic criteria and objective functions [*Moglen et al.*, 2003; *Tang et al.*, 2005; *Yeo et al.*, 2007]. For example, *Yeo et al.* [2007] developed an optimization approach for minimizing peak flows and *Tang et al.* [2005] for minimizing the change in runoff between future and existing conditions. In both of these approaches the minimizations were performed with respect to the overall watershed outlet. *Moglen et al.* [2003] used a multiobjective approach to account for various criteria, including hydrologic objectives, when optimizing changes in land use. Their emphasis was in understanding changes within a defined boundary but not

necessarily within a watershed or under the drainage conditions characteristic of watersheds. The methods of *Yeo et al.* [2007] and *Tang et al.* [2005] emphasize changes at a single location in the watershed, and are highly dependent on the local characteristics of watersheds and on the spatial resolution of the data sets used. This makes the methods useful for individual watershed studies but less so for understanding common patterns realized in heterogeneous watersheds. This also limits the application of optimized patterns as hypothetical land use scenarios for subsequent hydrologic modeling.

The optimization method proposed in this research is developed to include changes (i.e. increases in peak flows between urbanized and non-urbanized conditions in the watershed) along the entire stream network, not just at a single outlet point. This has the desirable conditions of accounting for the geometry of watersheds (i.e. their nested structure and dendritic network) and their drainage pattern [*Carter*, 1961; *Zheng and Baetz*, 1999; *Poff et al.*, 2006]. The proposed method is, in part, motivated by the intimate connection between watershed form and function expressed in the scaling of peak flows with drainage area [*Rodríguez-Iturbe and Rinaldo*, 1997; *Dawdy*, 2007]. This scaling is used to simplify the spatial optimization problem and obtain more general solutions. The simplification is achieved by using an empirical relation between peak flows, drainage area, and imperviousness. The results are generalized by their independence from local watershed conditions and their dependence on watershed geometry and the drainage pattern. This allows the results of the optimizations to be used as land use scenarios on watersheds with more diverse conditions. The optimization approach implemented was based on a similar algorithm to the one used by *Rodríguez-Iturbe et al.* [1992] to estimate distinct optimal channel network configurations. This

algorithm was selected because it can deal with spatially-oriented optimizations and is flexible in its handling of objective functions. Chapter 3 contains the details of the optimization approach and shows how the approach is able to estimate distinct patterns that can be interpreted in terms of hydrologic conditions and the watershed structure. The distinct imperviousness patterns obtained in Chapter 3 are used as imperviousness scenarios in Chapters 4 and 5. Thus the patterns also serve as a conceptual framework and a starting point to further investigate the role of the spatial distribution of imperviousness.

2.3 Hydrologic Response under Spatially Distributed Imperviousness

An interesting question that arises from the estimation of the different imperviousness patterns or scenarios is the ability to estimate and quantify the influence of the scenarios on the hydrologic response, where the response is viewed as a signature of the various hydrologic processes and their impacts from urbanization [*Weiler et al.*, 2003]. This question is important because it has been suggested that if one accounts for the uncertainty associated with hydrologic models and their limitations as evidenced by the difficulty of making predictions in ungaged watersheds, the answer is far from settled [*Grayson et al.*, 1992; *Sivapalan*, 2003, 2009; *McDonnell et al.*, 2007; *Wagener, 2007*; *Beven, 2008*; *Buytaert et al.*, 2008]. In fact, some hydrologists argue that hydrologic models of land use change are in their infancy and that unless process understanding and modeling is improved under generalizable principles and strategic field campaigns, substantial progress is unlikely [*Beven*, 2000; *McDonnell et al.*, 2007; *Buytaert et al.*, 2008]. The generalizable principles are meant to be simple conceptualizations that can

capture the essence of observations and represent the deeper regularities in hydrologic phenomena [*Dooge*, 1986; *McDonnell et al.*, 2007]. In parallel to these more scientific concerns, the hydrologic literature is filled with practical applications of hydrologic models that demonstrate reasonable predictions under widely diverse watershed, geologic, and climatic conditions [*Grimmond et al.*, 1986; *Troch et al.*, 1994; *Guo and Adams*, 1998; *Burges et al.*, 1998; *Olivera and Maidment*, 1999; *Valeo and Moin*, 2001; *Moramarco et al.*, 2005; *Easton et al.*, 2007; *Cuo et al.*, 2008; *Nicótina et al.*, 2008]. This duality, the ability to make reasonable predictions despite the processes not being completely understood [*Kirchner*, 2006], might be a reflection of the role of hydrology as both a scientific and engineering discipline. The hydrologic modeling performed in this dissertation strived for a balance between these dual roles of hydrology. Effort was made to consider actual hydrologic processes and to favor physical reasoning and parameters, and at the same time simplifications of a more practical nature were employed (e.g. separation of baseflows and linear routing) [*Philip*, 1960; *Beven and Kirkby*, 1979; *Rodríguez-Iturbe and Valdés*, 1979; *Sivapalan et al.*, 1987; *Szilagyi and Parlange*, 1998].

To simulate the hydrologic response, the event-based model proposed and developed by *Sivapalan et al.* [1987] and *Troch et al.* [1994] was extended to account for the imperviousness pattern. The modifications are explained in detail in Chapter 4. The model simulates runoff generation using Philip's two term equation for infiltration excess, a topographic index for saturation excess, and by accounting for the location of impervious areas where infiltration is inhibited [*Philip*, 1960; *Beven and Kirkby*, 1979]. The saturation excess is based on a TOPMODEL approach [*Beven and Kirkby*, 1979]. Impervious areas are determined from remotely sensed data [*USGS*, 2008b]. The

generated runoff is routed to the watershed outlet using a geomorphic instantaneous unit hydrograph (GIUH) [*Rodríguez-Iturbe and Valdés*, 1979]. The decision to include saturation excess was made because preliminary analysis of the data used in this research suggested the prevalence of this form of runoff generation over infiltration excess. This was also the recommendation made by Dr. Raffensperger, the groundwater specialist in the Maryland office of the United States Geological Survey (USGS). A TOPMODEL approach for saturation excess was chosen because it accounts in a simple way for important watershed heterogeneities using the so-called probability distributed approach [*Grayson and Blöschl*, 2000], is amenable to spatial data sets, and is applicable to conditions (e.g. humid climate and shallow soils) in the physiographic region used in this research. The modeling capabilities of the TOPMODEL have been tested for the hillslope and watershed scale under various conditions, including suburban watersheds [*Beven and Kirkby*, 1979; *Sivapalan et al.*, 1987; *Troch et al.*, 1994; *Franchini et al.*, 1996; *Grayson and Blöschl*, 2000; *Valeo and Moin*, 2001]. The TOPMODEL has also being used as a land surface parameterization, TOPLATS, for larger scale hydrologic modeling [*Famiglietti and Wood*, 1994].

The GIUH has been used widely in hydrologic research and practice [*Rodríguez-Iturbe and Valdés*, 1979; *Mesa and Mifflin*, 1986; *Troch et al.*, 1994; *Olivera and Maidment*, 1999; *Saco and Kumar*, 2002; *Nicótina et al.*, 2008]. It has proven to be a reasonable approximation in many cases for estimating the hydrologic response despite its linearity assumption [*Mesa and Mifflin*, 1986; *Troch et al.*, 1994; *Olivera and Maidment*, 1999; *Nicótina et al.*, 2008]. Since its inception into hydrologic research and practice various new concepts have modified the original GIUH theory of *Rodríguez-*

Iturbe and Valdés [1979]. *Gupta et al.* [1980] and *Rinaldo et al.* [1991] generalized the GIUH theory by specifying further its probabilistic structure and clarifying some physical assumptions. *Rosso* [1984] related the Nash instantaneous unit hydrograph to Horton's ratios to derive the GIUH. *Mesa and Mifflin* [1986] showed how the width function could be used instead of Horton's ratios to describe the geomorphology of the watershed. They also used the inverse Gaussian probability density function (pdf) to describe the GIUH. More recently the GIUH theory was extended to account for spatially variable forcing and parameters [*Olivera and Maidment*, 1999; *Saco and Kumar*, 2002; *Nicótina et al.*, 2008]. An interpretation of the GIUH which motivated its use in this dissertation, aside from its applicability and simplicity, is the possibility of approximating the response of a watershed while treating the watershed and the stream network as a single physical system. This interpretation emphasizes the idea of searching for regularity at the watershed scale despite the local heterogeneities [*Dooge*, 1986].

Because conceptual hydrologic models are imperfect representations of the actual physical system, there is uncertainty associated with their predictions. Recently, renewed effort has been devoted to better understand and quantify this uncertainty. These efforts have been largely motivated by recent advancements in computational mathematics and a greater acceptance of the limitations in hydrologic models [*Beven and Binley*, 1992; *Kuczera and Parent*, 1998; *Vrugt et al.*, 2003; *Kuczera et al.*, 2006; *Clark et al.*, 2008; *Vrugt et al.*, 2008a,b]. One approach has been to identify and quantify uncertainty according to its sources [*Kuczera et al.*, 2006; *Clark et al., 2008*; *Vrugt et al.*, 2008a,b]. The main sources of uncertainties typically identified are data, i.e. inputs and outputs, model structural, and parameter uncertainty [*Kuczera et al.*, 2006; *Clark et al.*, 2008;

Vrugt et al., 2008a,b]. Another approach has been to rely more heavily on parameter variability as a way to capture the uncertainty of predictions [*Beven and Binley*, 1992; *Vrugt et al.*, 2003]. This latter approach has used the concept of equifinality to describe the various problems that can normally occur with hydrologic parameters [*Beven and Binley*, 1992; *Beven*, 2000; *Ebel and Loague*, 2006; *Beven*, 2008]. The parameters can be poorly identified, highly sensitive, i.e. unstable, and non-unique, i.e. several parameter sets can be found [*Beven*, 2000; *Ebel and Loague*, 2006]. In this dissertation two of these uncertainty estimation methods are applied: the Generalized Likelihood Uncertainty Estimation (GLUE) and the Shuffled Complex Evolution Metropolis (SCEM) [*Beven and Binley*, 1992; *Vrugt et al.*, 2003]. The methods are used to understand if changes on the hydrologic response from the land use scenarios can be explained by the uncertainty associated with parameters, thus providing a simple way of measuring the significance of the changes. In essence, the goal is to distinguish the variations in the response due to changes in land use from those due to parameter variability.

2.4 Relating the Imperviousness Pattern to the Space-Time Variation in Rainfall, Runoff, and Routing

It is a difficult task to relate the imperviousness pattern to the space-time variation in rainfall, runoff, and routing in a simple manner. Typically, this relation is achieved as an indirect consequence of hydrologic modeling (i.e. rainfall-runoff modeling) such that the relations are not explicit or may be difficult to decipher. In the case of land use change from urbanization, the goal is normally to use the rainfall-runoff model to simulate streamflows continuously for a period of time and, after proper calibration-

evaluation of the model, different urban scenarios are tested by changing the land use [*Wigmosta and Burges*, 1990; *Ewen and Parkin*, 1996; *Niehoff et al.*, 2002; *Hundecha and Bárdossy*, 2004]. The evaluation usually entails the quantification and comparison of changes to the streamflows from the scenarios as a way to understand how the proposed land use will affect hydrologic conditions [*Niehoff et al.*, 2002; *Hundecha and Bárdossy*, 2004]. Despite the rainfall-runoff model requiring a relation between urbanization and the space-time pattern of rainfall and runoff, these relations can be quite difficult to understand beyond changes to the streamflows. This is the case because the model typically conceptualizes different processes using various mathematical formulations that are difficult to interrelate and express analytically in a simple form. Thus, it seems advantageous to develop a framework that can include the complex space-time variation of hydrologic systems in a more explicit manner and at the same time allow the development of relationships that express this complexity in a simpler way. Such a method could help in the understanding of results or guide the development of more detailed hydrologic models by providing additional insight about the importance of different space-time variations in hydrologic data and processes.

One approach hydrologists sometime take to simplify a complex system and provide a more unified view of a problem is through synthesis work [*Horton*, 1931; *Dooge*, 1986; *Blöschl*, 2006; *McDonnell et al.*, 2007]. One of such efforts of hydrologic synthesis was proposed by *Woods and Sivapalan* [1999]. However, their synthesis method was envisioned for natural conditions. In this dissertation their method is extended to account for the imperviousness pattern in a watershed. The goal of the

method is to make a tool available to simplify the space-time relations in data and processes, and use it to gain insight into a complex system.

Thus the research performed for this part of the dissertation was motivated and influenced largely by the work of Professor Sivapalan. In fact, the method proposed by *Woods and Sivapalan* [1999] embodies many of the research ideas developed by Professor Sivapalan. For instance, the conditions for the separation of rainfall variation into multiplicative, independent, space and time components were investigated in *Sivapalan and Wood* [1987], which is one of the assumptions made in the proposed method. The connections between the GIUH theory and runoff generation processes were investigated in *Sivapalan et al.* [1987, 1990], these connections are also part of the proposed method. The recognition of the stream network, hillslopes, and watershed scale as important units for the analysis of hydrologic phenomena were investigated in *Robinson et al.* [1995]. The importance of watershed scale is included in the proposed method with the understanding that the relative dominance of various hydrologic processes may vary depending on the watershed size [*Robinson et al.*, 1995]. Thus, regarding the research of Professor Sivapalan, it becomes evident that the method proposed in *Woods and Sivapalan* [1999] entails a profound aspiration for hydrologic synthesis. In this dissertation an effort is made to build on this synthesis.

2.5 Summary

The main research and concepts that motivated the three methods proposed in this dissertation were reviewed. The proposed methods are discussed in detail in Chapters 3, 4, and 5. Chapter 3 describes the optimization approach used to study the spatial

distribution of imperviousness. Chapter 4 discusses the simulation of the hydrologic response under spatially distributed imperviousness. Chapter 5 proposes a way to relate the imperviousness pattern to the space-time variation in rainfall, runoff, and routing. The description of the three proposed methods in Chapters 3, 4, and 5 discusses further the literature specific to each method.

CHAPTER 3 - OPTIMIZATION APPROACH FOR STUDYING THE SPATIAL DISTRIBUTION OF IMPERVIOUSNESS

> *"We found that each of the four regions has a unique distribution signature for land cover in watersheds of different scales. For example, urbanization tends to be focused in broad valley floors and floodplains in the SW... In contrast, urban land cover is 2.3 times higher in headwater catchments of the SE compared to the entire region."* [*Poff et al.*, 2006, p. 279]

3.1 Introduction

In this chapter a method is proposed to answer the question of, "Where in the watershed should new urban residential development be placed?" The purpose behind this question is to determine if there is a preferred way to organize imperviousness in a watershed. The method also aims at determining distinct imperviousness patterns that are general enough to be useful as future land use scenarios. To obtain general patterns the method is developed based on the nested structure of watersheds and their drainage pattern and dendritic stream network. The terms imperviousness, urbanization, and development are used interchangeably to mean the presence of impervious cover on a watershed.

3.2 Optimization Approach to Estimate Urban Patterns

The motivation behind the proposed approach is to find distinct patterns of urban development that reduce impacts to water resources. The specific way in which impacts

to water resources are quantified is discussed in Section 3.3. This section discusses the optimization approach in more general terms. It seems an optimization approach is well suited for studying where in the watershed to locate imperviousness because of the following considerations: (1) reduction of impacts to water resources can be conveniently stated as a minimization problem [*Moglen et al.*, 2003; *Yeo et al.*, 2004, 2007; *Tang et al.*, 2005; *Gabriel et al.*, 2006], (2) measures based on hydrologic variables and imperviousness can be expressed as objective functions within an optimization approach [*Moglen et al.*, 2003; *Yeo et al.*, 2004, 2007; *Tang et al.*, 2005; *Gabriel et al.*, 2006], and (3) idealizing urban development to be mainly concerned with locations in the undeveloped watershed where new residential development will minimize impacts, simplifies the problem to one of combinatorial analysis.

To account for the spatial form and location of the urban pattern, the proposed optimization approach is developed using a grid-based scheme. This scheme is implemented to take advantage of spatial data, e.g. digital elevation models (DEMs) [*USGS*, 2007], and grid techniques available. The grid techniques include using the DEM to determine flow directions and drainage areas at each grid cell [*O'Callaghan and Mark*, 1984; *Tarboton et al.*, 1991]. The optimization approach stated in general terms is as follows:

$$\min f_j(\mathbf{x}^*);\ \mathrm{j} = 1, ..., \mathrm{m}, \tag{3-1}$$

Subject to:

$$h(\mathbf{x}^*) \in H,$$

where $f_j(\mathbf{x}^*)$ denotes the j's objective function and $\mathbf{x}^*$ is a vector of decision variables [*Reeves*, 1993; *Pham and Karaboga*, 2000]. The optimization constraint is for $h(\mathbf{x}^*)$ to

belong to H, where $h(\mathbf{x}^*)$ represents an specific urban pattern configuration within the watershed and H is all the possible configurations or the feasible domain. The problem is simplified to finding the urban pattern configuration $h(\mathbf{x}^*)$ that belonging to H will give the lowest value of objective function $f_j(\mathbf{x}^*)$. The objective function can be, for example, the total change in imperviousness resulting from new development within a specified boundary [*Moglen et al.*, 2003]. The objective function used is described in detail in the next section.

A number of optimization techniques are available for the solution of the minimization problem in (3-1) [*Reeves*, 1993; *Pham and Karaboga*, 2000]. Because the problem is interpreted as one of combinatorial analysis and flexibility in the form of the objective function is desired, an effective approach to solve the problem is by heuristic optimization algorithms [*Rodríguez-Iturbe et al.*, 1992; *Reeves*, 1993; *Pham and Karaboga*, 2000; *Nunes et al.*, 2004]. Heuristic optimization algorithms can be classified as strictly descending or not strictly descending [*Nunes et al.*, 2004]. The main advantage of not strictly descending methods is they tend to search a larger portion of the feasible domain by allowing non-descending moves of the objective function or jumps from potential local optimum [*Reeves*, 1993; *Pham and Karaboga*, 2000]. This advantage of not strictly descending algorithms is seen as a way to ensure the global optimum is reached [*Reeves*, 1993; *Pham and Karaboga*, 2000]. Both types of algorithms were tested, a not strictly descending algorithm, simulated annealing [*Kirkpatrick et al.*, 1983; *Aarts and Korst*, 1990], and a strictly descending algorithm, iterative improvement [*Lin*, 1965; *Aarts and Korst*, 1990]. For the simulated annealing algorithm, computational time needed for the optimizations was found to be extremely

large. Therefore, the iterative improvement algorithm was selected to perform the optimizations in this study. Trial optimizations performed with both algorithms yielded the same urban spatial patterns. A similar optimization approach and algorithm was applied by *Rodríguez-Iturbe et al.* [1992] to develop distinct optimal channel network configurations. The form of the iterative improvement and simulated annealing algorithm is similar. They only differ in the acceptance rule [*Reeves*, 1993; *Pham and Karaboga*, 2000]. The main difference is in the iterative improvement algorithm only changes that decrease the value of the objective function are accepted while simulated annealing allows changes that cause slight increases. The increases are accepted base on a probabilistic condition that depends on the number of iterations. The term simulated annealing was coined from the first applications of the algorithm as a model of the change of energy in a system when subject to a cooling process. A more comprehensive explanation of simulated annealing is presented in *Reeves* [1993].

Before a detailed description of the iterative improvement algorithm is provided, it is useful to outline the general form of the algorithm, which is as follows [*Lin*, 1965; *Aarts and Korst*, 1990]:

1. Assume initial configuration h_o.
2. Randomly perturb configuration h_o to obtain h_1.
3. Find $\Delta f = f(h_1) - f(h_0)$.
4. If $\Delta f < 0$, configuration h_1 is accepted and $h_0 = h_1$, otherwise h_1 is rejected and h_o remains.
5. Repeat steps 2, 3, and 4 until completion condition is met.

The algorithm starts by assuming an initial configuration [*Lin*, 1965; *Aarts and Korst*, 1990]. In this case, the initial configuration consists of the watershed boundary and its stream network, and a hypothetical land use distribution which includes the set of grid cells that represent new development. Figure 3-1a illustrates an initial configuration where new development is randomly distributed within the watershed boundary. The initial configuration is defined as a grid and new development cells are assumed to have a 30 meter resolution which matches the DEM resolution. This assumption makes each grid cell approximately equal to the size of an average medium density residential lot [*NRCS*, 1986; *McCuen*, 1998]. New development cells at the start are randomly distributed within the watershed in places where new development is possible. Several initial configurations were tried and they did not change the results obtained for a given objective function. The algorithm proceeds by applying a random perturbation to the initial configuration [*Lin*, 1965; *Aarts and Korst*, 1990]. The perturbation consists of randomly selecting a new development cell and moving it to a new random location where development is possible [*Lin*, 1965; *Aarts and Korst*, 1990]. The location of the moved cell takes on its original land use designation. In this manner a perturbed configuration is obtained. This is illustrated in Figures 3-1b and c. Figure 3-1b shows a new developed cell being randomly selected (the selected cell is indicated by the circle) and moved to a randomly selected undeveloped location shown in Figure 3-1c (the undeveloped location is denoted by the circle). The selected cell in Figure 3-1b becomes undeveloped and the cell in Figure 3-1c becomes developed. This completes the determination of the perturbed configuration. The value of the objective function for the initial and the perturbed configuration are compared, and the configuration with the

lowest value is retained [*Lin*, 1965; *Aarts and Korst*, 1990]. In terms of Figure 3-1, if the perturbation illustrated in 3-1b and c results in a lower value of the objective function when compared to 3-1a, then the perturbation is accepted. The algorithm continues applying random perturbations until the completion criteria is met [*Nunes et al.*, 2004]. Normally the completion criteria is defined in terms of reductions to the relative change in the value of the objective function [*Nunes et al.*, 2004]. In this case the algorithm was stopped after a large number of iterations when changes in the objective function were very small, approximately less than 1% of the difference in the value of the objective function between two consecutive iterations. The number of iterations was found experimentally (200,000 iterations). The same number of iterations were used in every optimization performed in this chapter.

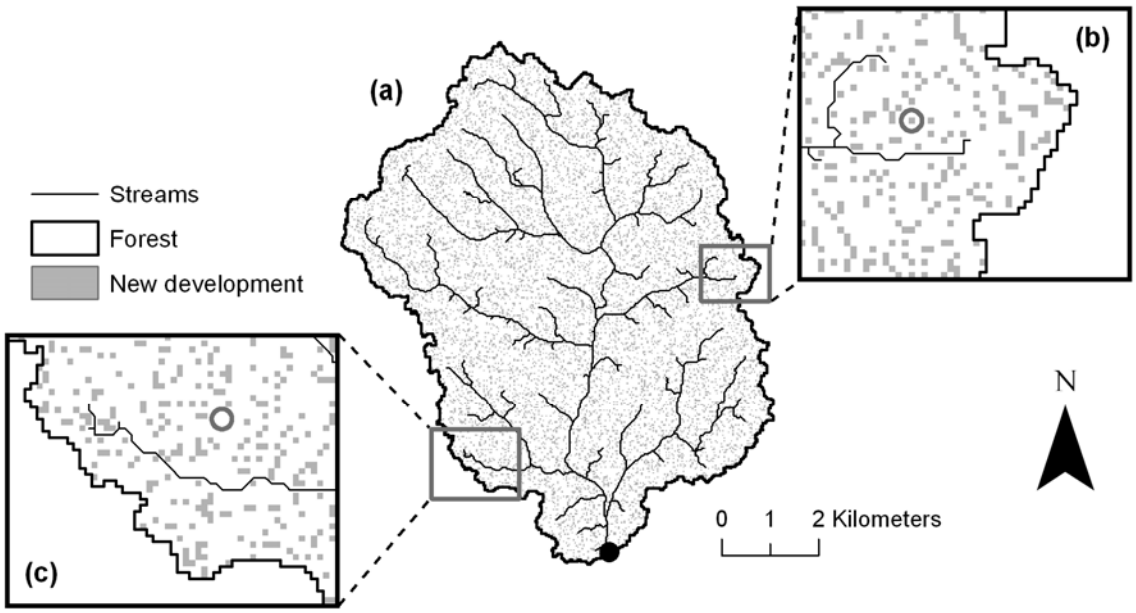

Figure 3-1. Illustration of the iterative improvement algorithm used for the optimization. (a) Initial land use configuration. (b) Random selection of a new developed cell (the cell is indicated with the circle). (c) Random selection of an undeveloped cell where the selected developed cell is placed (the cell is indicated with the circle). The black dot denotes the overall watershed outlet.

3.3 Urban Patterns Derived from Optimization Approach

In order to apply the proposed optimization approach, objective functions are required. The objective functions used in the optimizations are described in this section.

3.3.1 An Objective Function to Quantify Impacts to Water Resources

The objective functions were selected according to the following criteria: (1) the function should have a meaningful interpretation in terms of benefits or advantages to

water resources, and (2) the function needs to be defined in terms of a variable important to water resources whose spatial distribution can be readily estimated. Other optimization approaches developed to minimize impacts to water resources have used as objective function the total change in imperviousness resulting from new development within a specified boundary [*Moglen et al.*, 2003], the difference in runoff between proposed land use conditions and existing conditions [*Tang et al.*, 2005], and flood peaks at the watershed outlet [*Yeo et al.*, 2004, 2007]. In this study the ratio *r* is used to define the objective function. *r* is the ratio of the maximum annual flood flow of a given recurrence interval for a proposed land use condition (q_t^*) to the maximum annual flood flow of the same recurrence interval for an existing land use condition (q_t). *r*, for a given recurrence interval *t*, is defined as follows:

$$r_t(\mathbf{x}) = \frac{q_t^*(\mathbf{x})}{q_t(\mathbf{x})}, \tag{3-2}$$

where **x** is a space vector of the *x,y* coordinates of grid cells that constitute the stream network. Each *x,y* pair **x** has the important function of treating that grid cell as the outlet of a sub-watershed. The same ratio *r* was applied by *Carter* [1961] and *Anderson* [1970] to assess increases in flood peaks from urbanization. Flood peaks are commonly used to study the impacts from urbanization on streams and watersheds by directly analyzing streamflow data [*Carter*, 1961; *Anderson*, 1970; *DeWalle et al.*, 2000; *Galster et al.*, 2006; *Poff et al.*, 2006] or as part of hydrologic modeling [*Niehoff et al.*, 2002; *Hundecha and Bárdossy*, 2004; *Fohrer et al.*, 2005].

The objective function in terms of *r* is as follows:

$$f_j = \sum_{i=1}^{N} \left[r_t(\mathbf{x}_i) - k \right]^2; j = 1, ..., m, \tag{3-3}$$

where f_j denotes the j's objective function; N is the total number of grid cells that constitute the stream network; and k is a constant parameter. The parameter k allows the consideration of different water resources goals and of the patterns implied by these goals. N depends on the definition of the stream network. The stream network was defined using a constant area threshold equal to 0.225 km^2 [*Montgomery and Dietrich*, 1988]. Thus N is equal to the total number of cells in the watershed that have a drainage area greater than 0.225 km^2. i indexes the grid cell on the stream network where $r_t(\mathbf{x}_i)$ is being estimated. The physical interpretation of the objective function in (3-3) is described in Section 3.5.

3.3.2 Estimation of Changes in Flood Peaks from Urbanization

The flood peaks q_t^* and q_t in equation (3-2) can be estimated in a number of ways. Typically for urban watersheds, the rational method [*Kuichling*, 1889; *McCuen*, 1998; *DeFries and Eshleman*, 2004] or a lumped watershed model are used [*Singh and Woolhiser*, 2002; *DeFries and Eshleman*, 2004]. The interest in this study is to find flood peaks at each grid cell in the stream network, rendering a lumped model too unwieldy to be effectively used. Distributed watershed models available can simulate the hydrograph and flood peaks in space [*Singh and Woolhiser*, 2002]. However their implementation within the proposed optimization approach is unrealistic in terms of the computational and calibration time required by them. Instead regional flood peak regression equations are used [*Carter*, 1961; *Anderson*, 1970; *Dunne and Leopold*, 1978; *McCuen*, 1998; *DeWalle et al.*, 2000; *Moglen et al.*, 2006]. The regional regression equation used has the following form [*Moglen et al.*, 2006]:

$$q_t = C(t)A^{\alpha(t)}(I+1)^{\beta(t)} \tag{3-4}$$

where q_t is the flood peak for a *t*-year return period; *A* is the drainage area; *I* is the percent imperviousness in the watershed; the parameter *C(t)* and the exponents $\alpha(t)$ and $\beta(t)$ depend on the recurrence interval *t* and can be estimated from multiple regional regression analysis [*Carter*, 1961; *Anderson*, 1970; *McCuen*, 1998; *Ogden and Dawdy*, 2003; *Galster et al.*, 2006; *Moglen et al.*, 2006]. Equation (3-4) was used to determine the distribution of flood peaks within a watershed by making all variables a function of location as follows:

$$q_t(\mathbf{x}) = C(t)A(\mathbf{x})^{\alpha(t)}[I(\mathbf{x})+1]^{\beta(t)}, \tag{3-5}$$

where **x** is a space vector of the *x,y* coordinates. Both $A(\mathbf{x})$ and $I(\mathbf{x})$ are treated as grids. $A(\mathbf{x})$ is estimated from the DEM by determining the drainage area at each grid cell which is equal to the number of upstream cells that flow to cell **x** [*O'Callaghan and Mark*, 1984; *Tarboton et al.*, 1991]. $I(\mathbf{x})$ is defined as follows [*Moglen et al.*, 2006]:

$$I(\mathbf{x}) = 100\frac{\sum_{u=1}^{L} c_u a_u(\mathbf{x})}{A(\mathbf{x})}. \tag{3-6}$$

L is the number of land use types within the entire watershed. Three main types of land uses were considered: forest, urban-residential, and streams. c_u is the fraction of imperviousness associated with land use *u* and is constant for each land use [*NRCS*, 1986; *Moglen et al.*, 2006]. $a_u(\mathbf{x})$ is the total area occupied by land use *u* within $A(\mathbf{x})$ such that $\sum_{u=1}^{L} a_u(\mathbf{x}) = A(\mathbf{x})$, and is written in terms of **x** because it varies with location.

Equation (3-5) is used in this study because it accounts explicitly for changes in flood peaks from urbanization by means of imperviousness. It recognizes the fact that contributing drainage area, $A(\mathbf{x})$, is the dominant factor in the distribution of flood peaks as shown by the USGS regional regression studies of flood peaks [*Carter*, 1961; *Anderson*, 1970; *Ogden and Dawdy*, 2003; *Galster et al.*, 2006; *Moglen et al.*, 2006]. $A(\mathbf{x})$ can be used as a measure of watershed scale in the distribution of new development. Previous studies of urban development patterns have not explicitly considered the role of watershed scale, but have indicated its influential role in determining changes from urbanization [*Zheng and Baetz*, 1999; *Poff et al.*, 2006]. For example, *Zheng and Baetz* [1999] tested four different urban pattern scenarios at the site scale, approximately 1.9 km^2. They found the urban patterns were able to reduce flood peaks at the site scale but not at the main watershed scale, approximately 40 km^2. *Poff et al.* [2006] found changes in the distribution signature of urbanization across different watershed scales and noted their effects on streamflow conditions. Equation (3-5) also considers the effects of the stream network structure on changes from urbanization, because $A(\mathbf{x})$ and $I(\mathbf{x})$ are quantified using the drainage pattern of the watershed.

3.3.3 Urban Patterns and Their Relation to Flood Peaks

If k is equal to 0, then equation (3-3) becomes the ratio r, and substituting equation (3-2) into (3-3) gives the following expression for objective function f_1:

$$f_1 = \sum_{i=1}^{N} \left[r_t(\mathbf{x}_i) \right]^2 = \sum_{i=1}^{N} \left[\frac{q_t^*(\mathbf{x}_i)}{q_t(\mathbf{x}_i)} \right]^2 . \tag{3-7}$$

In equation (3-7) the goal is to minimize increases in flood peaks from urbanization for every grid cell in the stream network. Lower flood peaks are beneficial because they can reduce flooding and stream erosion [*Hammer*, 1972; *Hollis*, 1975; *Dunne and Leopold*, 1978; *Shuster et al.*, 2005; *Walsh et al.*, 2005].

As an illustration of the minimization of equation (3-7), the Cattail Creek watershed in Howard County, Maryland, was used. The DEM was obtained from the USGS at 30 meter resolution [*USGS*, 2007]. From the DEM the drainage pattern and stream network for Cattail Creek were derived. In equation (3-7) the parameters *C(t),* $\alpha(t)$, and $\beta(t)$ are equal to 37.01, 0.635, and 0.588, respectively, for the 2-year return period [*Moglen et al.*, 2006]. The c_u values for the three land uses considered are equal to 0, 0.38, and 0, for forest, medium density residential, and streams, respectively [*NRCS*, 1986; *Moglen et al.*, 2006].

Figure 3-2 shows the normalized value of objective function f_1 when minimized and the value objective functions f_2 and f_3 take while f_1 is being minimized. The functions are normalized by dividing the value of f_j at each iteration step by the maximum value of f_j from all the iterations. Objective functions f_2 and f_3, shown in Figure 3-2, are obtained by assuming different values of *k* in equation (3-3). The values of *k* assumed are 3.87 and 5, for f_2 and f_3, respectively. These values of *k* were chosen because they demonstrate the distinct set of urban patterns implied by equation (3-3). They also serve to illustrate how the patterns progress from a clustered downstream distribution ($k = 0$) to a random one ($k = 3.87$), and finally they return to a series of smaller headwater clusters ($k = 5$). The *k* value of 3.87 used in f_2 is the value of $r(\mathbf{x})$ at

the overall watershed outlet and it can be interpreted physically as the flood amplification factor that results in this example for a total area of development of 15%.

Figure 3-3 illustrates the minimization of f_1 starting with the land use configuration shown in Figure 3-3a, where residential development is randomly distributed and occupies 15% of the total watershed area. Figures 3-3b and 3-3c show the way development is clustered by the movement of residential grid cells toward the larger streams in the watershed as the minimization of f_1 continues. The minimization of f_2 starts with the land use configuration shown in Figure 3-3c. At the end of the minimization the land use configuration consists of development distributed randomly within the watershed as shown in Figure 3-3d, much like the starting condition in Figure 3-3a. The *k* value of 3.87 used in f_2 is the value of $r(\mathbf{x})$ at the overall watershed outlet, which is denoted as k_o. k_o can be interpreted physically as the flood amplification factor that results in this example for a total area of development of 15%.

The urban pattern resulting from the optimization f_3 is shown in Figure 3-4. In this optimization development moves to the headwaters of the smallest streams. The urban pattern from f_3 is then characterized by pockets of clustered development distributed across the watershed. From these results, and other optimizations performed for values of *k* greater than k_o not shown, it is deduce that the trend for values of $k > k_o$ is to move development upstream towards source areas in the watershed. In Figure 3-5 the minimization of f_3 causes the values of objective functions f_1 and f_2 to increase consistently, in this respect, f_3 has the inverse effect on both f_1 and f_2.

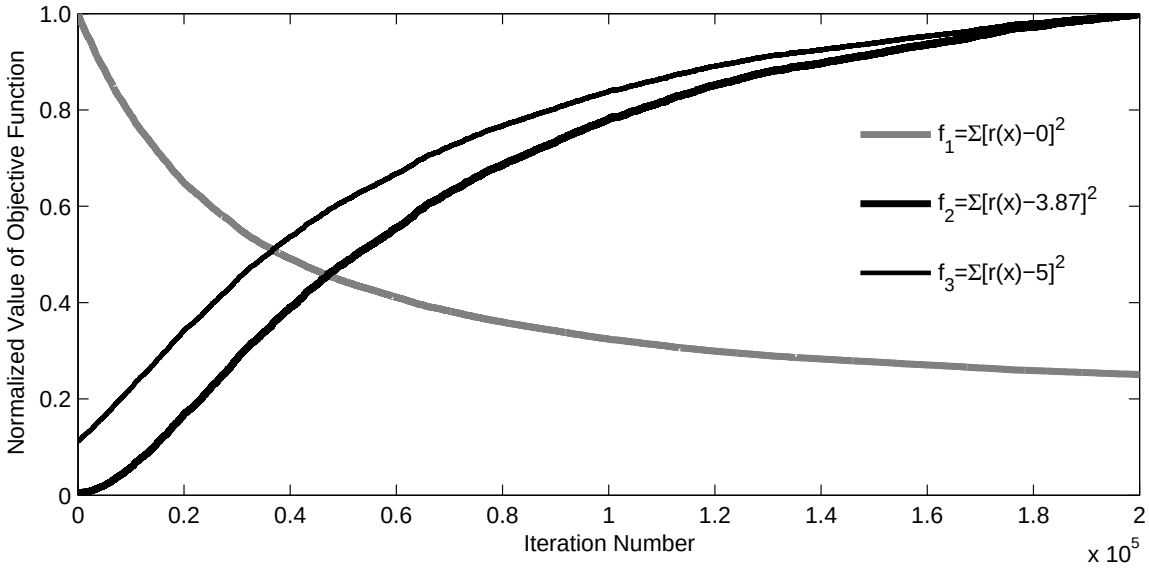

Figure 3-2. Normalized value of objective functions f_1, f_2, and f_3, when f_1 is minimized.

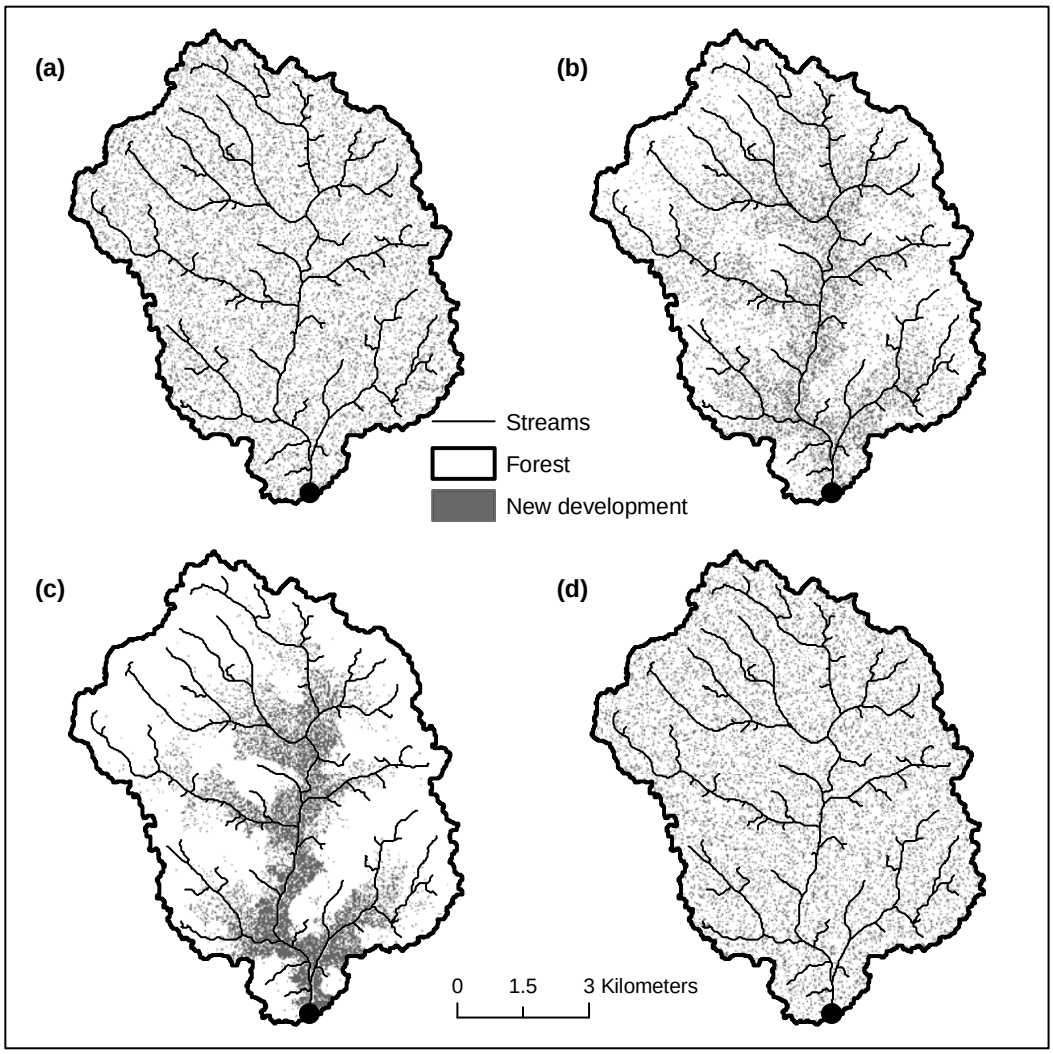

Figure 3-3. (a) Initial land use configuration used for the minimization of f_1. The new development is equal to 15% of the watershed area. (b) Urban pattern derived from the minimization of f_1 after 20,000 iterations and (c) at the end of the optimization, $2x10^5$ iterations. (d) Urban pattern derived from the minimization of f_2, where the initial land use configuration was the pattern in (c). The patterns in (a) and (d) are essentially the same, randomly distributed new residential development.

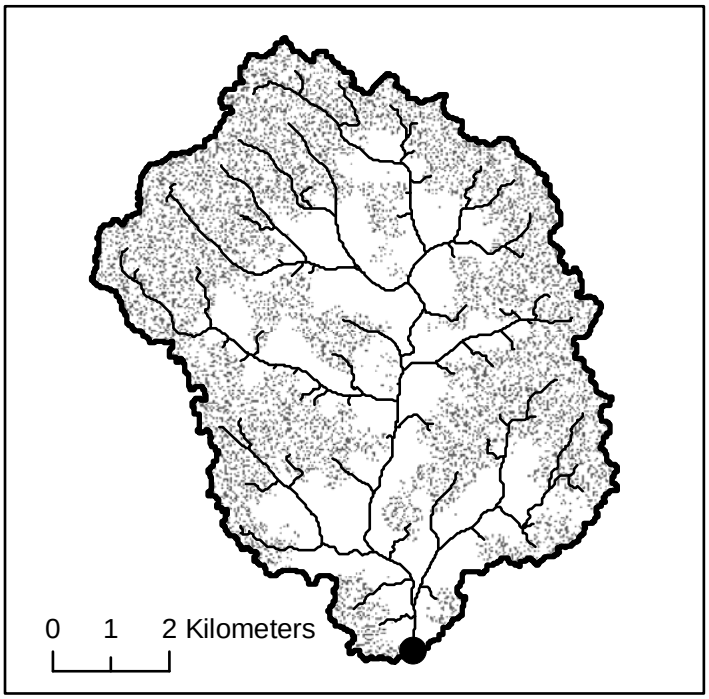

Figure 3-4. Urban pattern derived from the minimization of f_3.

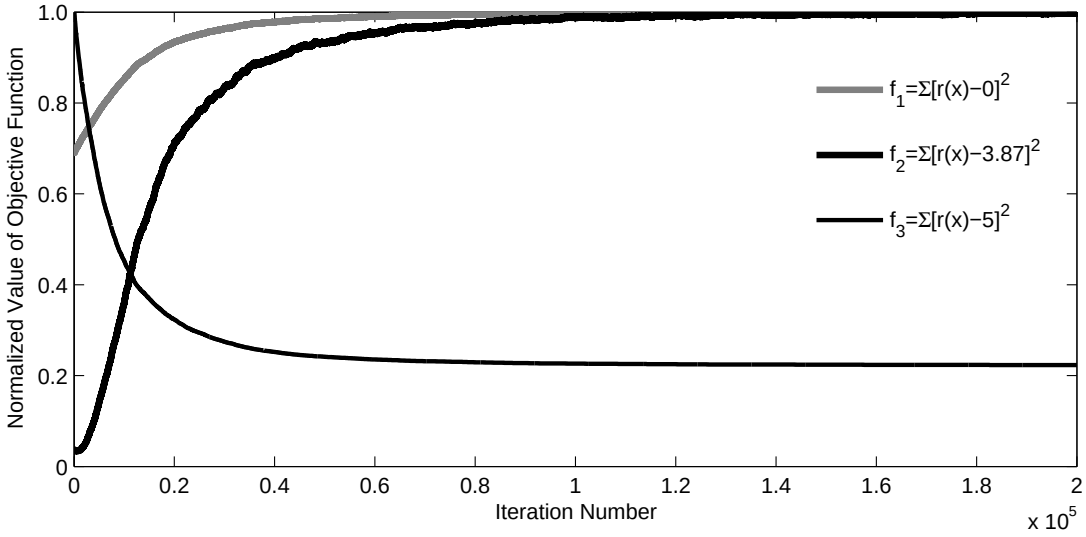

Figure 3-5. Normalized value of objective functions f_1, f_2, and f_3, when f_3 is minimized.

3.4 Urban Pattern Based on an Imperviousness Threshold

To illustrate the urban pattern that might arise from explicitly considering an imperviousness threshold a new objective function is defined. The objective function is as follows:

$$f_4 = \sum_{i=1}^{N} I_p(\mathbf{x}_i), \tag{3-8}$$

$$I_p(\mathbf{x}) = \begin{cases} 0 & I(\mathbf{x}) < I_t \\ I(\mathbf{x}) & I(\mathbf{x}) \geq I_t \end{cases}.$$

N is the total number of grid cells that constitute the stream network and $\mathbf{x}_i$ is the location of an individual grid cell in the stream network. $I(\mathbf{x}_i)$ is the percent imperviousness at location $\mathbf{x}_i$ estimated using equation (3-6). I_t is the imperviousness threshold set at 10% in this study because this value is often cited as a limit after which imperviousness causes environmental degradation to streams [*Schueler*, 1994; *Arnold and Gibbons*, 1996]. The minimization of f_4 resulted in the urban pattern shown in Figure 3-6a and 3-6c. The pattern appears as a combination of clustered development downstream near the main outlet and along the main stream, and uniformly distributed development on the remaining watershed area. The stream cells in the portion of the watershed with uniformly distributed development have less than 10% total imperviousness. Figure 3-7 contrasts the total imperviousness as a function of position along two stream traces in the watershed for both f_1 and f_4 and will be discussed further in the following section.

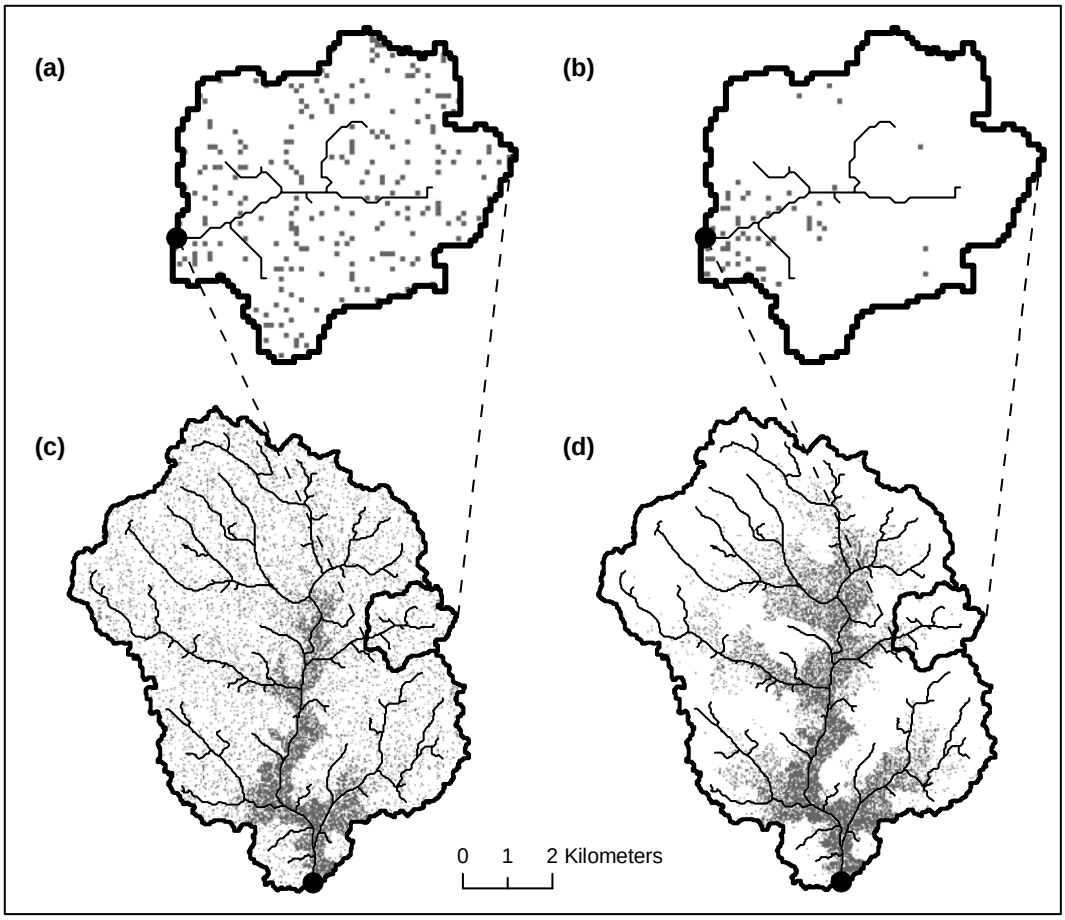

Figure 3-6. (a) Sub-watershed showing the distribution of urban development when f_4 is minimized and (b) same sub-watershed when f_1 is minimized. (c) Urban pattern derived from the minimization of f_4 and (d) from the minimization of f_1.

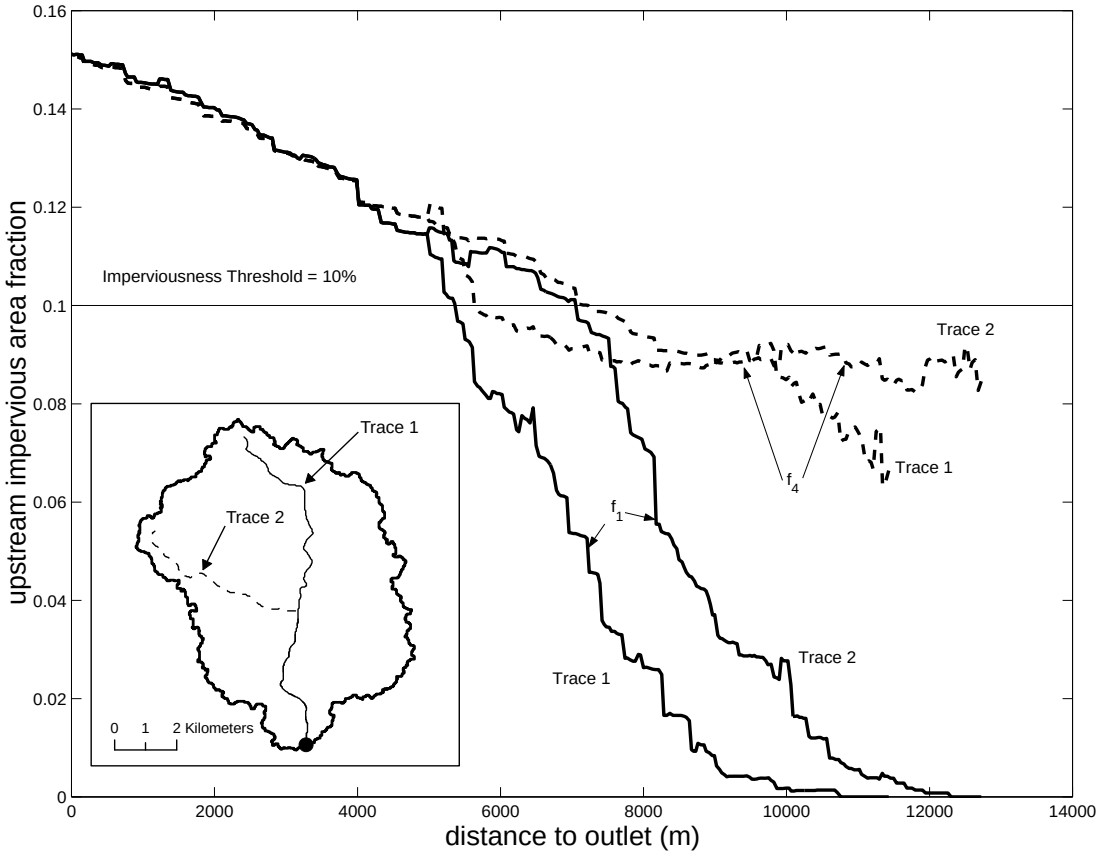

Figure 3-7. Imperviousness fraction along trace 1 and trace 2 for the urban patterns derived from the minimization of f_1 and f_4.

3.5 Interpretation of Objective Functions

Previously the mathematical representation of several different objective functions was emphasized. In this section these same objective functions are described quantitatively and interpretations of the land development patterns derived from the optimizations is provided.

Common characteristics for all objective functions: Each of the objective functions presented entails a summation over all locations along the stream network. From a computational standpoint, this means summing the observed value of r, the flood amplification factor, or $I_p(\mathbf{x})$, the aggregate imperviousness, at each grid point along the stream network. Since the sum is across all stream locations, each objective function gives equal weight to each unit of stream length, whether the stream is large or small. The role of land area within the watershed, but not directly on the stream network, is to provide a location for impervious cover to reside and to contribute to downslope locations that eventually reach the stream network.

Objective function f_1: This objective function seeks to minimize r^2 throughout the stream network. The optimized development pattern (Figure 3-3c) shows a propensity for f_1 to group all development as near as possible to the largest drainage area elements of the stream network. The objective function is thus optimized by development that is moved as far away from headwater streams as possible because this minimizes the amount of imperviousness that is drained by the most upland streams in the network. The appeal of such an objective is that the resulting development pattern supported by f_1 has the smallest overall effect on heightened flood peaks measured across the entire stream network as a system. Judging from Figure 3-3c, it should be clear that this is achieved by

having the most headwater-oriented stream locations essentially unaffected by development and instead concentrating and clustering adjacent to the stream all development at locations as far downstream as possible.

Objective function f_2: This objective function seeks to minimize $(r\text{-}k_o)^2$ throughout the stream network. The constant, k_o, physically corresponds to the flood amplification factor at the main watershed outlet. Thus minimizing f_2 corresponds to the goal of producing an urban development pattern that spreads the development evenly across the watershed. From the perspective of f_2, this objective would be absolutely minimized if each point along the stream network experiences the same flood amplification ratio as the overall watershed outlet. In contrast to f_1, the appeal of f_2 is that the resulting development pattern affects all locations in the stream network to the same degree - all flood peaks would be amplified after development by the same amount.

Objective function f_3: This objective function seeks to minimize $(r\text{-}5)^2$ throughout the stream network. The constant, 5, was chosen arbitrarily to illustrate optimization behavior for constants greater than k_o. In this case, the resulting landscape is the opposite of the objective function f_1 landscape. Objective f_3 promotes development at the most headwater locations in the watershed rather than the most downstream locations observed for f_1. While this optimization is instructive to understand the role of k in equation (3-3), this optimized landscape actually leads to the overall largest values of r when summed across the study watershed's stream network. Pursuing such a development pattern would lead to large flood amplification rations being experienced from the headwaters of the watershed on down.

Objective function f_4: This objective function has been crafted to replicate as closely as possible recent policy objectives that seek to limit imperviousness to less than a certain threshold level - often cited as around 10% [*Schueler*, 1994] to protect stream ecology. *EPA* [2004] identified the 10% threshold as an indicator of cumulative impacts. The EPA goes on to advocate the 10% threshold as a guideline for watershed based zoning to control land use. Optimizing this objective function therefore quantitatively and visually demonstrates how the landscape can be developed to most strategically accommodate imperviousness while maximizing the amount of stream network below this threshold. Figures 3-6a and 3-6c illustrate the optimal placement of imperviousness for this objective.

Contrasting f_1 and f_4: Figure 3-6 provides a comparison of the optimized urban development patterns resulting from these two objective functions. Both optimized patterns are similar in their favored clustering of development adjacent to the main stream of the study watershed. However, an important distinction between f_1 and f_4 patterns is evident at locations removed from the main channel. Objective f_1 is optimized as all land development is clustered to the main stream. In contrast, f_4 is optimized by moving a fraction of the total development to dispersed headwater locations throughout the watershed. Spot inspection at the streams draining these headwater areas confirms that the total imperviousness draining to these streams lies just under the threshold. This is borne out in Figure 3-7 by the two stream traces that correspond to f_4. These traces show a considerable length of the upstream portion of these traces at a value just below the imperviousness threshold. Objective f_4 is, in effect, gaming the policy objective by spreading as much development in a sprawl-type pattern across upstream areas of the

watershed to a degree that remains just below the specified imperviousness threshold, and then concentrating the remaining imperviousness at downstream locations that have total imperviousness well above the imperviousness threshold. In contrast, f_1 avoids upstream development altogether as shown by the headwater sub-watershed in Figure 3-6b and by the upstream portions of the stream traces for f_1 in Figure 3-7. This contrast between f_1 and f_4 helps illustrate a potential unintended consequence of policies that are structured to take advantage of the impervious cover threshold effects cited in the literature. Surely planners and policy makers did not develop impervious threshold polices (exemplified by objective f_4) with the intent of promoting low density sprawl in the headwater areas of the landscape. Results like these are important for planners and policy makers to consider before establishing regulations.

3.6 Conclusions

In this chapter an optimization approach was implemented to derive distinct urban patterns of development. Based on the urban patterns obtained and the analysis performed, the main conclusions are as follows:

1. The optimization approach is able to generate distinct patters of urban development by stating objective functions that embody a positive goal from a water resources perspective. Four different objective functions were defined. Objective functions f_1, f_2, and f_3, represented a continuous set of urban patterns with a common progression from clustered development at the most downstream locations in the stream network (f_1), to uniform distribution across the watershed (f_2), to clustered development focused on the upstream headwater locations in the watershed (f_3). The urban pattern derived from the

optimization of f_4 (which was crafted to approximate an imperviousness threshold policy) is similar to the pattern from f_1, but included a secondary characteristic of diffuse, low density development throughout the watershed that produced aggregate total imperviousness in the upstream portions of the stream network just below the optimization-enforced threshold.

2. The urban patterns derived from objective functions f_1 and f_2 were found to represent the meaningful spectrum of possible development from clustered development (f_1) to sprawl-type development (f_2). (The pattern from objective f_3, while plausible, actually amounts to a negative goal from a water resources perspective, since this pattern produces a maximum flooding configuration throughout the watershed.) The urban pattern from f_1 has the benefit of reducing flood peaks along the entire stream network and in the watershed as a whole. The pattern resulting from f_2 has the benefit of distributing the effects of urbanization equally across scales of sub-watersheds. In the f_2 pattern, all locations in the stream network experience the same level of impact from urbanization.

Even though the urban pattern from f_1 tends to reduce peak flows along the stream network, it also places urbanization in locations prone to flooding or within the floodplains. The effect of the floodplains on the pattern from f_1 could be included in the optimization. The pattern will be similar but the clustering will occur adjacent to the areas just outside of the restricted floodplain areas. The goal with f_1 is not to encourage development in the floodplain. The goal is to describe how to place development relative to the stream network to reduce peak flows.

3. An important new finding of this study is that the urban pattern resulting from objective f_4 indicates that land use policies structured to keep total imperviousness below a fixed threshold may result in the unintended consequence of favoring sprawl-type development. The optimization performed shows that such policies would promote urban development patterns in which total aggregate imperviousness remains just below the policy threshold. Such a pattern consumes the landscape with widespread, diffuse development. Further, the development pattern is optimized just below the policy threshold and is, thus, sensitively dependent on the accuracy and precision of the research that promoted the threshold. Past research has shown [*Moglen and Kim*, 2007] that certainty about the existence and actual value of the threshold is poor. Such research coupled with the f_4 optimization outcome should be a significant concern for those within the planning community who espouse threshold-based controls on land development.

3.7 Summary

A question that emerges from this chapter is whether the different optimized patterns have an impact on the hydrologic response at the overall outlet of a watershed. The empirical relation between peak flows and imperviousness used in this chapter, equation (3-5), predicts at the overall outlet the same peak flow for the different optimized patterns. This is because it treats imperviousness as a uniform aggregate measure. Normally, hydrologic conceptual models used to simulate land use changes also tend to aggregate imperviousness, if not at the overall outlet, at least within some defined sub-areas in the main watershed. It is likely that any estimation method that aggregates imperviousness will tend to mask the impact of the location of imperviousness

on the response. The next chapter develops a simple event-based model to investigate the influence on the hydrologic response of the different optimized patterns. The event-based model, albeit simple, is conceptualized to consider spatially distributed impervious conditions.

CHAPTER 4 - HYDROLOGIC RESPONSE UNDER SPATIALLY DISTRIBUTED IMPERVIOUSNESS

4.1 Introduction

This chapter describes the development and application of an event-based model for simulating the spatially distributed hydrologic response of a watershed under spatially distributed imperviousness conditions. The spatially distributed response means the simulation of the excess rainfall hydrograph at the overall outlet as well as any internal stream location within the overall watershed that can be treated as the outlet of a nested sub-watershed. The aim of the modeling approach is to study and understand the influence of the imperviousness pattern on the hydrologic response. For the study the optimized imperviousness patterns obtained in Chapter 3 are used as land use scenarios.

4.2 Description of Modeling Approach

The description of the modeling approach is divided into four sub-sections: runoff generation, hydrologic response, initial conditions, and baseflow separation. Each of these sub-sections is described next.

4.2.1 Runoff Generation

To simulate runoff generation the modeling approach developed and implemented by *Sivapalan et al.* [1987] and *Troch et al.* [1994] is adapted to account for urbanized

conditions. The modeling approach is largely based on the original TOPMODEL [*Beven and Kirkby*, 1979]. This approach was chosen because of its simplicity: the approach is event-based, requires few parameters, accounts for spatially distributed data, evidence indicates its applicability to conditions in the watershed and climate used for this study, and is computationally efficient given the spatially distributed data used. However, the model proposed by *Sivapalan et al.* [1987] and *Troch et al.* [1994] is generalized by including a more general assumption about the subsurface transmissivity profile [*Ambroise et al.*, 1996; *Duan and Miller*, 1997]. The assumption is described in the next section. In summary, the runoff generation approach uses a topographic index to estimate the initial saturated areas and track the amount of saturation during the storm event, and uses Philip's two-term infiltration equation to simulate infiltration excess runoff [*Philip*, 1960; *Beven and Kirkby*, 1979]. The method is briefly described here. The complete explanation and derivation of equations can be found elsewhere [*Beven and Kirkby*, 1979; *Sivapalan et al.*, 1987; *Ambroise et al.*, 1996; *Duan and Miller*, 1997].

Runoff from saturation excess: The following condition is used to estimate the initial saturated areas in the watershed [*Duan and Miller*, 1997]:

$$1-\frac{\bar{\delta}}{n} \geq \frac{\omega}{\sqrt[n]{\xi}}, \tag{4-1}$$

where $\bar{\delta}$ is the ratio of the initial average storage deficit, $\bar{S}$ [L], to the maximum storage deficit, S_{max} [L], or

$$\bar{\delta} = \frac{\bar{S}}{S_{\max}}. \tag{4-2}$$

$\bar{S}$ is an initial condition of the model in this case and S_{max} can be interpreted as some effective soil depth, the depth of the soil times a drainable porosity, for which lateral

subsurface flow is important. n is the dimensionless generalizing factor for the transmissivity profile, it allows theoretically the consideration of various profile forms (e.g. linear, power, and exponential). ξ is defined as

$$\xi = \frac{a}{T_o \tan\beta}, \tag{4-3}$$

where a [L] is the area drained per unit contour width, T_o [L^2/T] is the transmissivity constant, and $tan\ \beta$ is the local topographic slope. ω is the expected value of ξ which is estimated as

$$\omega = \frac{1}{A}\int_A \sqrt[n]{\xi}, \tag{4-4}$$

where A [L^2] is the total drainage area. The variables a and $tan\ \beta$ can be estimated from the Digital Elevation Model (DEM) and vary locally. S_{max} and T_o can be estimated from calibration and they are assumed to be watershed-wide constants in this application [*Franchini et al.*, 1996].

To determine the local deficits at the start of the simulation, the following expression is used [*Duan and Miller*, 1997]:

$$\delta_i = n - \frac{\sqrt[n]{\xi}}{\omega}\left(n - \bar{\delta}\right). \tag{4-5}$$

The local scaled storage deficit, δ_i, is dimensionless and equal to the ratio of the local deficit (S_i) and S_{max}. New saturated areas during the storm event are formed where and when δ_i becomes equal or less than 0. The rate at which δ_i is filled depends in this case on the infiltration capacity or rainfall rate. This implies within a TOPMODEL approach that saturated areas during the storm event are formed due to infiltration. These

dynamics can be explained with the following condition [*Beven and Kirkby*, 1979; *Romanowicz*, 1997]:

$$S_1(t+1) = \min\{S_2(t), \max[0, S_1(t) - Q_f]\}, \tag{4-6}$$

where S_1 and S_2 are the unsaturated and saturated storages, respectively, and Q_f [L] is simply the amount of infiltrated water at time step t. It is assumed that S_2 does not become less than S_1, therefore the minimum in equation (4-6) is controlled by the unsaturated storage, assuming at the start of the event S_1 and S_2 are the same. A similar assumption was previously used by *Woods and Sivapalan* [1999]. It is also assumed that vertical recharge to the water table is instantaneous and equal to the infiltration rate. This last assumption seems acceptable since evidence suggests the presence of a shallow perched water table [*Turner*, 2006].

Runoff from infiltration excess: Philip's infiltration equation is used [*Philip*, 1960], under the assumption of the time compression approximation (TCA), to simulate infiltration excess. TCA allows the treatment of variable rainfall and the substitution of time in Philip's equation for the cumulative infiltration [*Philip*, 1960; *Milly*, 1986; *Sivapalan et al.*, 1987]. The infiltration equation is as follows [*Milly*, 1986]:

$$f_i^*(F_i) = CK_s \left\{ 1 + \left[\left(1 + \frac{4CK_s F_i}{S_r^2} \right)^{1/2} - 1 \right]^{-1} \right\}, \tag{4-7}$$

where f_i^* [L/T] is the potential infiltration capacity as determined from Philip's equation at cell i, F_i [L] is the cumulative infiltration at i, C is a parameter representing the effects of gravity, S_r [$LT^{-1/2}$] is the sorptivity, and K_s [L/T] is the surface saturated hydraulic conductivity. Both C and S_r depend on the soil texture. It is assumed for simplicity that

C is equal to 1, the parameter is normally estimated from calibration. To estimate S_r, the following relation is used [*Dingman*, 1994]:

$$S_r = \left[(\phi - \theta_o) K_s |\psi| \left(\frac{2B+3}{B+3} \right) \right]^{1/2}, \tag{4-8}$$

where ϕ is the soil porosity, θ_o is the initial soil moisture, ψ [L] is the air-entry tension, and B is the pore-size distribution index. The average value of these soil properties can be estimated from published data for soil textures [*Dingman*, 1994].

From equation (4-7), the actual infiltration rate at any time during the storm is:

$$f_i = \min\left[f_i^*(F), P_i \right]. \tag{4-9}$$

P_i [L/T] is the rainfall at cell i for the given time step. Infiltration excess is estimated when at a particular unsaturated cell the condition $P_i > f_i$ is met and the amount of pervious runoff generated at the cell is $r_i = (P_i - f_i)(1 - w_i)$ [L/T], where w_i is the impervious fraction of cell i, otherwise all the rain infiltrates provided the soil storage, S_i, is large enough.

Runoff from impervious surfaces: The assumption is made that rain falling on impervious cells immediately becomes runoff and available for routing. Therefore, infiltration of runoff from impervious cells is not considered. This last assumption is less constraining when most of the imperviousness is connected. The watershed selected for this study is mostly connected. The runoff from impervious cells is $r_i = w_i P_i$ [L/T].

The assumption that water from impervious areas does not infiltrate has a direct implication on the topographic index, which was addressed by *Valeo and Moin* [2001]. *Valeo and Moin* [2001] proposed using a modified upslope drainage area value to reflect the expected reduction in watershed infiltration from the impervious cover [*Valeo and*

Moin, 2001]. The modified value is estimated as $a_i' = a_i(1 - v_i)$, where v_i is the total impervious fraction upstream of a_i and equal to $\frac{1}{A_i}\int_{A_i} w_i$. Therefore a_i' [L] is the actual pervious amount of drained area per unit contour width upstream from cell *i*.

4.2.2 Hydrologic Response

The excess rainfall is routed from hillslopes and channels using a geomorphologic unit hydrograph (GIUH). A GIUH is used because of its simplicity and it has been shown to be useful for urbanized conditions [*Olivera and Maidment*, 1999; *Smith et al.*, 2005]. Typically the GIUH is expressed in terms of Strahler streams or channel links [*Rodríguez-Iturbe and Valdés*, 1979; *Rinaldo and Rodríguez-Iturbe*, 1996; *Rodríguez-Iturbe and Rinaldo*, 1997]. In this case the grid cells are used to obtain a GIUH described in terms of individual flow paths [*Olivera and Maidment*, 1999; *Nicótina et al.*, 2008]. The use of grid cells to describe the flow paths is convenient because it matches the format of other data sets used. The travel time distribution, *f(t)*, of all the paths in the watershed that contribute runoff to the outlet can be expressed as follows [*Saco and Kumar*, 2002; *D'Odorico and Rigon*, 2003]:

$$f(t) = \sum_{\gamma \in \Gamma} p(\gamma, t) f_{h_\gamma} * f_{c_\gamma}(t), \tag{4-10}$$

where $p(\gamma,t)$ is the probability of water following path γ, Γ is the set of all possible paths, f_{h_γ} and f_{c_γ} [T^{-1}] are the probability density functions (pdfs) describing the travel times within the hillslope and channel section of path γ, respectively, and the asterisk (*) indicates the convolution operator [*Saco and Kumar*, 2002; *D'Odorico and Rigon*, 2003]. For both the hillslope and channel travel time pdfs, a two-parameter inverse Gaussian

distribution (IG) is assumed because of its physical basis and applicability [*Mesa and Mifflin*, 1986; *Rinaldo and Rodríguez-Iturbe*, 1996; *Olivera and Maidment*, 1999; *Saco and Kumar*, 2002; *D'Odorico and Rigon*, 2003; *Nicótina et al.*, 2008]. IG can be derived from the parabolic model of the Saint Venant equations [*Rinaldo and Rodríguez-Iturbe*, 1996]. IG has the following form:

$$f_{c_\gamma}(t) = \frac{L_c}{\sqrt{4\pi D_c t^3}} \exp\left[-\frac{(L_c - u_c t)^2}{4 D_c t} \right], \tag{4-11}$$

where L_c [L] is the path length, u_c [L/T] is the kinematic wave celerity for the path, and D_c [L^2/T] is the coefficient of hydrodynamic dispersion for the path. The parameters u_c and D_c can be constant or vary depending on the path γ while L_c is always varied, this is not reflected in the notation of equation (4-11) for simplicity. IG is also used for routing water from the hillslope in which case the path parameters are L_h, u_h, and D_h, and u_h and D_h can also be treated as constant or varied [*Saco and Kumar*, 2002; *D'Odorico and Rigon*, 2003; *Nicótina et al.*, 2008]. The parameters L_c and L_h can be estimated from the DEM, while u_c, u_h, D_c, and D_h are normally, in practical applications, obtained from calibration [*Olivera and Maidment*, 1999; *Nicótina et al.*, 2008]. The parameters u_c and u_h will be referred herein as the channel and hillslope velocities, respectively.

The discharges at the outlet of the watershed, $Q_i(t)$ [L/T], from the excess rain are found from the convolution of the instantaneous response, equation (4-10), and the spatially averaged rate of runoff generation:

$$Q_i(t) = \sum_{\gamma \in \Gamma} \int_0^t R(\tau) * p(\gamma, \tau) f_\gamma(t - \tau) d\tau. \tag{4-12}$$

The subscript *i* indicates that *Q(t)* can be estimated at any location of the channel network; for example, *i* can be the main watershed outlet or an outlet chosen inside the main watershed. *R(t)* [L/T] is simply the total amount of runoff generated at time *t* in the watershed divided by the total drainage area of the watershed. To simplify the convolution in equation [4-10], f_γ is used to represent $f_{h_\gamma} * f_{c_\gamma}(t)$, and an IG pdf is assumed for f_γ [*Olivera and Maidment*, 1999; *Saco and Kumar*, 2002]. The path dependent parameters in equation (4-11) are estimated in the same manner as *Saco and Kumar* [2002], therefore these equations are not shown here.

GIUH path probabilities and impervious surfaces: The term *p(γ,t)* in equation (4-12) is used to account in part for the effects of imperviousness in the GIUH formulation. The meaning of *p(γ,t)* is the likelihood that a given path *γ* will carry water to the outlet and it acts as a weighting factor when summing all the possible paths *Γ* in the watershed. In the original formulation of the GIUH, *p(γ,t)* is defined in terms of Horton's ratios [*Rodríguez-Iturbe and Valdés*, 1979; *Rinaldo and Rodríguez-Iturbe*, 1996]. Other definitions of *p(γ,t)* have been used, for example, *Mesa and Mifflin* [1986] used the width function of the watershed and *Woods and Sivapalan* [1999] used a generalized form of the area function. It is desirable for *p(γ,t)* to reflect the effects of imperviousness and rainfall variability. *p(γ,t)* as originally defined assumes a uniform input forcing and constant probabilities in time. These assumptions are relaxed, similar to the way *Nicótina et al.* [2008] did, leading to the following expression for *p(γ,t)*:

$$p(\gamma,t) = \frac{r(\mathbf{x},t)}{\int_A r(\mathbf{x},t)d\mathbf{x}} = \frac{r(\mathbf{x},t)}{R(t)}. \tag{4-13}$$

It is assumed every cell to be a possible path. The probabilities must meet the condition $\sum_{\gamma\in\Gamma} p(\gamma,t)=1$. *r(***x**,*t)* [L/T] is the runoff generated on cell **x** at time *t* , where **x** is a vector with the *x,y* location of the cell. *A* [L^2] is the total watershed area. Thus the numerator in equation (4-13) is the runoff at a given cell at time *t* while the denominator is the total runoff in the watershed at time *t*. *p(γ,t)* is the fraction of runoff generated on a given cell. Because *p(γ,t)* is defined in terms of the generated runoff, the imperviousness pattern has an effect on the likelihood of a path. Also, substituting equation (4-13) into (4-12) simplifies (4-12) and provides a more straightforward convolution between the path GIUH and the runoff generated at a given cell at time *t*, the simplified equation (4-12) is:

$$Q_i(t)=\sum_{\gamma\in\Gamma}\int_0^t r(\mathbf{x},\tau)*f_\gamma(t-\tau)d\tau. \tag{4-14}$$

4.2.3 Initial Conditions

A common problem in event-based modeling is the estimation of initial conditions due in part to their dependence on conditions prior to the storm and the inability to assume a warm-up period as usually done in continuous rainfall-runoff modeling [*Franchini et al.*, 1996; *Vrugt et al.*, 2003]. Two initial conditions are required by the chosen modeling approach, the average soil moisture and the average storage deficit in the watershed. To estimate the initial average soil moisture, results from the analysis of seasonal soil moisture data from an urbanizing watershed located in close proximity to the study area selected for this investigation are used [*Tenenbaum et al.*, 2006]. The location and characteristics of the study area selected are described in the next section. The watershed studied by *Tenenbaum et al.* (2006) has similar underlying

geology, soils, and imperviousness to the study area. Additionally, the assumption of using a regional average value for the initial soil moisture has little effect within the chosen modeling scheme and climatic conditions, since infiltration excess plays a minor role in runoff generation.

To estimate the initial depth of the water table or the initial storage deficit, the method proposed by *Troch et al.* [1993] was tried. The initial depth to the water table and the initial storage deficit are interchangeable conditions within a TOPMODEL approach provided a proper drainable porosity is chosen [*Romanowicz*, 1997]. However, the *Troch et al.* [1993] method requires a specific form for the recession hydrograph that does not conform well to the recessions observed in the study area. Another drawback of this method within the current application is the need to add another initial condition, the drainable porosity, to convert the initial depth to an initial storage [*Romanowicz*, 1997]. Hence, the initial deficit is treated as a parameter that needs to be calibrated.

4.2.4 Baseflow Separation

An expression for the baseflow discharge at the watershed outlet can be derived from the topographic index and the average storage deficit. Instead of using this expression, the streamflow data was used to estimate the baseflow discharge following the method of *Brutsaert and Nieber* [1977] and the extension proposed by *Szilagyi and Parlange* [1998]. Using a baseflow separation technique in this case helps reduce the number of parameters in the model and is justified given the few data available about subsurface and groundwater flow dynamics in the study area. Additionally, there is some evidence of the presence of a perched water table [*Turner*, 2006], and to include these

dynamics, in a topographic index-based model, is foreseen that at least 3 new parameters are needed [*Scanlon et al.*, 2000]. Since the emphasis here is on the effects of imperviousness on surface runoff, a simplified lumped approach to baseflow contributions seems acceptable.

The method proposed by *Brutsaert and Nieber* [1977] and *Szilagyi and Parlange* [1998] assumes the following relation holds for the recession part of the streamflow hydrograph:

$$\frac{dQ(t)}{dt} = -bQ(t)^c, \tag{4-15}$$

where b and c are fitting parameters. The assumption can be verified graphically and by line fitting. The details about the exact way in which the separation is done are described in *Szilagyi and Parlange* [1998], and therefore are omitted from this description.

4.3 Study Area

For this study, a suburban watershed located within the Northwest Branch Anacostia River watershed (NW Branch watershed), in the State of Maryland, U.S., was selected. The map in Figure 4-1 illustrates the location of the NW Branch watershed within Maryland, together with the stream network, the imperviousness pattern, and the two United States Geological Survey (USGS) streamflow gages. The watershed has a total drainage area of 124 km^2 and a total imperviousness of 17%. The watershed extends into Montgomery and Prince George's Counties in Maryland and joins downstream the Potomac River within the Washington, D.C. boundaries [*Miller et al.*, 2007]. The watershed has a tidal portion mostly located within Washington, D.C. The study area selected is limited to the non-tidal portion of the watershed.

The NW Branch watershed was selected mainly because it has a characteristic suburban pattern (mixed pervious-impervious land use) and an imperviousness gradient. The gradient in this case consists of imperviousness accumulating as one moves from the most upstream areas in the watershed, farthest from the main outlet, to the main watershed outlet as illustrated in Figure 4-2a. Figure 4-2a shows at the main outlet, at x = 0 km, the total imperviousness in the watershed is approximately 17%, as one moves away from the main outlet, along the main stream of the watershed, the imperviousness decreases for the most part at a constant rate. There are two locations in Figure 4-2a, when the distance is approximately equal to 1.5 and 18.9 km, where the cumulative imperviousness is characterized by a pronounced downward jump. These are the locations where two significant tributaries in the watershed join the main stream with their respective amounts of total imperviousness. Figure 4-2b illustrates the mixed pervious-impervious character of the suburban pattern in NW Branch. Each cell in the imperviousness grid consists of the fraction of imperviousness in the cell estimated from remotely sensed data [*Homer et al.*, 2007]. The imperviousness fraction of a cell is referred herein as the local imperviousness. Figure 4-2b shows that approximately 40% of the watershed is pervious, approximately 55% of the watershed has a local imperviousness of less than 0.1, and only a small percentage of the watershed, approximately 2%, has a local imperviousness greater than 0.9. This means almost half of the NW Branch watershed is essentially pervious and most of the remaining areas are mixed pervious-impervious land uses.

The NW Branch watershed has two locations where USGS streamflow measurements are available. The USGS gage number 01651000 is located at the overall

outlet of the NW Branch watershed and drains an area of 124 km^2 out of which 17% is impervious. This gage and its drainage area are referred herein as HG because the gage is located near the town of Hyattsville, Maryland. The USGS gage number 01650500 in Figure 4-1 drains an area of 54 km^2 out of which 7% is impervious. This internal gage and its sub-watershed are referred herein as CG because the gage is located near the town of Colesville, Maryland. There is no rain gage data available within the watershed, Next Generation Weather Radar (NEXRAD) stage-III rainfall data is used instead [*NOAA*, 2008a]. The climate in the watershed is humid-temperate with an annual wetness index of approximately 1.4 [*Tenenbaum et al.*, 2006]. The physiography of the watershed is mostly described by the Piedmont Plateau region, although a small downstream portion of the watershed is in the Atlantic Coastal Plain region. The Piedmont is characterized by rolling hilly terrain conformed by a well-defined system of ridges, hills, and valleys, and shallow soils. The Coastal Plain has flatter topography and deeper soils [*Miller et al.*, 2007]. The land cover consists mostly of suburban and grassland areas. A small amount of commercial and cultivated crop cover is also present. The percentages of the main aggregated land cover classes are approximately 60% urban and suburban development, 29% forest and grasslands, and 11% of cultivated crop areas.

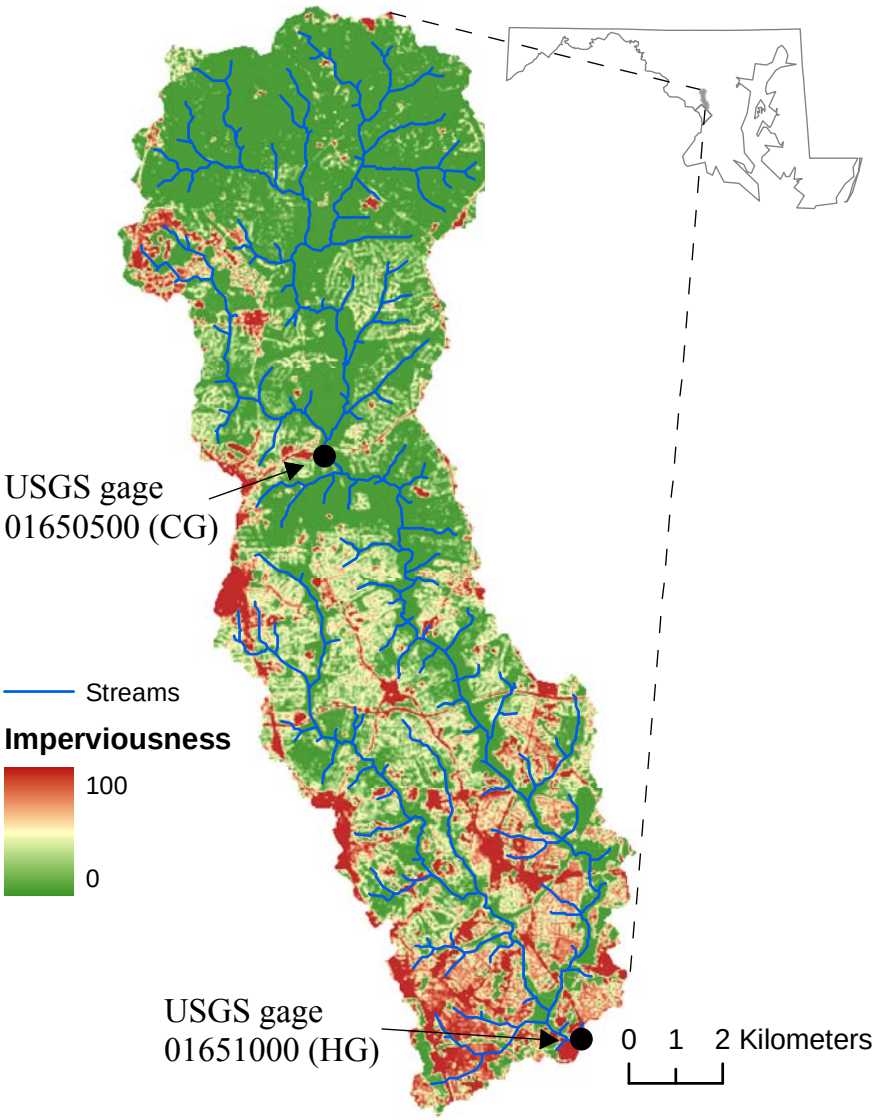

Figure 4-1. Map illustrating the location of the NW Branch watershed within the State of Maryland, U.S. The watershed map illustrates the stream network derived from DEM data, the imperviousness pattern, and the two locations where USGS streamflow data are available.

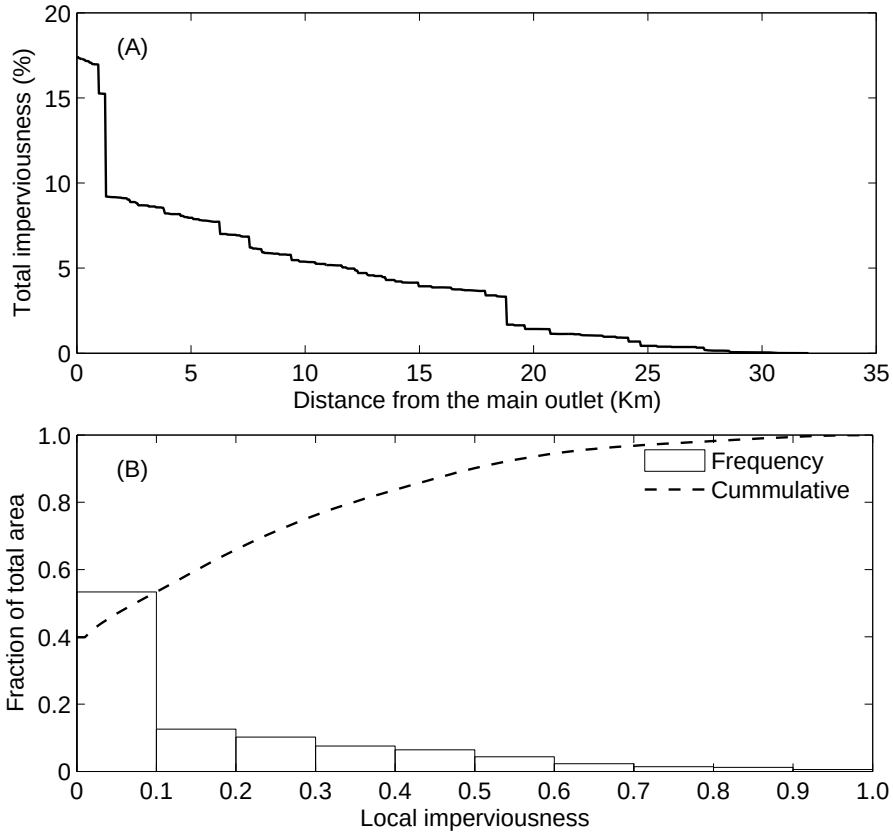

Figure 4-2. (a) Accumulation of total imperviousness along the main stream of the NW Branch watershed, starting from the main outlet to the most upstream location in the watershed at a distance of 32.4 km. The downward steps at the distances of 1.5 km and 18.9 km are the locations where the two largest tributaries join the main stream. (b) Distribution of local imperviousness within NW Branch, local imperviousness is the degree of imperviousness of each cell with 0 being a completely pervious cell and 1 a completely impervious cell.

4.4 Data Sets

For the input or forcing data the NEXRAD stage-III radar rainfall at the 1 hour time resolution and at approximately 4 km spatial resolution was used [*NOAA*, 2008a]. The stage-III radar data is used not only because of the lack of gaged data but also because the spatial distribution of rainfall is known to be particularly important in urbanized watersheds [*Smith et al.*, 2005; *Segond et al.*, 2007]. Since the imperviousness data used depicts conditions in the year 2001, storm and streamflow data between the 1999 and 2001 time period were selected, where land use conditions can be assumed to be approximately stationary. The 1999-2001 time window also matches the period where both radar rainfall and higher resolution streamflow data are available for HG and CG. Six well documented storms were carefully selected with the help of the U.S. National Climatic Data Center (NCDC) Storm Event database [*NOAA*, 2008b], the storms and their characteristics are shown in Table 4-1. Using the NCDC Storm Event database, the storms were selected to represent average rainfall conditions, as opposed to extreme conditions where severe flooding is recorded, and to have caused soil saturation during the storm duration. The streamflow data needed for the gages at HG and CG was obtained from the USGS Instantaneous Data Archive (IDA) at the 15 minute resolution [*USGS*, 2008a]. To match the spatial resolution of the imperviousness data, the rainfall radar data was interpolated using the inverse distance squared weighting of the rainfall amounts at the center of the radar cells [*Smith et al.*, 2005], as shown next:

$$\tilde{P}(t,x) = \sum_{k=1}^{Z} \lambda_k P(t,x_k) \tag{4-16}$$

and

$$\lambda_k = \frac{\frac{1}{(x - x_k)^2}}{\sum_{j=1}^{Z} \frac{1}{(x - x_j)^2}} \tag{4-17}$$

where $\widetilde{P}(t,x)$ [L] is the hourly rainfall amount estimated for location x at time t, $P(t,x_k)$ [L] is the measured rainfall at time t and radar cell k located at x_k, and λ_k are the weights associated with each radar cell. Beyond the corrections done as part of the development of the stage-III data set [*Young et al.*, 2000], it was not possible to further unbias the radar data given the lack of additional rain gages.

The DEM and imperviousness data were obtained from the USGS at a resolution of approximately 30 meters [*USGS*, 2007, 2008b]. In order to preserve the resolution of both of these data sets, this same spatial resolution is used in the model to partition rainfall and route the runoff produced. The DEM is used to determine the area draining to each cell, the D∞ and D8 flow directions, and the stream network [*Tarboton*, 1997]. The D∞ flow directions are used to estimate the topographic index because they can reproduce more realistically the drainage tendencies of hillslopes [*Tarboton*, 1997]. The D8 flow directions are used to route the generated runoff and avoid having multiple flow routing paths for hillslope cells. The stream network was derived using a fixed area threshold [*Montgomery and Dietrich*, 1988]. The threshold used is 0.2 km^2 which compares well with blue lines from the 1:100k NHDPlus hydrography data set of the U.S. Environmental Protection Agency (EPA) [*EPA and USGS*, 2006]. The soil data was obtained from the U.S. Natural Resources Conservation Service (NRCS). Both SSURGO [*NRCS*, 2008a] and STATSGO [*NRCS*, 2008b] data are used, since the higher resolution data, SSURGO data, was not available for the entire study area. However, after

classifying soils in the study area according to soil textures, it was found that soils are highly homogeneous and characterized by a single soil class, silt-loam. The soil parameters associated with silt-loam soils were obtained from the literature and their values are K_s = 2.59 cm/hr, ϕ = 0.485, ψ = 78.6 cm, and B = 5.30 [*Dingman*, 1994]. The soil parameters are needed to estimate the infiltration capacity at the soil surface, and they are used in the estimation of equations 4-7 and 4-8. All the grid data used was projected from its original coordinate system to Maryland State Plane coordinates in meters [*Stern*, 1990].

Table 4-1. Characteristics of the storm events selected for this study. The storms were selected with the help of the NCDC Storm Event database. The storm data is NEXRAD stage-III radar rainfall at the 1 hour time resolution and approximately 4 km spatial resolution.

Storm	Depth (cm)	Maximum intensity (cm/hr)	Duration (hr)	COV[b]	Recurrence interval[c]
March 21, 1999 [a]	2.17	1.71	8	0.22	1.5
August 25, 1999	1.67	0.90	7	0.12	1
March 21, 2000 [a]	2.21	1.17	12	0.18	1
April 17, 2000 [a]	2.17	0.80	12	0.12	1
March 29, 2001	0.95	0.64	8	0.066	<1
July 4, 2001[a]	2.57	1.58	8	0.38	4

[a] Storms selected for calibration in the split sample test, the remaining two storms were used for evaluation.
[b] Coefficient of variation from the accumulated rainfall amounts at every grid cell.
[c] Estimated from NOAA Atlas 14 [*NOAA*, 2008c].

4.5 Results

The results from applying the event model are divided into three sections. In the first section, Section 4.5.1, the event model is assessed using a split sample test and by analyzing the parameters. The assessment is not intended to be an exhaustive evaluation of the chosen modeling approach, more complete evaluations are available in the literature. For example, *Valeo and Moin* [2001] evaluated the application of a TOPMODEL approach to suburban watersheds, and *Olivera and Maidment* [1999] evaluated the application of a spatially distributed unit hydrograph to an urbanized watershed. In Sections 4.5.2 and 4.5.3, the event model is used to investigate the role of the imperviousness gradient and pattern after accounting for limitations in the model. In Section 4.5.2, the storm hydrographs at various internal locations in the watershed are compared. Section 4.5.3 compares changes in the hydrologic response from various imperviousness scenarios.

4.5.1 Assessment of Modeling Approach

In order to determine suitable values for the parameters S_{max}, u_h, u_c, D_c, and D_h, and the initial condition $\overline{S}$ a model calibration was performed; the calibration was also done to better understand the behavior of parameters and identify limitations in the modeling approach. The soil parameters required by equation 4-7 were assumed to be equal to their average value and constant for all the simulations. It was assumed for the calibrations different parameter sets for the two watersheds where streamflow data are available, HG and CG, and for each of the four storms identified in Table 4-1. The calibrations were performed in three steps. The first step was to manually adjust

parameters and choose the form of the transmissivity profile. In the second step the Generalized Likelihood Uncertainty Estimation (GLUE) method was used to investigate the identifiability and sensitivity of parameters [*Spear and Hornberger*, 1980; *Beven and Binley*, 1992]. In the third step the parameters were tuned with the Shuffled Complex Evolution algorithm to obtain an optimum parameter set for the evaluation [*Duan et al.*, 1992]. The goodness of fit of simulations was quantified using the Nash Sutcliffe efficiency (*NS*) [*Nash and Sutcliffe*, 1970] and the modified correlation coefficient (R_{mod}) [*McCuen and Snyder*, 1975].

From the manual calibrations an exponential transmissivity profile was chosen, choosing the form of the transmissivity profile is the equivalent of deciding the value of *n* in equations 4-1 and 4-5 [*Duan and Miller*, 1997]. A preference for larger values of *n* was observed in the calibrations and because from the baseflow separation the recession exponent *b* in equation (4-15) was found to be approximately equal to 2, the exponential transmissivity profile was chosen for all the simulations [*Ambroise et al.*, 1996; *Duan and Miller*, 1997]. The relation between *n* and other model parameters was not explored further. Such an investigation would need to include more specific soil profile data than was available in this study. Another simplification made was to ignore the imperviousness when estimating the topographic index. The calibration results remained essentially the same when the reduction in upslope contributing area due to imperviousness was not considered, a similar result was found by *Valeo and Moin* [2001]. This lack of sensitivity of the topographic index is described and explained in detail by *Franchini et al.* [1996].

For the identifiability and sensitivity analysis, the version of GLUE [*Beven and Binley*, 1992] in the Monte Carlo Analysis Toolbox was used (MCAT) [*Wagener et al.*, 2004]. For each behavioral parameter set Θ_i, the *NS* efficiency was used to find the normalized pseudo-likelihood function [*Beven and Binley*, 1992], $L(\Theta_i)$, which can be defined as:

$$L(\Theta_i \mid Y) = \frac{NS_i}{\sum_{i=1}^{M} NS_i}, \tag{4-18}$$

where Y are the streamflow observations, i is in this case a given behavioral parameter set, and M is the total number of behavioral sets selected from the Monte Carlo realizations. Figure 4-3 shows the scattergram obtained from 10,000 model simulations and a single storm event, using the criteria $NS > 0.8$ to select the behavioral set, analogous scattergrams were found for the other storms. It is evident in the scattergram the channel velocity is very sensitive and well identified, while the other parameters are less identifiable. The regional sensitivity analysis, as implemented in MCAT [*Spear and Hornberger*, 1980; *Wagener et al.*, 2004], indicated the channel velocity to be the most sensitive parameter, while the other parameters were relatively less sensitive with D_h being the most insensitive. The Kolmogorov-Smirnov test (*KS*-test) comparing the behavioral set pdf of each parameter to a uniform pdf bounded by the parameter range indicated all parameters to be sensitive except D_h [*Spear and Hornberger*, 1980]. The estimated *KS* statistic d for D_h was less than d_{max} ($d_{max} = 0.13$ at the 0.005 level of significance) for all the storms, while the other parameters had d values greater than d_{max}. The apparent lack of identifiability in Figure 4-3 is in part due to the combination of spatially distributed conditions and observations at a point used to estimate *NS*, where

grid cells can contribute unevenly to the simulations. Another way of identifying parameters is to take parameters within their role in the simulations. Thus the scattergram for the initial value of the ratio $\overline{S}/S_{\max}$, *E[δ]*, the mean travel time, *E[f(t)]*, and the variance of the travel times, *var[f(t)]*, was determined and are shown in Figure 4-4. The initial *E[δ]* has the role of deciding the degree of soil saturation in the watershed just before the rain starts, and thus its identifiability is perhaps more relevant in this case than S_{max} alone. Similarly, for the routing parameters, *E[f(t)]* and *var[f(t)]* are important properties of the GIUH that characterize the form of the response [*Rinaldo and Rodríguez-Iturbe*, 1996; *Rodríguez-Iturbe and Rinaldo*, 1997; *Nicótina et al.*, 2008]. *E[f(t)]* and *var[f(t)]* were found using the expression of *Saco and Kumar* [2002] and by integrating the time in equation (4-10) to obtain *p(γ)*. It becomes apparent in Figure 4-4 that the role of the parameters is identifiable and one expects the parameters to have a role in the simulations.

The split sample test resulted in different parameter values for each of the four storms used in calibration, these values were averaged to obtain a single parameter set for HG and CG. This parameter set is shown in Table 4-2. Table 4-2 shows a consistent value of S_{max} for HG and CG while the routing parameters varied between the two watersheds, the velocities increased with drainage area and the dispersions decreased. This scale dependency of the routing parameters was expected as supported by empirical studies, e.g. *Leopold and Maddock* [1953]. Figure 4-5 shows the final calibration results for the March 21, 2000, storm event for HG and CG. Figure 4-5a shows the calibration results for CG, the *NS* and R_{mod} values for this calibration are 0.96 and 0.95, respectively. Figure 4-5b shows the results for HG, in this case the *NS* and R_{mod} values are 0.91 and

0.90, respectively. Overall the calibrated results performed reasonably well, but when a single parameter set was used to perform the evaluation, the goodness-of-fit coefficients decreased. The *NS* efficiency decreased on average by 20% and R_{mod} by 18%. The hydrographs estimated for the two storms used in the evaluation are shown in Figures 4-6 and 4-7. In general, the simple event model was found to have a better ability to predict peak flows than other parts of the hydrograph, it performs better when calibrated, and it appears sensitive to storm dependency in the routing parameters, possible biases in the forcing data, and uncertainty in the estimate of the initial condition.

Some of the limitations of the modeling approach are visible in Figures 4-7a and b. In Figure 4-7a, the overestimated flows on the receding limb of the simulated hydrograph are mostly due to the last pulse of rainfall, but this pulse has no equivalent in the observed hydrograph. It is possible that rainfall is somewhat overestimated for this particular storm. Biases in the radar rainfall data are well-documented [*Young et al.*, 2000; *Smith et al.*, 2005]. Additionally, the impervious cover can increase the sensitivity of the hydrologic response to spatially distributed rainfall which, in turn, can increase the effects of potential biases [*Smith et al.*, 2005; *Segond et al.*, 2007]. The overestimation of observed flows on the rising limb of the hydrographs in Figures 4-7a and b suggests areas where the model structure could be improved. The overestimation is likely due in part to the unaccounted effects of initial rainfall storage on localized depressions, and uncertainty in the estimate of the initial condition $\overline{S}$. An average calibrated value for $\overline{S}$ was used that changed for spring and summer flows, but a tendency for $\overline{S}$ to vary within seasons was observed. The storm dependency of routing parameters was a lesser concern in this case because average rainfall conditions and storms with similar return periods

were used. However, during calibration it was found u_c to range from 0.78 to 1.28 m/sec, instead of having a single value. For instance, in Figure 4-3, if u_c is chosen to be 0.7 instead of the optimum value of 0.96, one expects the *NS* efficiency to decrease by approximately 25%. The storm dependency of u_c, or its time-variant character, was somewhat expected, since it was present in the original formulation of the GIUH [*Rodríguez-Iturbe and Valdés*, 1979]. An interesting result of this study is the increasing relevance of channel routing for the case of a mixed pervious-impervious land use and this will likely be an important concern when trying to consider more diverse climatic conditions than average rainfall. The relevance of channel routing in the case of an urbanizing watershed may be enhanced by the direct connection between rainfall and channel routing provided by the stormwater network. In the remaining analysis, some of the limitations found in the event-model will be considered.

Table 4-2. Single parameter set found from the calibration of four storms. The single parameter set was obtained by averaging the parameter values obtained for each of the four calibrated storms.

Watershed	S_{max} (cm)	V_h (m/s)	V_c (m/s)	D_h (m^2/s)	D_c (m^2/s)
HG	50	0.55	0.90	100	200
CG	50	0.40	0.80	300	500

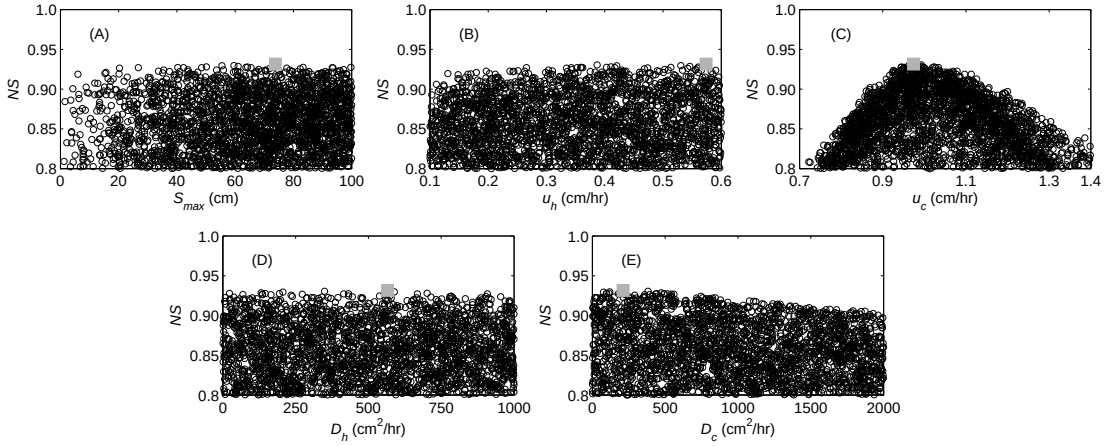

Figure 4-3. Scattergram obtained from 10,000 Monte Carlo simulations and the March, 21, 2000, storm event, for the five parameters in the model: (a) S_{max}, (b) u_h, (c) u_c, (d) D_h, and (e) D_c. Each dot in the plots is a simulation with parameter values sampled from a uniform pdf. The bounds of the pdfs were the same as the ranges shown for the *x*-axis above. Only the simulations that met the condition $NS > 0.8$ are shown. The solution with the highest *NS* value is indicated by the square symbol.

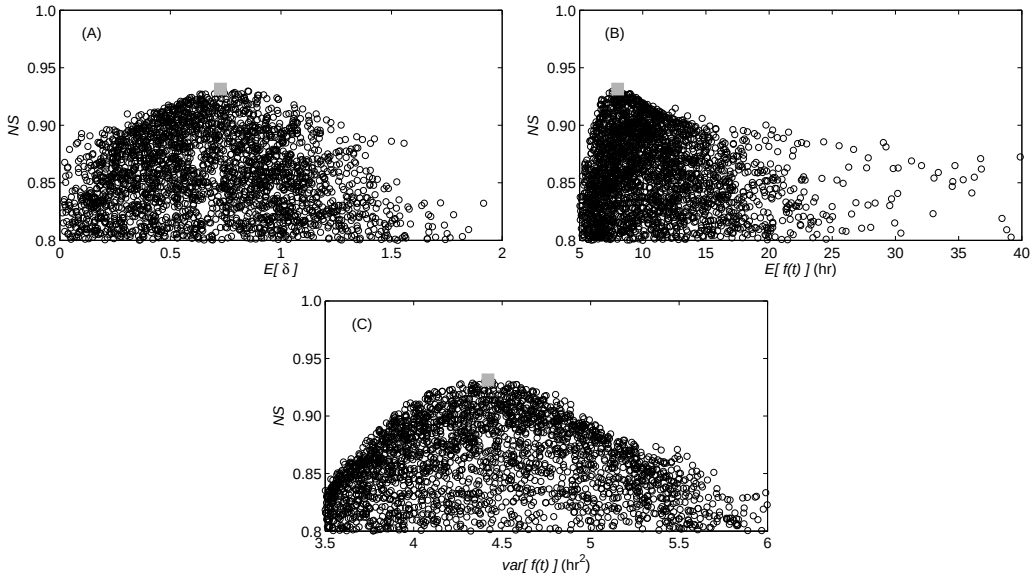

Figure 4-4. Scattergram obtained from 10,000 Monte Carlo simulations and the March, 21, 2000, storm event, for the (a) initial ratio of $\overline{S}/S_{\max}$, *E[δ]*, (b) the mean travel time *E[f(t)]*, and (c) the variance of the travel times, *var[f(t)]*. Each dot in the plots is a simulation run with parameter values (the five parameters in the model) sampled from a uniform pdf. Only the simulations that met the condition *NS* > 0.8 are shown. The solution with the highest *NS* value is indicated by the square symbol.

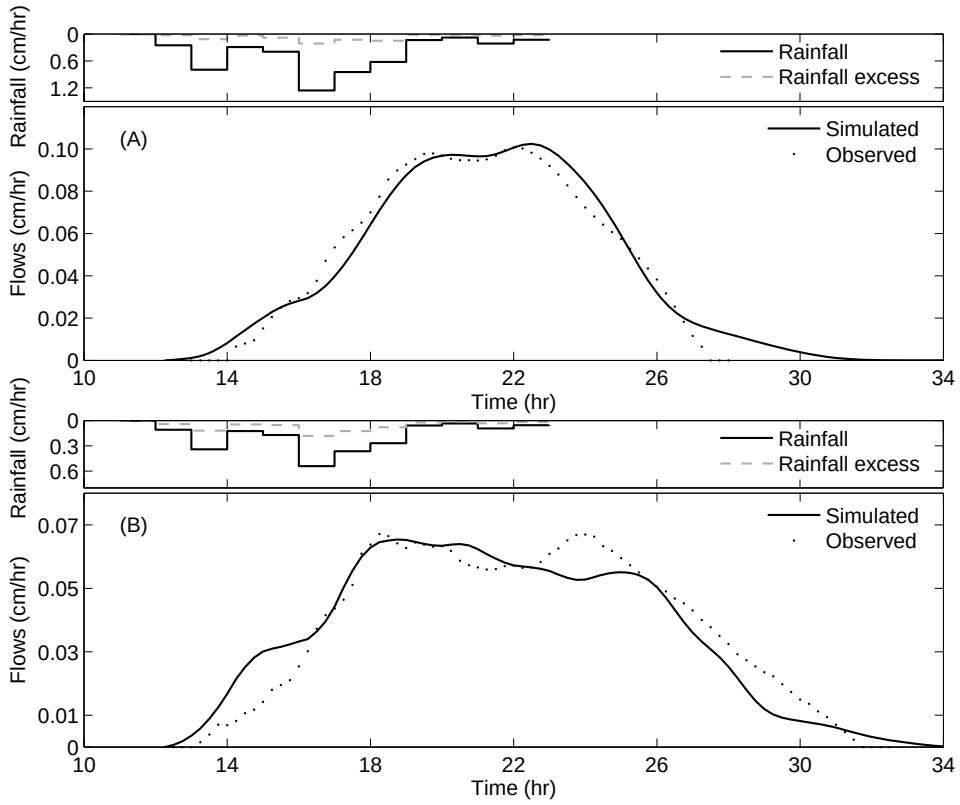

Figure 4-5. Calibration results for the March 21, 2000, storm event at HG and CG. (a) Observed and simulated flows at CG, and (b) HG. Observed flows are at the 15 min. resolution and were obtained from the USGS IDA. The rainfall and rainfall excess are the areal averaged values obtained from the radar rainfall data and the spatially simulated runoff, respectively. The areal averaged rainfall and rainfall excess are only shown for illustrative purposes, they were not used directly in the simulations. The horizontal axis is the starting time on the day of the storm.

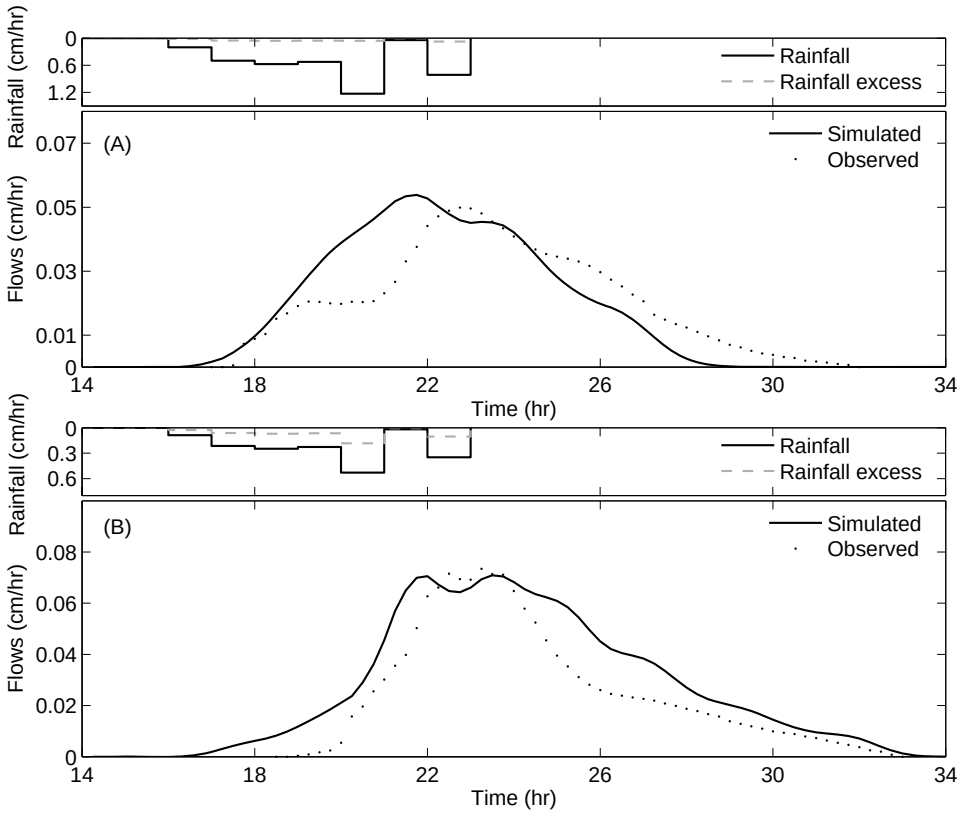

Figure 4-6. Evaluation results for the August 25, 1999, storm event at HG and CG. (a) Observed and simulated flows at CG, and (b) HG. Observed flows are at the 15-min resolution and were obtained from the USGS IDA. The rainfall and rainfall excess are the areal averaged values obtained from the radar rainfall data and the spatially simulated runoff, respectively. The areal averaged rainfall and rainfall excess are only shown for illustrative purposes, they were not used directly in the simulations.

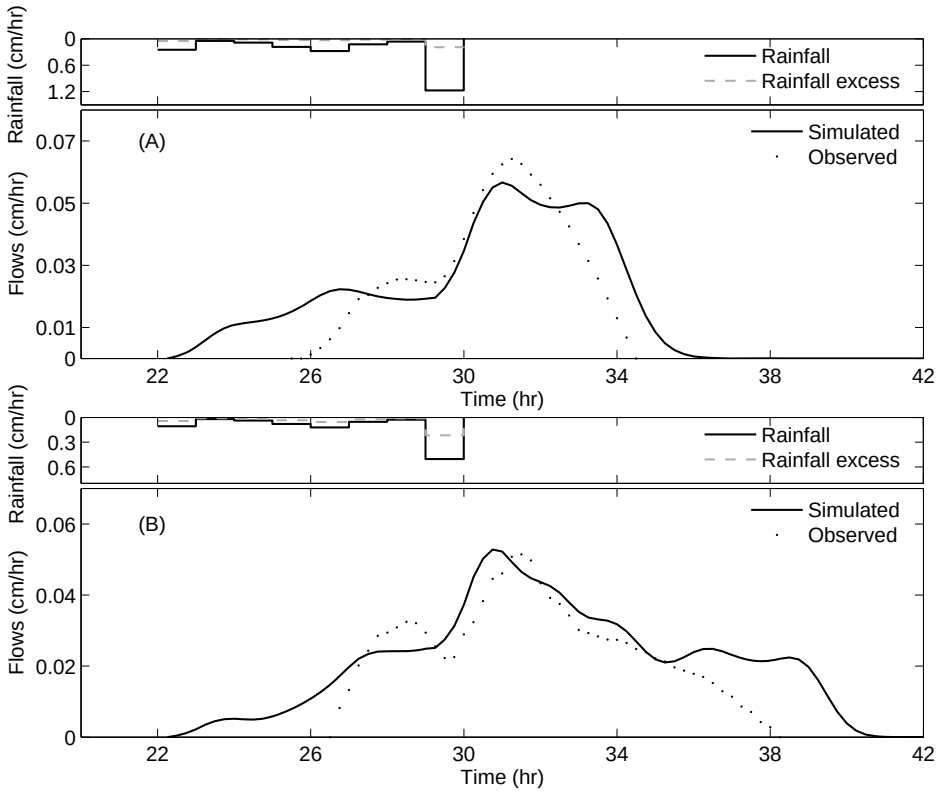

Figure 4-7. Evaluation results for the March 29, 2001, storm event at HG and CG. (a) Observed and simulated flows at CG, and (b) HG. Observed flows are at the 15-min resolution and were obtained from the USGS IDA. The rainfall and rainfall excess are the areal averaged values obtained from the radar rainfall data and the spatially simulated runoff, respectively. The areal averaged rainfall and rainfall excess are only shown for illustrative purposes, they were not used directly in the simulations.

4.5.2 Effects of the Imperviousness Gradient

For the remaining of the analysis the focus will be on the March 21, 2000, storm event shown in Figure 4-5. This storm event is characteristic of average rainfall conditions in the study area selected. The objective is to use this storm event to perform a series of comparisons and clarify further the role of imperviousness on the response. Effort will be made to account for the scale dependency of the routing parameters but they will be assumed time-invariant throughout the storm. There is more interest, in this case, in the spatial variation of the routing parameters, in particular the velocities, because their scale dependency makes it difficult to explore the role of imperviousness at internal locations in the watershed. The emphasis in the next comparisons will be on peak flows and the time to peak since the assumption of time-invariant velocities is more suitable for estimating peak flows [*Rodríguez-Iturbe and Valdés*, 1979]. To estimate the velocity field, the use of a Leopold-Maddock type parameterization for channel velocities is proposed [*Leopold and Maddock*, 1953]. The proposed parameterization is as follows:

$$u_i \propto A_i^{\alpha} I_i^{\beta} \tag{4-19}$$

where u_i [L/T] is the velocity at location i, A [L^2] is the drainage area at i, and I is the total imperviousness upstream of location i. The proportionality constant and the exponents α and β in equation (4-19) were estimated by calibration. The proportionality constant was found to be equal to 0.37 m/sec, α = 0.04, and β = 0.15. The value of α compares well with empirical values [*Leopold and Maddock*, 1953]. In addition, a similar mathematical relation to equation (4-19) was found for peak flows of a given return period for gaged urban watersheds in the Maryland Piedmont province [*Moglen et al.*, 2006]. Equation (4-19) is also written in terms of imperviousness in order to identify

the dependency of u on imperviousness. For the dispersion, the following parameterization is used:

$$D_i \propto u_i \tag{4-20}$$

where the proportionality constant was found by calibration to be equal to 272 m^2/sec. The parameterization for the dispersion was kept simpler because there is little empirical evidence about its scaling with drainage area [*Toprak and Cigizoglu*, 2008]. A parameterization for the dispersions similar in form to equation (4-19) was tried first, but only minor improvements in the *NS* efficiency were found when compared to equation (4-20). This last parameterization of dispersion was tried as one way to account for the relation of dispersion to flow depth, under the assumption that flow depth is related to the drainage area [*Leopold and Maddock*, 1953]. The basis for equation (4-20) is the larger correlation found between dispersion and velocity than with other hydraulic variables [*Toprak and Cigizoglu*, 2008].

To evaluate the calibrated parameters for equations (4-19) and (4-20), a simplified version of the proxy-watershed test was performed [*Ewen and Parkin*, 1996]. Identifiability and sensitivity analysis for the parameters in equations (4-19) and (4-20) were not performed because the structure of the model was not changed. The proxy-watershed test performed consisted of using the CG watershed for calibration and the HG watershed for evaluation. Figure 4-8 shows the results of this simplified version of the proxy-watershed test. The *NS* and R_{mod} for the calibration, Figure 4-8a, are 0.92 and 0.94, respectively. For the evaluation, Figure 4-8b, the *NS* and R_{mod} are 0.82 and 0.90, respectively. In Figure 4-8 the model demonstrates a reasonable ability to match peak flows, as expected from the assumption of time-invariant velocities, but a tendency to

overestimate the recession flows in the case of HG and underestimate in the case of CG. The calibrated model with the spatially varying velocities and dispersions was used to investigate the role of the imperviousness gradient by selecting and comparing four internal sub-watersheds.

The selected sub-watersheds are shown in Figure 4-9. The sub-watersheds were selected to constitute two pairs of watersheds with approximately the same drainage area but strikingly different level of imperviousness (see Table 4-3). For the pair SB3 and SB4, the hydrographs obtained for the March 21, 2000, storm are shown in Figure 4-10a. This figure shows the peak flow for SB4 is 25% larger than for SB3, even though SB4 has a much lower amount of total imperviousness than SB3. SB4 is only 3.5% impervious while SB3 is 37.7%. The main reason for this is the uneven space-time distribution of rainfall and runoff. The rainfall amounts are greater on the upper portions of the watershed, where SB4 is located, than near the overall outlet, where SB3 is located. In Figure 4-10b the peak flow for SB1 is 20% larger than SB2, this time the sub-watershed with greater imperviousness has the largest peak. No differences in the time to peak were observed in Figures 4-10a and b. The same comparison just performed was repeated assuming spatially uniform rainfall, this emphasizes the role of imperviousness by removing the effects of spatially variable rainfall. The uniform rainfall was obtained from the areal average of the radar rainfall. The model was recalibrated using the simple proxy-watershed test previously described. The *NS* and R_{mod} for the recalibration were 0.94 and 0.87, respectively, and 0.78 and 0.79 for the evaluation, respectively. The results from the uniform rainfall assumption are consistent with the general observation of increasing peak flows with increasing imperviousness as illustrated in Figures 4-10c

and d. In Figure 4-10c the peak flow increased by 28% and in Figure 4-10d by 18%, in both cases the sub-watershed with the largest imperviousness, SB1 and SB3, produced the largest peak flow. The time to peak did not change for SB3 and SB4, but between SB1 and SB2 the time to peak arrived earlier by 1 hour for SB1.

The comparisons performed in this section illustrate the complex interplay between spatially variable rainfall and imperviousness. This complexity becomes more apparent if one accounts for the various nested sub-watersheds in HG and their respective peak flows, instead of just using four sub-watersheds as previously done. Figure 4-11 shows the peak flow for nested sub-watersheds in HG with a drainage area larger than 3 km^2 for the March 21, 2000, storm. The peak flows were normalized, Q_p/A, using the drainage area to further emphasize the role of imperviousness, and Q_p/A is plotted against A, where A in this case serves as an index of watershed size. It is apparent in the box area shown in Figure 4-11 that for a given watershed size, say A is approximately 9 km^2, the normalized peak flow can be approximately 0.16 cm/hr in a sub-watershed with 10% or less imperviousness and 0.12 in a sub-watershed with greater imperviousness, between 20 and 30%. Figure 4-11 also illustrates the fact that many sub-watersheds that are mostly pervious (with less than 10% imperviousness) have greater normalized peak flows than watershed with 40 to 50% imperviousness. Overall, the results in this section indicate that pervious areas can have an important effect on the runoff generated and the peak flows of suburban watersheds. A similar result was found by *Burges et al.* [1998] for pervious areas on an urbanized hillslope. Here the results show how pervious areas can be important at a wide range of scales beyond the hillslopes. Also the wide variability illustrated in Figure 4-11 suggests that the spatial distribution of

imperviousness and rainfall are important factors when trying to understand changes in the hydrologic response from urbanization at the watershed scale. Much of this variability is often neglected by aggregating imperviousness and assuming spatially uniform rainfall. This spatial understanding and estimation of the impacts from urbanization could be useful when designing mitigation measures, such as stream restoration projects, that are aimed at recovering natural conditions along the stream network [*Wohl et al.*, 2005].

Table 4-3. Drainage area and total imperviousness of the sub-watersheds selected to examine the role of the imperviousness gradient. The pairs SB1-SB2 and SB3-SB4 are used together in the comparisons.

Sub-watershed	Drainage area (km^2)	Imperviousness (%)
SB1	12.58	24.5
SB2	12.63	2.5
SB3	2.93	37.7
SB4	2.97	3.5

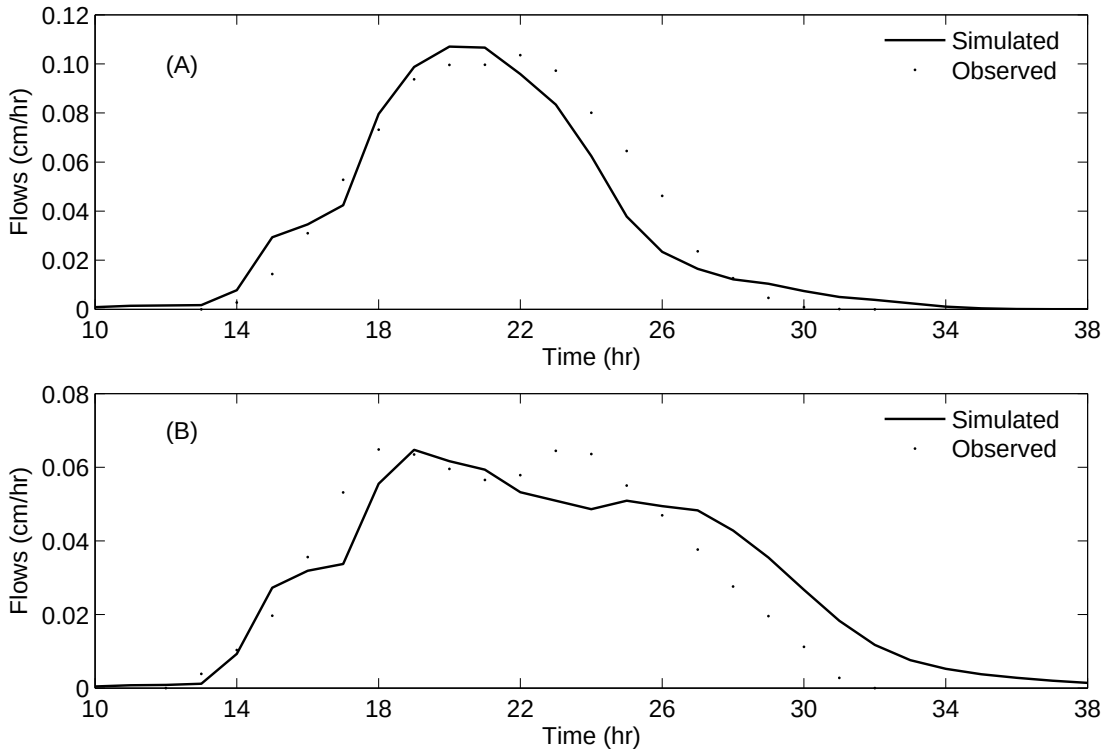

Figure 4-8. Results from the simplified proxy-watershed test used for the calibration-evaluation of the spatially distributed routing parameters. (a) Calibration based on the CG streamflows and (b) evaluation based on the HG streamflows, for the March 21, 2000, storm event.

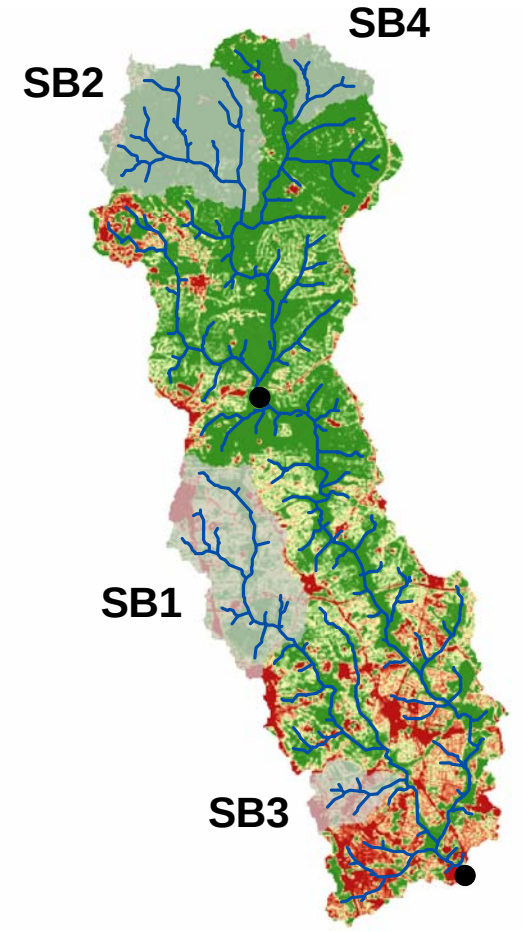

Figure 4-9. Sub-watershed chosen to investigate the role of the imperviousness gradient on the hydrologic response. The pair SB1-SB2 each has a drainage area of approximately 12.6 km^2 and total imperviousness of 24.5 and 2.5%, respectively. The pair SB3-SB4 each has a drainage area of approximately 2.9 km^2 and total imperviousness of 37.7 and 3.5%, respectively.

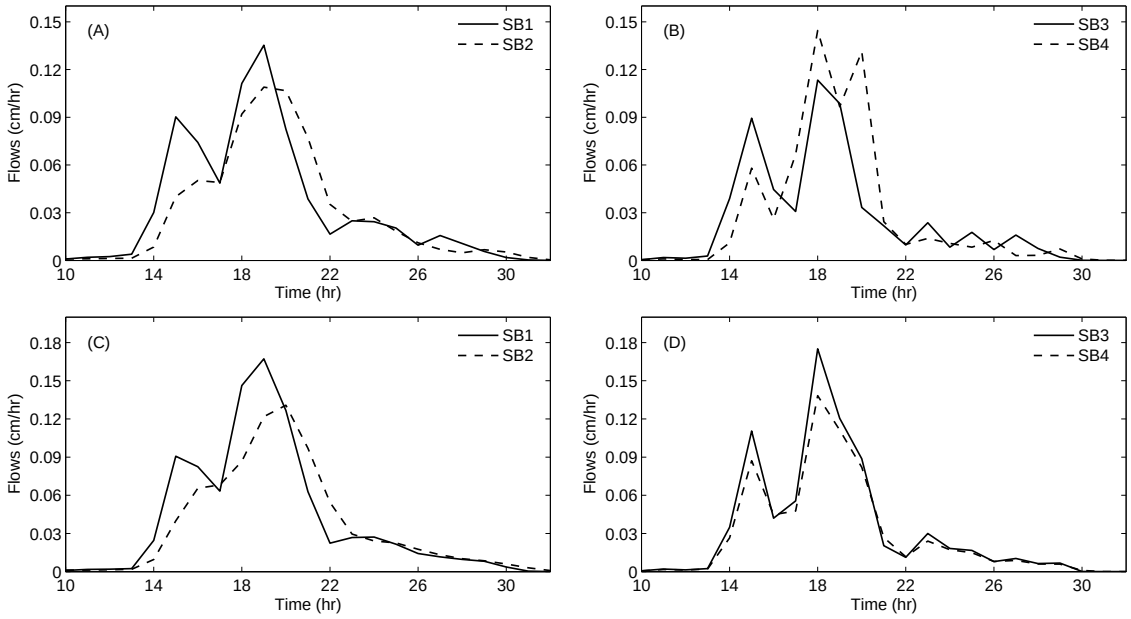

Figure 4-10. Comparison of simulated hydrographs for the selected sub-watersheds. (a) Comparison for the pair SB1-SB2 and (b) SB3-SB4 using spatially distributed rainfall. (c) Comparison for the pair SB1-SB2 and (D) SB3-SB4 using uniform rainfall. The pair SB3-SB4 each has a drainage area of approximately 2.9 km^2 while SB1-SB2 each is approximately 12.6 km^2.

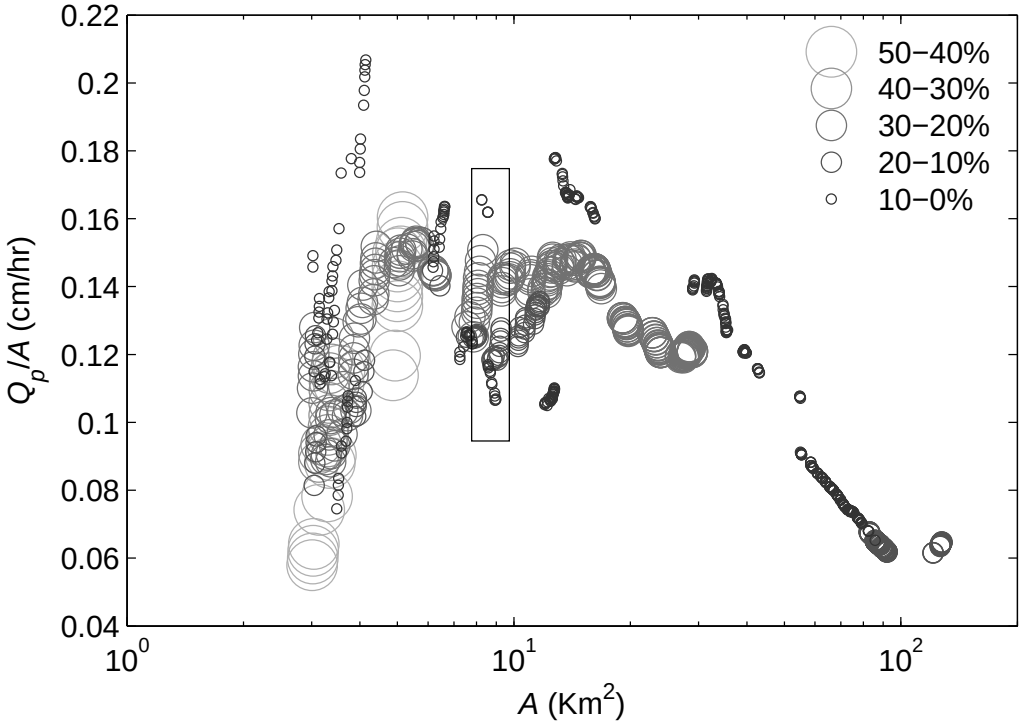

Figure 4-11. Effect of the imperviousness gradient on the normalized peak flows, Q_p/A. Each circle in the plot is a nested sub-watershed of HG, and the area-size of the circles indicates the level of imperviousness as shown in the legend. The horizontal axis is the drainage area of the sub-watershed, A, and is used as an index of watershed size. For the vertical axis the peak flows, Q_p, were normalized by A.

4.5.3 Effects of the Imperviousness Pattern

The previous comparison between sub-watersheds could be extended to analyze the role of the imperviousness pattern by selecting a pair of sub-watersheds with the same drainage area and amount of imperviousness, but contrastingly different development patterns. The HG sub-watersheds that meet this criterion have relatively small drainage areas, where the effect of hillslopes are likely to be dominant and the modeling approach gives preference to channel routing in its structure and calibration-evaluation data. Therefore, this comparison is not recommended in this case, instead simulated imperviousness patterns were used. The patterns were simulated using the results from Chapter 3. The patterns typify extreme and predictable ways of organizing imperviousness in the watershed. Figure 4-12 illustrates the three patterns that were used. The pattern in Figure 4-12a is the actual NLCD pattern (current scenario). The patterns in Figures 4-12b and c represent different ways of clustering imperviousness. Figure 4-12b has the advantage of reducing peak flows along the channel network while 4-12c will tend to increase peak flows but at the same time it stirs development away from the floodplains. The pattern in Figure 4-12b is referred herein as the channel clustering scenario and the one in Figure 4-12c as the source clustering scenario. Figure 4-12d shows uniformly distributed imperviousness in the watershed, this pattern is mimicking an extreme case of urban sprawl and it is referred herein as the uniform scenario. All the scenarios maintain the total imperviousness and the distribution of local imperviousness in the main watershed the same level as the current scenario, with only the spatial organization being changed.

It is important when comparing the hydrologic response from the various scenarios to understand the significance of changes, say changes in peak flows, by estimating the uncertainty associated with the model's simulations. In this case the uncertainty in the parameters and the initial condition is determined [*Beven and Binley*, 1992; *Vrugt et al.*, 2003; *Kuczera et al.*, 2006]. This is important because land use changes as reflected on the hydrologic response could have a lesser impact than parameter uncertainty. This will be the case if changes on the response from the land use scenarios are completely contained within the estimated uncertainty bounds. To estimate the uncertainty associated with parameters and the initial condition the Shuffled Complex Evolution Metropolis algorithm (SCEM) and GLUE were used [*Beven and Binley*, 1992; *Vrugt et al.*, 2003]. The details of the SCEM and GLUE methodologies are not described here; the complete descriptions of SCEM and GLUE can be found in *Vrugt et al.* [2003] and *Beven and Binley* [1992], respectively. To determine convergence in the SCEM estimates the scale reduction score (*SR*) was used with the criteria being $\sqrt{SR} < 1.2$ [*Vrugt et al.*, 2003]. The behavioral parameter set for GLUE was selected by using the lowest *NS* value obtained from the solutions in SCEM, recall from equation (4-18) that *NS* was used to define the likelihood function for the GLUE analysis [*Beven and Binley*, 1992]. This value was found to be 0.85 for HG and 0.9 for CG.

Figures 4-13 and 4-14 show the simulation results for HG and CG, respectively, and the various imperviousness scenarios. The uncertainty bounds in Figures 4-13 and 4-14 do not necessarily contain all the observations. This is mainly because the bounds only account for uncertainty in the parameters and initial condition, and not for model structural uncertainty. Both the GLUE and SCEM bound are shown for the 95% interval.

The GLUE bounds are generally wider, although the similarities between the SCEM and GLUE bounds are striking, as the two approaches require very different methodologies. In Figure 4-13, the peak flow relative to the simulated peak flow for the current scenario decreased by 6% (Figure 4-13b), 1% (Figure 4-13c), and 4% (Figure 4-13d) for the channel clustering, source clustering, and uniform scenario, respectively. The most noticeable change in Figure 4-13 is a delay in the time to peak of approximately 4 hours for both the source clustering and uniform scenarios. However, in both scenarios the change in the peak flow and time to peak is outside the SCEM and GLUE estimated uncertainty, indicating the change is bigger than the uncertainty associated with parameters and the initial condition. This is important because it suggests that the imperviousness pattern can influence the hydrologic response at the watershed scale. In Figure 4-14 for CG, the time to peak did not change but the peak flow increased relative to the current scenario by 18% (Figure 4-14b), 30% (Figure 4-14c), and 27% (Figure 4-14d) for the channel clustering, source clustering, and uniform scenarios, respectively. The increases in peak flow are all greater than the estimated uncertainty indicating their importance, albeit the increases in this case are due in part to increases in the total imperviousness in CG. Overall, these results suggest that the imperviousness pattern can have an impact in the shape of the hydrologic response at the watershed scale. This becomes even more evident when impacts at internal locations within the overall watershed are examined. At internal locations the impacts can be magnified by the large scale re-ordering of imperviousness locations produced by the various patterns as illustrated by Figure 4-14.

To further illustrate the impacts from the various scenarios a sub-set of 150 nested sub-watersheds from HG were sampled. For the sampled sub-watersheds, Q_p/A was plotted against the level of imperviousness, this plot is shown in Figure 4-15. All the possible sub-watersheds were not selected for clarity and because the trends shown in Figure 4-15 do not change by using a sub-set. The sub-set was sampled by assuming all sub-watersheds to be equally likely. Each circle in the plot represents a sub-watershed and the size of the circle indicates the relative size or drainage area of the watershed. Figure 4-15 shows how the scenarios re-order imperviousness differently within the overall watershed by changing the level of imperviousness in the nested sub-watersheds. For example, the uniform scenario has approximately 17% total imperviousness for all watershed sizes while the current scenario is characterized by a wide range of imperviousness from approximately 2% to 48%. This internal variability in imperviousness affects the degree of changes in flows along the stream network. This last observation is illustrated in Figure 4-15 in two ways. First, the scenarios produce different ranges for the minimum and maximum normalized peak flows. The source clustering scenario has normalized peak flows that range from 0.02 to 0.24 cm/hr while the range for the channel clustering scenario is 0.035 to 0.19 cm/hr. Second, the maximum normalized peak flow for each scenario can be produced by sub-watersheds of different sizes. The source clustering scenario has a maximum normalized peak flow of approximately 0.24 cm/hr for a watershed size between 2.4 and 6.6 km^2 while the maximum normalized peak flow for the channel clustering scenario, 0.19 cm/hr, is due to a watershed size between 6.6 and 17.7 km^2. This spatial variability in normalized peak flows produced by the different scenarios is important because it could lead to uneven

patterns of impacts. For instance, excessive stream erosion and disturbance to stream ecosystems will likely vary in space depending on the stream locations where peak flow increases are largest or most variable, and peak flows, in turn, can depend on the distribution of imperviousness, as illustrated in Figure 4-15. Our ability to recognize, characterize, and predict this spatial variability could have important implications in our understanding of changes to stream ecosystems and geomorphic processes in urbanized watersheds; since changes in these processes are very often correlated to changes in hydrologic conditions, such as peak flows [*Poff et al.*, 1997].

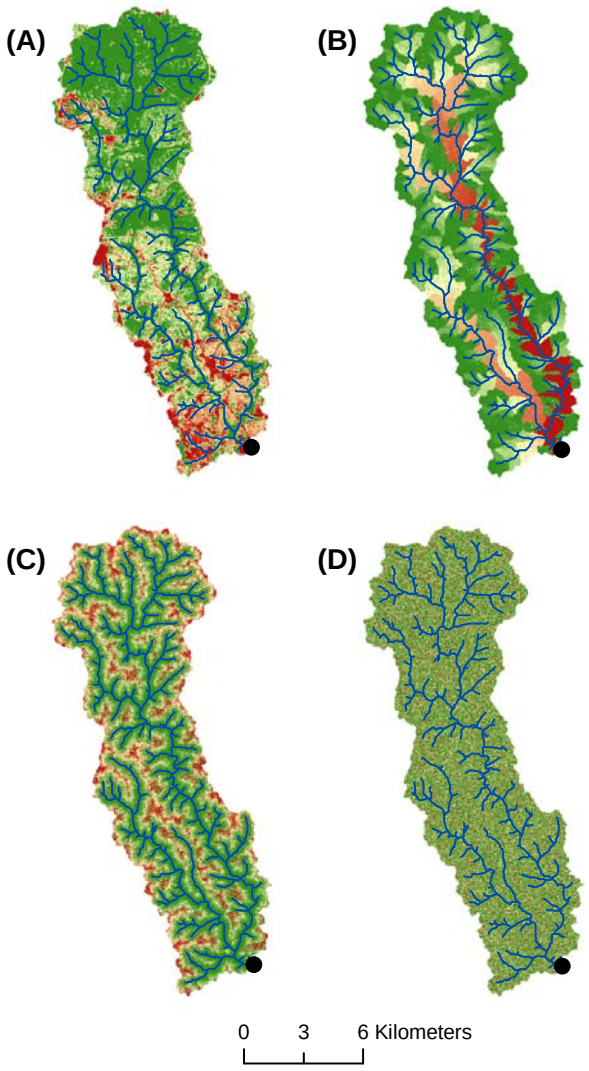

Figure 4-12. Current and simulated imperviousness patterns used for the comparison of scenarios: (a) current scenario, (b) channel clustering scenario, (c) source clustering scenario, and (d) uniform scenario.

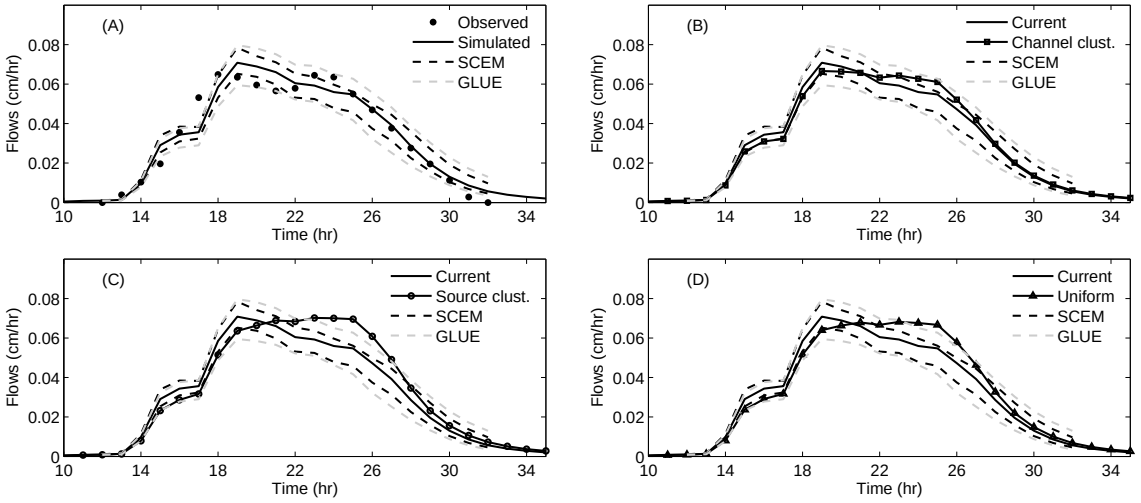

Figure 4-13. Comparison of the hydrographs obtained from the imperviousness scenarios at HG, including the 95% uncertainty bounds associated with the parameters and the initial condition. (a) Observed flows and current scenario, (b) current and channel clustering scenario, (c) current and source clustering scenario, and (d) current and uniform scenario.

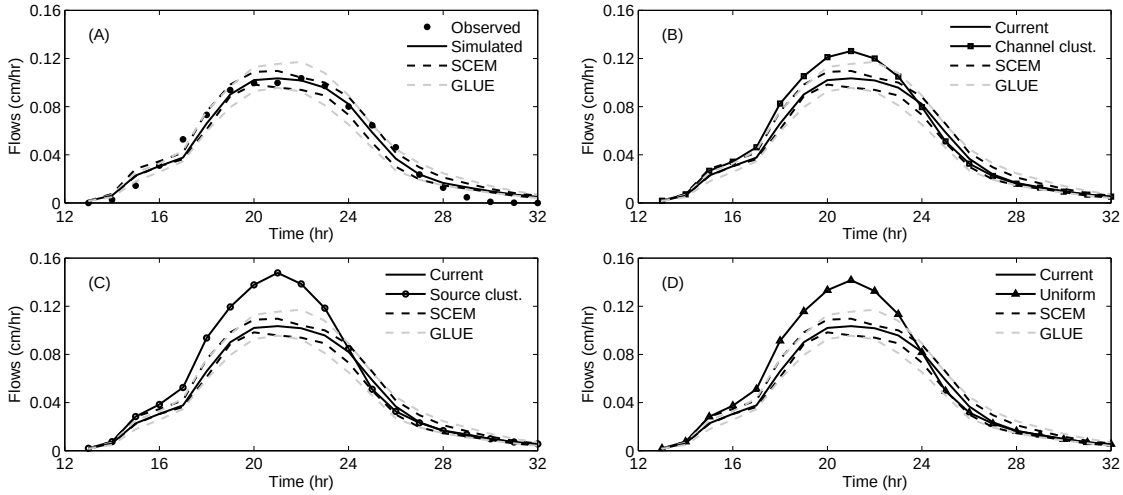

Figure 4-14. Comparison of the hydrographs obtained from the imperviousness scenarios at CG, including the 95% uncertainty bounds associated with the parameters and the initial condition. (a) Observed flows and current scenario, (b) current and channel clustering scenario, (c) current and source clustering scenario, and (d) current and uniform scenario.

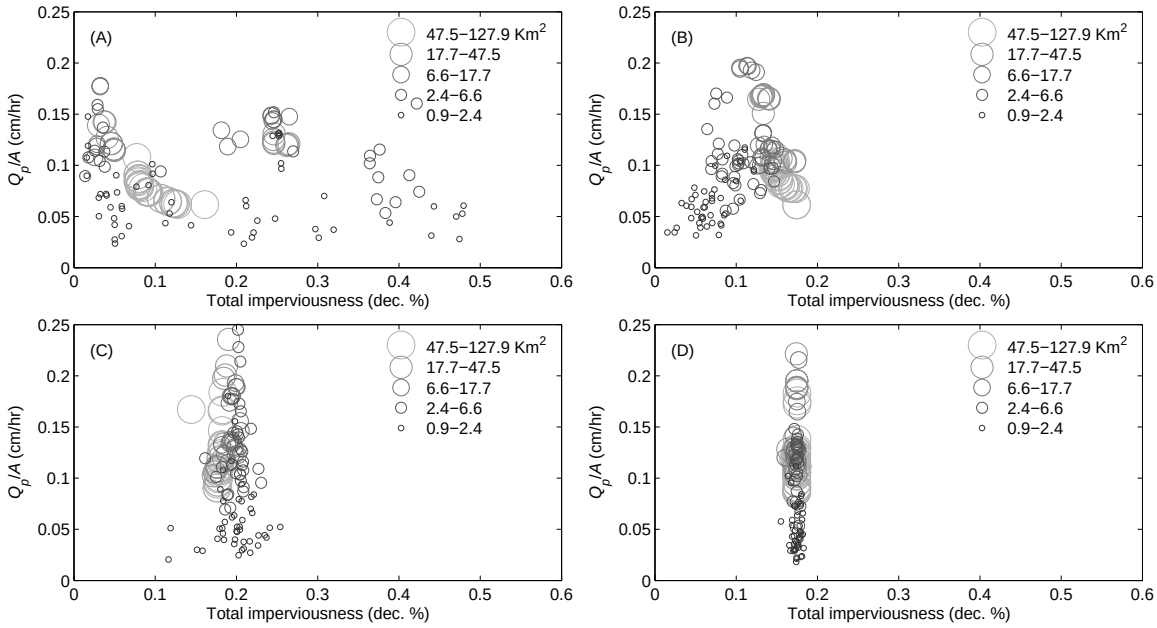

Figure 4-15. Effect of the imperviousness scenarios on the distribution of normalized peak flows, Q_p/A, for sub-watersheds of various sizes (the sizes considered are described by the intervals in the legend). Distribution for the (a) current, (b) channel clustering, (c) source clustering, and (d) uniform scenario.

4.6 Conclusions

An event-based model, previously developed [*Sivapalan et al.*, 1987; *Troch et al.*, 1994], was modified and applied to an urbanized watershed by making several simplifying assumption about the effects of imperviousness. To begin the development of the model a suburban watershed, where the land use is characterized by both pervious and impervious conditions, was assumed [*Guo and Adams*, 1998; *Valeo and Moin*, 2001; *Cuo et al.*, 2008]. To model pervious conditions a topographic index and Philip's infiltration equation were used to account for both saturation and infiltration excess, respectively [*Philip*, 1960; *Beven and Kirkby*, 1979]. To model the effects of imperviousness, rain falling on impervious cells was immediately converted to runoff because most of the impervious surfaces in the study area are connected. This assumption was reasonable in this case, but it is expected for reinfiltration to be a source of soil saturation and runoff in watersheds with disconnected impervious surfaces [*Easton et al.*, 2007]. A unit hydrograph was used for routing all the runoff [*Rodríguez-Iturbe and Valdés*, 1979; *Rinaldo and Rodríguez-Iturbe*, 1996], assuming the effects of imperviousness on surface flows could be represented by a time-invariant velocity field [*Olivera and Maidment*, 1999].

The assessment of model parameters showed the channel velocity to be very sensitive and an important variable in estimating the response for urbanized watersheds. Effort in the direction of a more realistic representation of channel routing appears promising at improving predictions. It is likely the sensitivity of channel routing parameters is enhanced by the stormwater system which links rainfall directly to the channel routing process without the modulating effect of hillslope processes. This also

reinforces the need for accurate estimates of the spatial pattern of rainfall, as imperviousness will tend to increase the role of rainfall spatial variability on the response [*Segond et al*., 2007]. The comparison of internal sub-watersheds revealed an interesting fact about the pervious-impervious land use condition. The coincidence of higher rainfall intensity on the most pervious portions of the watershed led to higher peak flow in these areas than the most urbanized ones. Generally, it is thought that higher imperviousness leads to higher peak flows. This general perception seems to be more consistent when rainfall is assumed uniform and some of the interactions between the spatial pattern of imperviousness and rain are neglected. The various imperviousness scenarios tried led to considerable changes in the hydrographs at the two gaged locations, after accounting for uncertainties in the parameters and initial condition. The changes consisted of delays in the time to peak at the overall outlet and increases in the peak flows at the internal gage location. Overall, the results indicate the imperviousness pattern, its distribution within the watershed, has an important effect on the distribution of peak flows along the stream network and on the form of the hydrologic response at the watershed scale. Particularly, the relation between the spatial imperviousness and rainfall pattern seems to be an important factor in understanding and estimating the impacts of urbanization on the response.

4.7 Summary

The simulations of the hydrologic response performed in this chapter, under different imperviousness scenarios, revealed a complex system. The system is complex in this case because of the space-time variability in the rainfall data and the runoff

process, and the spatial variability in the routing process and in the imperviousness data. After observing this complexity, one may be tempted to ask questions such as "Which source of variability is more dominant?" or "How are these different variability related to each other?" To help answer these questions a synthesis method is proposed in the next chapter. The synthesis method is developed as an analytical tool for relating the different sources of variability encountered in this chapter (i.e. rainfall, runoff, routing and imperviousness), and simplify some of the observed complexity.

CHAPTER 5 - RELATING THE IMPERVIOUSNESS PATTERN TO THE SPACE-TIME VARIATION IN RAINFALL, RUNOFF, AND ROUTING

5.1 Introduction

The method proposed in this chapter builds on the analytical framework of *Woods and Sivapalan* [1999] by including the spatial distribution of imperviousness. The framework is based on the simplifying assumption of the space-time separability of rainfall and the runoff generation function [*Eagleson*, 1967; *Sivapalan and Wood*, 1987; *Woods and Sivapalan*, 1999], as well as any other specific assumptions made about the hydrologic processes themselves. The method allows the analytical expression of the space-time variability of rainfall, runoff, and the hydrologic response, such that these space-time variabilities can be tracked and compared when estimating useful hydrologic relationships [*Woods and Sivapalan*, 1999]. The hydrologic relationships are described in Section 5.4. The method in this case is also used to gain insight into the role of the imperviousness pattern by providing a basis for comparing scenarios and identifying dominant controls. To present the method, the space-time variability of the data and processes is described and identified first. Then the analytical approach is developed and used to determine hydrologic relationships based on the space-time variability identified. Lastly, the relationships obtained are used to study the role of the spatial distribution of imperviousness.

5.2 Space-Time Variabilities from Pervious and Impervious Areas

The main interest here is in relating the space-time components of rain, runoff, and the routing process to the spatial distribution of imperviousness. The aim is also to express these relations analytically in order to make them tractable and gain insight about their interactions. In order to achieve this, the space-time variability of runoff, *R(x,y,t)* [LT^{-1}], is expressed as follows:

$$R(x,y,t) = P(x,y,t)W(x,y,t)[1-I(x,y)] + P(x,y,t)I(x,y), \tag{5-1}$$

where *P(x,y,t)* [LT^{-1}] is the rainfall space-time pattern, *W(x,y,t)* is the runoff generation function space-time pattern, and *I(x,y)* is the spatial imperviousness pattern. The *x,y* coordinates identify the location where the variable is being estimated and *t* is time during the storm event. The watershed is discretized into a grid of regular squares such that *x,y* represents the different cells in the grid. *W(x,y,t)* is the fraction of rain that becomes runoff at a given cell, it can take a value ranging from 0 to 1, where 0 means all the rain falling on a given *x,y* cell at time *t* infiltrates and 1 means all the rain becomes runoff. In practice, the runoff generation function can be determined by various methods such as an infiltration equation, topographic index, or curve number, as long as the runoff function is properly normalized to be between 0 and 1 [*Philip*, 1960; *Kirkby and Beven*, 1979; *NRCS*, 1986]. Equation (5-1) can be used to classify the generated runoff into pervious and impervious contributions. This classification is useful because it can track these two sources of runoff and compare their relative importance as shown later. The first term in the sum of (1) is the runoff generated from pervious areas,

$$R(x,y,t)_p = P(x,y,t)W(x,y,t)[1-I(x,y)], \tag{5-2}$$

and the last term in (1) is the runoff from impervious areas,

$$R(x,y,t)_i = P(x,y,t)I(x,y). \tag{5-3}$$

equation (5-1) assumes all the rainfall falling on impervious areas becomes runoff which can be a reasonable assumption for connected imperviousness. In equations (5-2) and (5-3), and in the remainder of this paper, the subscript *p* is used to refer to pervious areas and *i* for impervious ones. To study how the space-time variability of *P(x,y,t)*, *W(x,y,t)*, and the spatial *I(x,y)* pattern contribute to runoff, it is assumed that they can be separated into multiplicative space and time processes. The separability assumption was first used by *Eagleson* [1967] and later by *Woods and Sivapalan* [1999] to investigate space and time contributions in hydrologic processes. The way these processes are separated is discussed in the next section.

5.2.1 Rainfall and Runoff Variability

Using the separability assumption the rainfall space-time pattern, *P(x,y,t)*, can be represented by independent space, $P_t(x,y)$ [ ], and time variations, $P_{x,y}(t)$ [LT^{-1}], such that [*Eagleson*, 1967; *Woods and Sivapalan*, 1999]:

$$P(x,y,t) = P_{x,y}(t)P_t(x,y), \tag{5-4}$$

where $P_{x,y}(t)$ is the areal averaged rainfall and equal to

$$P_{x,y}(t) = \frac{1}{A}\iint_A P(x,y,t)dxdy, \tag{5-5}$$

A [L^2] is the drainage area of the watershed, and $P_t(x,y)$ is the spatial pattern of rainfall determined by dividing the total rainfall falling on every grid cell in the watershed by the total average rainfall falling over the entire watershed for a given storm event such that

$$P_t(x,y) = \frac{\int_0^{T_s} P(x,y,t)dt}{\int_0^{T_s} P_{x,y}(t)dt}, \tag{5-6}$$

where T_s [T] is the storm duration assuming at the start of the storm the time is 0. A similar assumption is made for the space and time variations of the runoff generation function such that:

$$W(x,y,t) = W_{x,y}(t)W_t(x,y), \tag{5-7}$$

where $W_{x,y}(t)$ is the areal averaged value of W and determined as follows:

$$W_{x,y}(t) = \frac{1}{A}\iint_A W(x,y,t)dxdy, \tag{5-8}$$

and $W_t(x,y)$ is the runoff generation function space pattern and estimated similarly to (5-6) as follows:

$$W_t(x,y) = \frac{\int_0^{T_s} W(x,y,t)dt}{\int_0^{T_s} W_{x,y}(t)dt}, \tag{5-9}$$

W as defined here is amenable to the representation of imperviousness and in particular to remotely sensed impervious data [*Homer et al.*, 2007]. Remotely sensed impervious data represents the amount of imperviousness on each grid cell as a continuous value between 0 and 1, where 0 is a fully pervious cell and 1 a fully impervious cell [*Homer et al.*, 2007]. In the case of the imperviousness pattern, the space-time field is as follows:

$$I(x,y,t) = I(x,y), \tag{5-10}$$

where the imperviousness pattern is assumed constant in time. Then the space and time variations for I are as follows:

$$I_t(x,y) = \frac{I(x,y)}{f}, \tag{5-11}$$

and

$$I_{x,y}(t) = f, \tag{5-12}$$

f is the total fraction of imperviousness in the watershed and equal to:

$$f = \frac{1}{A}\iint_A I(x,y)dxdy. \tag{5-13}$$

Even though $I(x,y)$ is only a function of space and constant in time, the notation in equation (5-11) will be retained to refer to the normalized $I(x,y)$ value.

5.2.2 Runoff Routing Variability

The variability associated with the hydrologic response is quantified using the mean and variance of the travel times assuming a GIUH approach, the same routing approach that was used in Chapter 4 [*Rinaldo and Rodríguez-Iturbe*, 1996; *Rodríguez-Iturbe and Rinaldo*, 1997]. In this case the GIUH is a convenient assumption because analytical relations are available that can be used to approximate the variations induced on the response from pervious and impervious surfaces [*Rinaldo and Rodríguez-Iturbe*, 1996]. Also, the approach has been used widely by others researches and shown to be useful for suburban watersheds [*Olivera and Maidment*, 1999; *Smith et al.*, 2005]. The estimation of the response with the GIUH can be expressed as follows [*Rinaldo and Rodríguez-Iturbe*, 1996]:

$$Q_k(t) = \sum_{\gamma\in\Gamma}\int_0^t R_{x,y}(\tau) * p(\gamma) f_\gamma(t-\tau)d\tau, \tag{5-14}$$

where $R_{x,y}(t)$ is the time component of the runoff generation process or the time series of rainfall excess. The exact way in which $R_{x,y}(t)$ is estimated is shown in the next section. The subscript k indicates that $Q(t)$ can be estimated for any location along the stream network by treating the location as an outlet. $p(\gamma)$ is the likelihood of a given path γ to carry water to the outlet, and $f_\gamma(t)$ is the path response function or the distribution of the travel times [*Rinaldo and Rodríguez-Iturbe*, 1996]. It is assumed that $f_\gamma(t)$ includes both the hillslope and channel sections of a path and is defined by an inverse Gaussian probability density function (pdf) [*Mesa and Mifflin*, 1986; *Rinaldo and Rodríguez-Iturbe*, 1996]. It is assumed that $p(\gamma)$ is equal to:

$$p(\gamma) = \frac{R_t(x,y)}{\iint_A R_t(x,y)dxdy}. \tag{5-15}$$

$R_t(x,y)$ is the spatial pattern of runoff and its estimation is shown on the next section. Equation (5-15) is divided by the total value of $R_t(x,y)$ to ensure the sum of all the path probabilities, $p(\gamma)$'s, is 1. To determine the mean and variance of the travel times previously derived equations by *Rinaldo et al.* [1991] are used. The runoff produced on pervious and impervious cells is tracked and used to separate the mean and variance of the travel times into pervious and impervious times. This separation is done as a simple way to measure the relative effects of pervious and impervious areas on the response. The mean travel time for impervious surfaces is determined as follows [*Rinaldo et al.*, 1991; *Saco and Kumar*, 2002]:

$$E[T_i] = \sum_{\gamma \in \Gamma_i} p(\gamma) \frac{L_\gamma}{u_\gamma}, \tag{5-16}$$

where L_γ [L] and u_γ [L/T] are the path dependent length and wave celerity, respectively. Γ is the set of all possible paths. The subscript i in equation (5-16) indicates runoff that

originated from impervious areas. This can be replaced by p to obtain an expression for the mean travel time for runoff originating from pervious areas. The total expected travel time for the watershed is:

$$E[T_b] = E[T_i] + E[T_p]. \tag{5-17}$$

T_b [T] is the travel time after accounting for both pervious and impervious contributions. To estimate the variance of the travel times the following expression is used:

$$\begin{aligned} Var(T_i) = 2\sum_{\gamma\in\Gamma_i} p(\gamma)\frac{L_\gamma D_\gamma}{u_\gamma^3} + \sum_{\gamma\in\Gamma_i} p(\gamma)\left(\frac{L_\gamma}{u_\gamma}\right)^2 - \left(\sum_{\gamma\in\Gamma_i} p(\gamma)\frac{L_\gamma}{u_\gamma}\right)^2 \\ -\left(\sum_{\gamma\in\Gamma_i} p(\gamma)\frac{L_\gamma}{u_\gamma}\right)\left(\sum_{\gamma\in\Gamma_p} p(\gamma)\frac{L_\gamma}{u_\gamma}\right). \end{aligned} \tag{5-18}$$

$Var(T_i)$ indicates equation (5-17) is for the impervious portion of the watershed. D_γ [L^2/T] is the path dependent dispersion coefficient. By substituting the subscript i above for p, a similar expression for the variance of the pervious portion of the watershed, $Var(T_p)$, can be obtained. The expression in equation (5-18) is similar to the one proposed by *Saco and Kumar* [2002]. However this time the expression was rearranged to separate the total variance into pervious and impervious components based on $p(\gamma)$. The variance of the travel times measures the spread of the response [*Saco and Kumar*, 2004]. The usefulness of the variance is demonstrated in Section 5.6.2 where is used to define the peakedness of the response. Additionally, it is possible to separate the terms in (5-18) into geomorphologic, kinematic, and hydrodynamic dispersion which has been shown to be useful for studying the response of watersheds under various conditions [*Rinaldo et al.*, 1991; *Saco and Kumar*, 2002, 2004; *Nicótina et al.*, 2008]. Here the emphasis is placed instead on pervious and impervious contributions to the variance. The total variance of the travel times from pervious and impervious surfaces is as follows:

$$Var(T_b) = Var(T_i) + Var(T_p). \quad (5\text{-}19)$$

Equations (5-16) and (5-18) can be compared to a time of concentration and the response duration, respectively [*Woods and Sivapalan*, 1999; *Saco and Kumar*, 2004]. They are useful because they provide, analytically, a simple way of explaining the influence of imperviousness on the hydrologic response. The path probabilities *p(γ)* account for the space variations as they decide the relative importance of a given path. It is possible to further separate the time and space components in the mean and variance of the travel times [*Woods and Sivapalan*, 1999], but in this case the space variation of the response is defined as a function of the travel times to emphasize instead the pervious and impervious components.

5.3 Data

To illustrate the application of the proposed method, the NW Branch Anacostia River watershed (NW Branch), located in the Maryland Piedmont province, was selected. This is the same watershed used in Chapter 4. A brief description of the data needed by the proposed method is provided below.

The NW Branch watershed is characterized by a suburban pattern where the main land use categories are pervious forested and grassed areas and impervious residential developments. The watershed has a drainage area of 124 km^2, of which approximately 17% is impervious. The imperviousness in the watershed tends to increase as one moves from the most upstream areas towards the overall watershed outlet. Figure 5-1c illustrates the imperviousness distribution in the watershed. To represent imperviousness NLCD 2001 remotely sensed data was used [*USGS*, 2008b]. NEXRAD stage-III radar

data was used for the space-time rainfall [*NOAA*, 2008a]. The NLDC data represents imperviousness using a grid scheme with cells having values that range from 0 to 1, where 0 is a fully pervious cell and 1 is fully impervious. The NEXRAD data has a time resolution of 1 hour and space resolution of approximately 4 km. To interpolate the rainfall an inverse squared distance weighting scheme was used which has been found to be applicable [*Smith et al.*, 2005]. The DEM data was obtained from the USGS [*USGS*, 2007]. Figure 5-1a shows the storm event chosen to illustrate the application of the method. Figure 5-1b is the space pattern, $P_t(x,y)$, obtained using equation (5-6). The space pattern in Figure 5-1b resembles several of the individual hourly space patterns in Figure 5-1a. It resembles the patterns that contribute the most rainfall and it can be interpreted as an average space pattern.

To estimate the runoff generation function, $W(x,y,t)$, the runoff production approach of the event-based model in Chapter 4 was used. The generated runoff on cell x,y at time t is normalized by the rain falling on the cell to obtain a value between 0 and 1 for $W(x,y,t)$. Additionally, the imperviousness in the NW Branch watershed is mostly connected as assumed by equation (5-1).

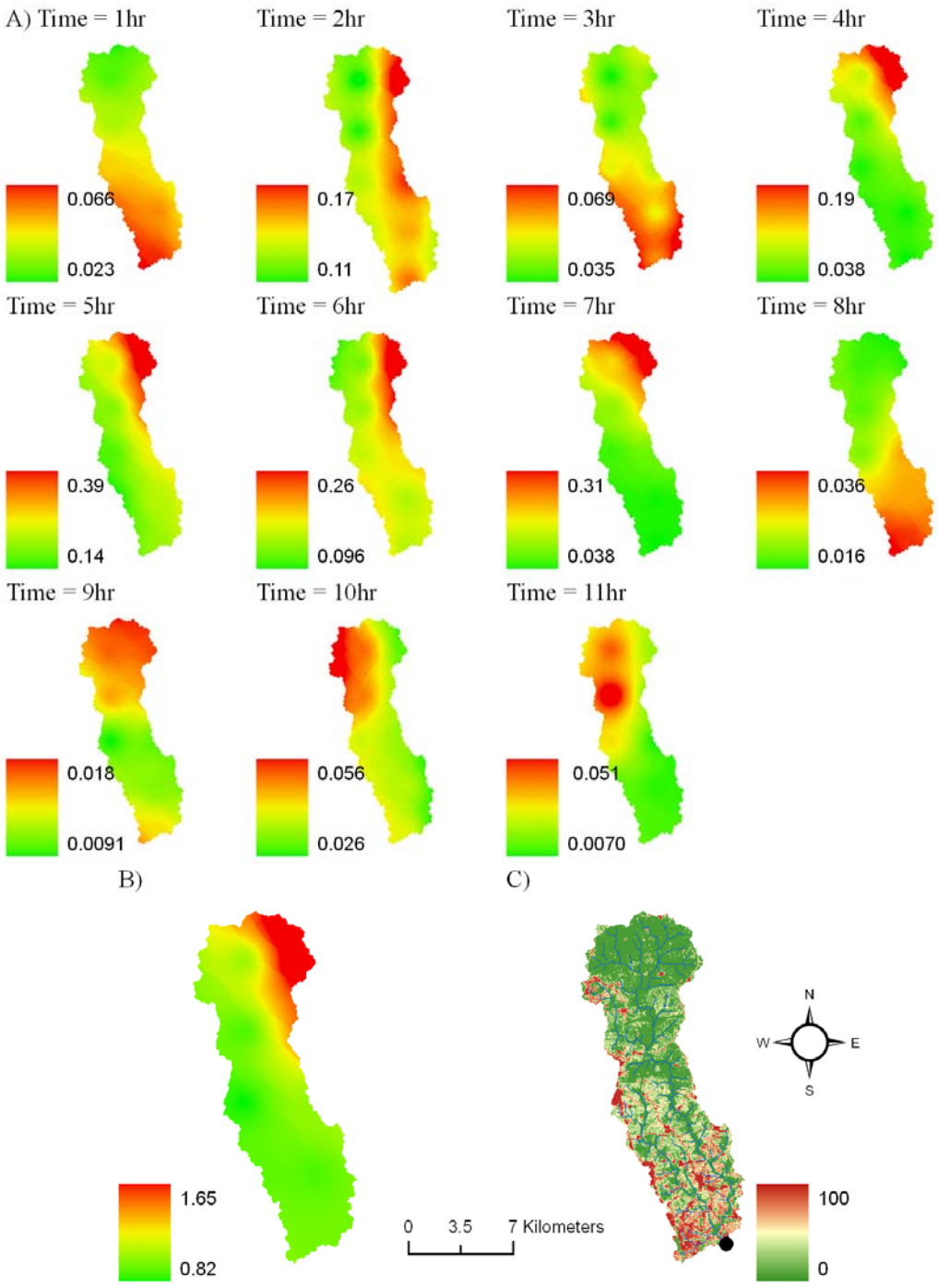

Figure 5-1. (a) Spatial distribution of rainfall for the March 21, 2000, storm, in cm/hr and (b) the $P_t(x,y)$ pattern, obtained using equation (5-6). (c) Map illustrating the NW Branch watershed, including the stream network and the imperviousness pattern, the dot indicates the location of the main outlet.

5.4 Space-Time Relationships for Pervious and Impervious Areas

In this section the separation and estimation of variations in rainfall, runoff, and routing presented in Section 5.2 are used to develop several hydrologic relationships. The relationships estimated are: (1) the instantaneous rainfall excess, (2) the storm-averaged watershed rainfall excess, (3) the ratio of instantaneous rainfall excess, (4) the ratio of storm-averaged watershed rainfall excess, and (5) the mean and variance of the watershed runoff time. The ratio in measures (3) and (4) is the runoff from the pervious-impervious land use to the runoff assuming a fully pervious land use. The estimation of these five relationships is presented below based on the data for the NW Brach.

5.4.1 Instantaneous Rainfall Excess

Within the proposed framework, the space-time pattern of runoff generation is as follows:

$$R(x,y,t) = R(x,y,t)_i + R(x,y,t)_p, \tag{5-20}$$

where $R(x,y,t)_p$ and $R(x,y,t)_i$ are defined by equations (5-2) and (5-3), respectively. $R(x,y,t)_p$ is the runoff from pervious areas where saturation or infiltration excess occurs and $R(x,y,t)_i$ is the runoff from impervious areas or the impervious fraction of individual cells. The sum of $R(x,y,t)_p$ and $R(x,y,t)_i$ results in the total amount of runoff generated, $R(x,y,t)$, on cell x,y at time t.

To determine the instantaneous rainfall excess, $R_{xy}(t)$, the areal averaged value of equation (5-20) can be used as follows:

$$R_{x,y}(t) = \frac{1}{A}\iint_A P(x,y,t)W(x,y,t)[1-I(x,y)]dxdy + \frac{1}{A}\iint_A P(x,y,t)I(x,y)dxdy, \tag{5-21}$$

using the separability assumption for *P(x,y,t)* and *R(x,y,t)* defined in equations (5-4) and (5-7), respectively, letting $W(x,y,t)[1-I(x,y)]$ be equal to a new variable, $W^*(x,y,t)$, and by taking out the time dependent terms from the integrals, equation (5-21) can be expressed as follows:

$$R_{x,y}(t) = P_{x,y}(t)W^*_{x,y}(t)\frac{1}{A}\iint_A P_t(x,y)W^*_t(x,y)dxdy + P_{x,y}(t)f\frac{1}{A}\iint_A P_t(x,y)I_t(x,y)dxdy. \tag{5-22}$$

W^* is the amount of runoff that can be generated on the pervious portion of an individual grid cell with a mixed land use. Using the relation between the covariance and the expected value of two random variables, *cov(x,y) =E[xy]-E[x]E[y]*, and by noting that the integrals in (5-22) can be interpreted as the expected value of two random variables, equation (5-22) can be written as follows:

$$R_{x,y}(t) = R_{x,y}(t)_p + R_{x,y}(t)_i, \tag{5-23}$$

where

$$R_{x,y}(t)_p = P_{x,y}(t)W^*_{x,y}(t)\{1+\mathrm{cov}[P_t(x,y),W^*_t(x,y)]\}, \tag{5-24}$$

and

$$R_{x,y}(t)_i = P_{x,y}(t)f\{1+\mathrm{cov}[P_t(x,y),I_t(x,y)]\}. \tag{5-25}$$

Also notice that, in the determination of equations (5-24) and (5-25), $E[P_t(x,y)]$, $E[W_t(x,y)]$, and $E[I_t(x,y)]$ are each equal to 1. Equations (5-24) and (5-25) are the time series of rainfall excess due to the pervious and impervious areas of the watershed,

respectively. However the rainfall excess is expressed this time in terms of the different variations and including the imperviousness pattern, $I_t(x,y)$.

The illustration of equations (5-24) and (5-25) is shown in Figure 5-2. In Figure 5-2 the rainfall excess due to pervious areas is larger than that due to impervious areas. Also, the value of $W^*_{x,y}(t)$ remains nearly constant in Figure 5-2, indicating the time variations in $R_{x,y}(t)$ for pervious areas are due to the time variation in rainfall, as it was found that $cov[P_t(x,y), W^*_{x,y}(t)]$ is small, approximately -0.01. However it was also observed that $cov[P_t(x,y),I_t(x,y)]$ is equal to -0.08. This value is of a similar magnitude, as a reference, to the areal reduction amount indicated by TP-40 for a 12 hour storm over an 180 km^2 watershed [*NWS*, 1961]. The comparison of the magnitude of $cov[P_t(x,y),I_t(x,y)]$ with the areal reduction amount indicated by TP-40 suggests that the interaction between the rainfall and imperviousness pattern can have an important effect on the estimation of rainfall excess. The effect of $cov[P_t(x,y),I_t(x,y)]$ on the generated runoff from impervious areas is explored further in Section 5-5.

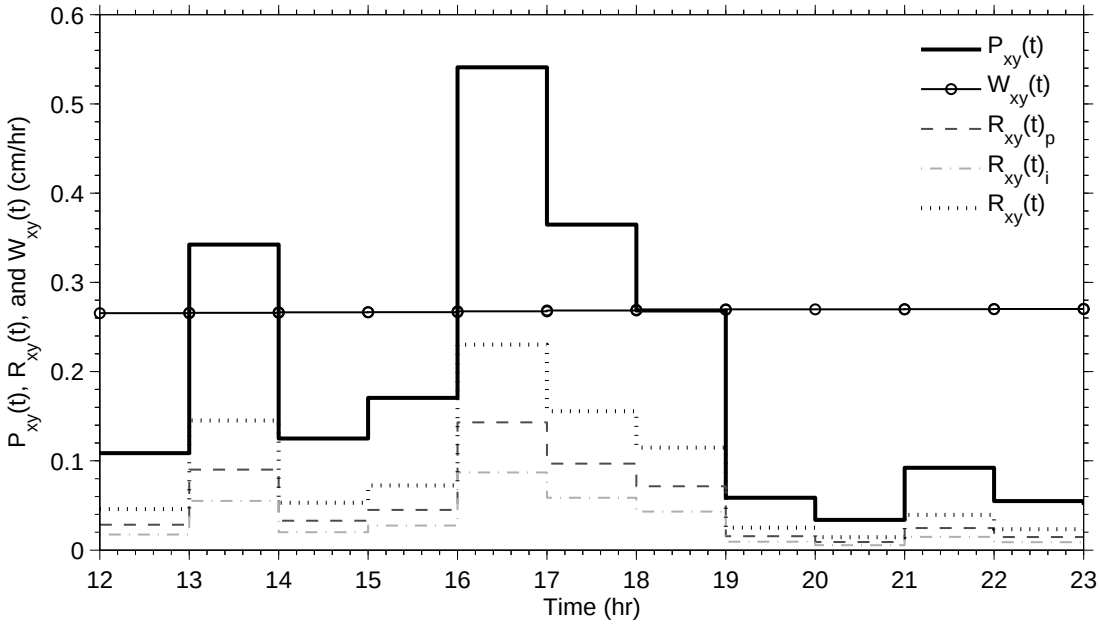

Figure 5-2. Illustration of the instantaneous rainfall excess, $R_{xy}(t)$, and the separated pervious, $R_{xy}(t)_p$, and impervious series, $R_{xy}(t)_i$. The runoff generation function, $W^*_{x,y}(t)$, and rainfall series, $P_{xy}(t)$, are also shown.

5.4.2 Storm-Averaged Watershed Rainfall Excess

The storm-averaged watershed rainfall excess is estimated from the time series of rainfall excess, equations (5-24) and (5-25), by integrating the rainfall excess over the storm duration as follows [*Woods and Sivapalan*, 1999]:

$$R_{x,y,t} = \frac{1}{T_s}\int_o^{T_s} R_{x,y}(t)dt, \tag{5-26}$$

for pervious and impervious areas equations (5-24) and (5-25), respectively, are substituted into (5-26), yielding the following expression:

$$R_{x,y,t} = \frac{1}{T_s}\int_o^{T_s} P_{x,y}(t)W^*_{x,y}(t)\{1+\text{cov}[P_t(x,y),W^*_t(x,y)]\}dt + \frac{1}{T_s}\int_o^{T_s} P_{x,y}(t)I_{x,y}(t)\{1+\text{cov}[P_t(x,y),I_t(x,y)]\}dt. \quad (5\text{-}27)$$

The time independent terms can be taken out of the integrals in (5-27). The terms $T_s^{-1}\int_o^{T_s} P_{x,y}(t)W^*_{x,y}(t)dt$ and $T_s^{-1}\int_o^{T_s} P_{x,y}(t)I_{x,y}(t)dt$ can both be interpreted as the expected value of two random variables, and using the relation between the covariance and the expected value of two random variables, the expression in (5-27) can be written now as:

$$R_{x,y,t} = (R_{x,y,t})_p + (R_{x,y,t})_i, \quad (5\text{-}28)$$

where

$$(R_{x,y,t})_p = \{1+\text{cov}[P_t(x,y),W^*_t(x,y)]\}\{P_{x,y,t}W^*_{x,y,t} + \text{cov}[P_{x,y}(t),W^*_{x,y}(t)]\}, \quad (5\text{-}29)$$

and

$$(R_{x,y,t})_i = \{1+\text{cov}[P_t(x,y),I_t(x,y)]\}P_{x,y,t}f. \quad (5\text{-}30)$$

Equations (5-29) and (5-30) are the averaged runoff generated from pervious and impervious areas, respectively, in units of length over time.

The estimated value of the terms in (5-29) and (5-30) for the main watershed in NW Branch are included in Table 5-1. The storm-averaged watershed rainfall excess for the pervious areas is approximately equal to 0.058 cm/hr and for the impervious areas 0.032 cm/hr, which was expected since the rainfall excess from pervious areas was larger than from impervious areas as illustrated in Figure 5-2.

Table 5-1. Estimates of the terms in equations (5-29) and (5-30) for the main watershed.

Terms in equations (5-29) and (5-30)	Value
$P_{x,y,t}$ (cm/hr)	0.201
$W^*_{x,y,t}$	0.293
$P_{x,y,t}W^*_{x,y,t}$ (cm/hr)	0.0588
$P_{x,y,t}f$ (cm/hr)	0.0351
$\mathrm{cov}[P_t(x,y),W^*_t(x,y)]$	-0.0102
$\mathrm{cov}[P_{x,y}(t),W^*_{x,y}(t)]$ (cm/hr)	$-1.15\text{x}10^{-4}$
$\mathrm{cov}[P_t(x,y),I_t(x,y)]$	-0.0771
$(R_{x,y,t})_p$ (cm/hr)	0.0583
$(R_{x,y,t})_i$ (cm/hr)	0.0324

5.4.3 Instantaneous Ratio of Rainfall Excess

A common way of quantifying the impacts from urbanization on watershed hydrology is to compare the value of a hydrologic variable after imperviousness to the value of the variable before imperviousness [*Carter*, 1961; *Anderson*, 1970]. This method of quantifying impacts is used for the next two relationships. The relationships are determined by dividing equations (5-23) and (5-28) by the equivalent relationship for fully pervious conditions where *I(x,y)* is zero for all *x,y* cells. The determination of the relationships for fully pervious conditions is similar to the way equations (5-23) and (5-28) were obtained, therefore a detail derivation of these is not shown.

For the instantaneous ratio of rainfall excess, one can start with the following expression:

$$r(x,y,t) = \frac{P(x,y,t)W^*(x,y,t) + P(x,y,t)I(x,y)}{P(x,y,t)W(x,y,t)}. \quad (5\text{-}31)$$

In equation (5-31), *W(x,y,t)* is the runoff generation function assuming every cell is fully pervious, therefore the denominator in (5-31) is the runoff that would be expected if the imperviousness were not in the watershed. After some manipulations one can obtain the following expression for the ratio of rainfall excess:

$$r_{x,y}(t) = r_{x,y}(t)_p + r_{x,y}(t)_i, \quad (5\text{-}32)$$

where

$$r_{x,y}(t)_p = \frac{W^*_{x,y}(t)\{1 - \mathrm{cov}[P_t(x,y), W^*_t(x,y)]\}}{W_{x,y}(t)\{1 + \mathrm{cov}[P_t(x,y), W_t(x,y)]\}}, \quad (5\text{-}33)$$

and

$$r_{x,y}(t)_i = \frac{f\{1 - \mathrm{cov}[P_t(x,y), I_t(x,y)]\}}{W_{x,y}(t)\{1 + \mathrm{cov}[P_t(x,y), W_t(x,y)]\}}. \quad (5\text{-}34)$$

$W_{x,y}(t)$ and $W_t(x,y)$ are the equivalent of equations (5-8) and (5-9), respectively, but they are now determined assuming a fully pervious watershed. The numerators in (5-33) and (5-34) are equal to $R_{x,y}(t)_p$ and $R_{x,y}(t)_i$, respectively. The denominators in both (5-33) and (5-34) are the same and equal to $R_{x,y}(t)_{fp}$. The subscript *fp* indicates the value is for fully pervious conditions where imperviousness is 0 everywhere in the watershed.

The estimation of equations (5-33) and (5-34) is shown in Figure 5-3. The rainfall excess series for fully pervious conditions decreases overall by approximately 25% when compared to the mixed pervious-impervious series. The ratio of rainfall excess decreases slightly for both pervious and impervious conditions. This is likely the case here because the pervious portions of the watershed are contributing the most runoff and only a small amount of saturated areas are formed during the storm event. However

it is still possible for the change between mixed pervious-impervious and fully pervious conditions to vary with time. This change is often assumed constant during the storm. This suggests that when the ratio is assumed constant it only represents an average condition.

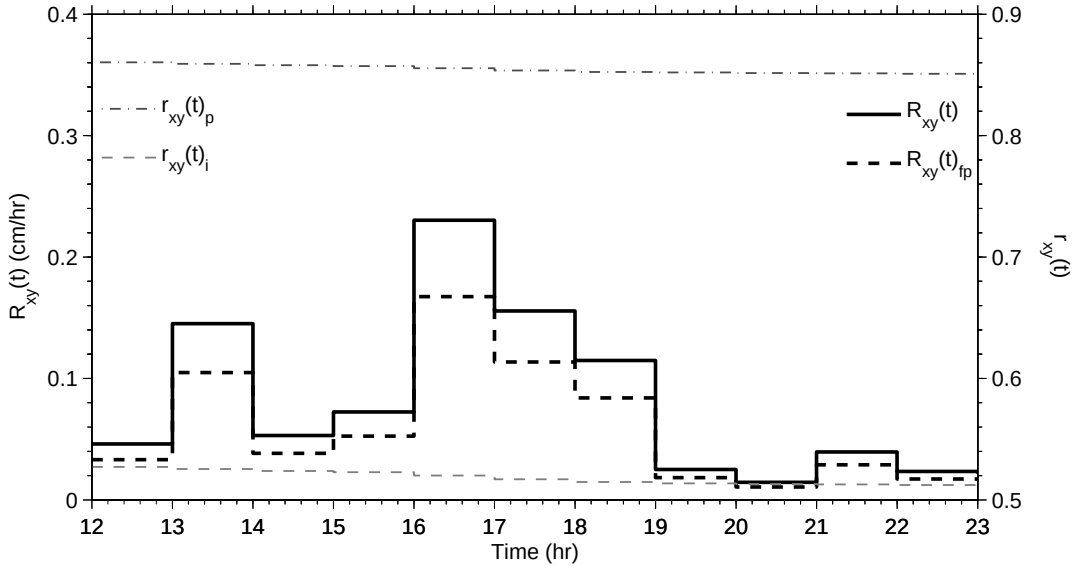

Figure 5-3. Illustration of the instantaneous ratio of rainfall excess for pervious, $r_{x,y}(t)_p$, and impervious areas, $r_{x,y}(t)_i$. The rainfall excess series for the pervious-impervious, $R_{x,y}(t)$, and the fully pervious land use condition, $R_{x,y}(t)_{fp}$, are also shown.

5.4.4 Storm-Averaged Ratio of Watershed Rainfall Excess

The ratio of rainfall excess between the mixed pervious-impervious and fully pervious conditions can be used to determine the ratio of storm-averaged rainfall excess

similar to the way equations (5-29) and (5-30) were obtained. One can start from the following expression:

$$r_{x,y,t} = \frac{T_s^{-1}\int_o^{T_s} R_{x,y}(t)dt}{T_s^{-1}\int_o^{T_s} R_{x,y}(t)_{fp}\,dt}, \tag{5-35}$$

where $R_{x,y}(t)_{fp}$ is for a fully pervious watershed and $R_{x,y}(t)$ is for the mixed pervious-impervious land use condition. After substituting for the terms in the integrals and some manipulations, the following relation is obtained:

$$r_{x,y,t} = (r_{x,y,t})_p + (r_{x,y,t})_i, \tag{5-36}$$

where

$$(r_{x,y,t})_p = \frac{\{1+\mathrm{cov}[P_t(x,y),W_t^*(x,y)]\}\{P_{x,y,t}W_{x,y,t}^* + \mathrm{cov}[P_{x,y}(t),W_{x,y}^*(t)]\}}{\{P_{x,y,t}W_{x,y,t} + \mathrm{cov}[P_{x,y}(t),W_{x,y}(t)]\}\{[1+\mathrm{cov}[P_t(x,y),W_t(x,y)]\}}, \tag{5-37}$$

and

$$(r_{x,y,t})_i = \frac{\{1+\mathrm{cov}[P_t(x,y),I_t(x,y)]\}\{P_{x,y,t}f\}}{\{P_{x,y,t}W_{x,y,t} + \mathrm{cov}[P_{x,y}(t),W_{x,y}(t)]\}\{[1+\mathrm{cov}[P_t(x,y),W_t(x,y)]\}}. \tag{5-38}$$

The numerators in (5-37) and (5-38) are equal to $(R_{x,y,t})_p$ and $(R_{x,y,t})_i$, respectively. The denominators are the storm-averaged value when the watershed is fully pervious and the value is the same for (5-37) and (5-38).

The estimate for the new terms in equations (5-37) and (5-38) is included in Table 5-2, the other terms were included in Table 5-1. In Table 5-2, the value of r_{xyt} for the pervious areas is 0.855 instead of 1, because for the fully pervious condition some of the cells that had a fraction of impervious cover in the mixed land use condition are now fully saturated. This suggests that when impervious cover is located in areas prone to soil saturation, the generated runoff can remain approximately the same for fully pervious or

mixed land use conditions. This can also indicate locations where runoff from imperviousness might be mitigated. For example, *Naef et al.* [2002] used similar information, together with field observations, to map different runoff mechanisms and showed how these can help manage land use changes. The sum of $(r_{x,y,t})_p$ and $(r_{x,y,t})_i$ is equal to 1.33, accounting for the impervious cells in the soil saturated areas indicates that 36% of 1.33 is due to the impervious cover. The estimate is slightly larger than the 33% that would likely be assumed if saturation excess were not considered.

Table 5-2. Estimates of the terms in equations (5-37) and (5-38) for the overall watershed.

Terms in equations (5-37) and (5-38)	Value
$W_{x,y,t}$	0.341
$P_{xyt}W_{xyt}$ (cm/hr)	0.0684
$\mathrm{cov}[P_{x,y}(t), W^*_{x,y}(t)]$ (cm/hr)	-2.04×10^{-4}
$\mathrm{cov}[P_t(x,y), I_t(x,y)]$	-0.0771
$(r_{x,y,t})_p$	0.855
$(r_{x,y,t})_i$	0.476

5.5 Mean and Variance of the Runoff Time

To estimate the mean and variance of the runoff time, it is assumed that the runoff time can be separated into two successive stages, each characterized by a holding time and a independent random variable. The same holding time assumption was made by *Rodríguez-Iturbe and Valdés* [1979] and *Woods and Sivapalan* [1999]. The first stage is the time it takes for runoff to be produced, including the waiting time for rain to fall, and

the second stage is the combined hillslope and channel routing times or the time for runoff to reach the outlet after its generation. The total time for water to reach the outlet, T_o, is expressed as:

$$T_o = T_r + T_b, \tag{5-39}$$

T_r is the holding time for rainfall excess and T_b for the hillslope and channel routing. Since the times in equation (5-39) are assumed independent random variables, the mean and variance of T_o are equal to the sum of the mean and variance of the individual terms. Thus, to determine the mean runoff time one can take the expectation of the terms in equation (5-39):

$$E[T_o] = E[T_r] + E[T_b], \tag{5-40}$$

the term $E[T_b]$ is estimated using equations (5-16) and (5-17), and $E[T_r]$ needs to be determined. To determine $E[T_r]$ one can assume the distribution of T_r, f_{T_r}, is defined as follows [*Woods and Sivapalan*, 1999]:

$$f_{T_r}(t) = \frac{R_{x,y}(t)}{\int_o^{T_s} R_{x,y}(t)dt}, \tag{5-41}$$

such that

$$E[T_r] = \int_0^{T_s} t f_{T_r}(t)dt. \tag{5-42}$$

After equations (5-23), (5-24), and (5-25) are substituted into (5-41) and some manipulations are performed, one can obtain the following result:

$$E[T_r] = E[T_r]_p + E[T_r]_i, \tag{5-43}$$

where

$$E[T_r]_p = \{1 + \mathrm{cov}[P_t(x,y), W_t^*(x,y)]\} \times \frac{\{E[T]E[P_{x,y}(T)W_{x,y}^*(T)] + \mathrm{cov}[T, P_{x,y}(T)W_{x,y}^*(T)]\}}{R_{x,y,t}}, \quad (5\text{-}44)$$

and

$$E[T_r]_i = \{1 + \mathrm{cov}[P_t(x,y), I_t(x,y)]\} \times \frac{\{E[T]E[P_{x,y}(T)f] + \mathrm{cov}[T, P_{x,y}(T)f]\}}{R_{x,y,t}}. \quad (5\text{-}45)$$

The terms in (5-44) and (5-45) were defined earlier with the exception of the random variable *T*. It is assumed that *T* is the time during the storm and to be uniformly distributed between 0 and the total duration of the storm, T_s, [*Woods and Sivapalan*, 1999]. Thus, in this case *E[T]* is 5.5 hours since the storms lasts a total of 11 hours.

Similarly for the variance of the runoff time, assuming T_r and T_b to be independent, one can express the variance as follows:

$$Var(T_o) = Var(T_r) + Var(T_b), \quad (5\text{-}46)$$

where $Var(T_b)$ can be estimated using (5-18) and (5-19), and $Var(T_r)$ needs to be determined. To determine $Var(T_r)$ one can use the relation between the variance of a random variable and its expected value,

$$Var(T_r) = E[T_r^2] - E[T_r]^2, \quad (5\text{-}47)$$

together with (5-44) and (5-45). The second term in (5-47), $E[T_r]^2$, is obtained by taking the square of (5-43). The term $E[T_r^2]$ is obtained by substituting t^2 into (5-42). After performing some additional substitutions and manipulations, one can obtain the following expressions for $E[T_r^2]$:

$$E[T_r^2]_p = \{1 + \mathrm{cov}[P_t(x,y), W_t^*(x,y)]\} \times \frac{\{E[T^2]E[P_{x,y}(T)W_{x,y}^*(T)] + \mathrm{cov}[T^2, P_{x,y}(T)W_{x,t}^*(T)]\}}{R_{x,y,t}}, \quad (5\text{-}48)$$

$$E[T_r^2]_i = \{1 + \mathrm{cov}[P_t(x,y), I_t(x,y)]\} \times \frac{\{E[T^2]E[P_{x,y}(T)f] + \mathrm{cov}[T^2, P_{x,y}(T)f]\}}{R_{x,y,t}}, \quad (5\text{-}49)$$

Ultimately, $Var(T_r)$ is estimated by substituting equations (5-44), (5-45), (5-48), and (5-49) into the following relation, which is another way of expressing (5-47):

$$Var(T_r) = \{E[T_r^2]_p + E[T_r]_p^2\} + \{E[T_r^2]_i + E[T_r]_i^2\} + 2E[T_r]_p E[T_r]_i. \quad (5\text{-}50)$$

In order to separate $Var(T_r)$ into pervious and impervious contributions one can use:

$$Var(T_r)_p = \{E[T_r^2]_p + E[T_r]_p^2\} + E[T_r]_p E[T_r]_i, \quad (5\text{-}51)$$

and

$$Var(T_r)_i = \{E[T_r^2]_i + E[T_r]_i^2\} + E[T_r]_p E[T_r]_i, \quad (5\text{-}52)$$

where $Var(T_r) = Var(T_r)_p + Var(T_r)_i$. Equations (5-51) and (5-52) are useful because they can quantify the relative contributions from pervious and impervious areas. R_{xyt} and the variance can be used together as a measure of peakedness, where a large R_{xyt} and a small variance would indicate a larger peakedness. Also, the mean runoff time, equation (5-40), is comparable to a time of concentration, so separating the mean time into pervious and impervious contributions provides a measure of their relative impacts on the time of concentration.

Figure 5-4a illustrates the estimation of $E[T_r]$ and $E[T_b]$ for both pervious and impervious areas for a range of watershed sizes. The figure shows that pervious areas have a larger mean runoff time than impervious areas and therefore contribute the most to

the total mean runoff time. This also indicates that runoff from impervious areas takes less time to reach the outlet. Figure 5-4a can also help identify the importance of different processes in the runoff time. It shows for the pervious areas how the influence of runoff generation on the mean travel time and variance decreases as the watershed size increases while the routing time becomes more dominant. This ability to distinguish between the contribution of different processes and between pervious and impervious areas is precisely the goal behind the proposed method. For example, in this case, for watershed sizes greater than approximately 64 km^2, $E[T_b]_p$ becomes more dominant than $E[T_r]_p$. This suggests that in watersheds greater than 64 km^2 for the selected storm event the routing process becomes a more dominant process. Similarly, in Figure 5-4b, the variance of travel times from pervious areas, $var(T_r)_p$ and $var(T_b)_p$, contribute the most and the importance of processes can vary across the different watershed sizes.

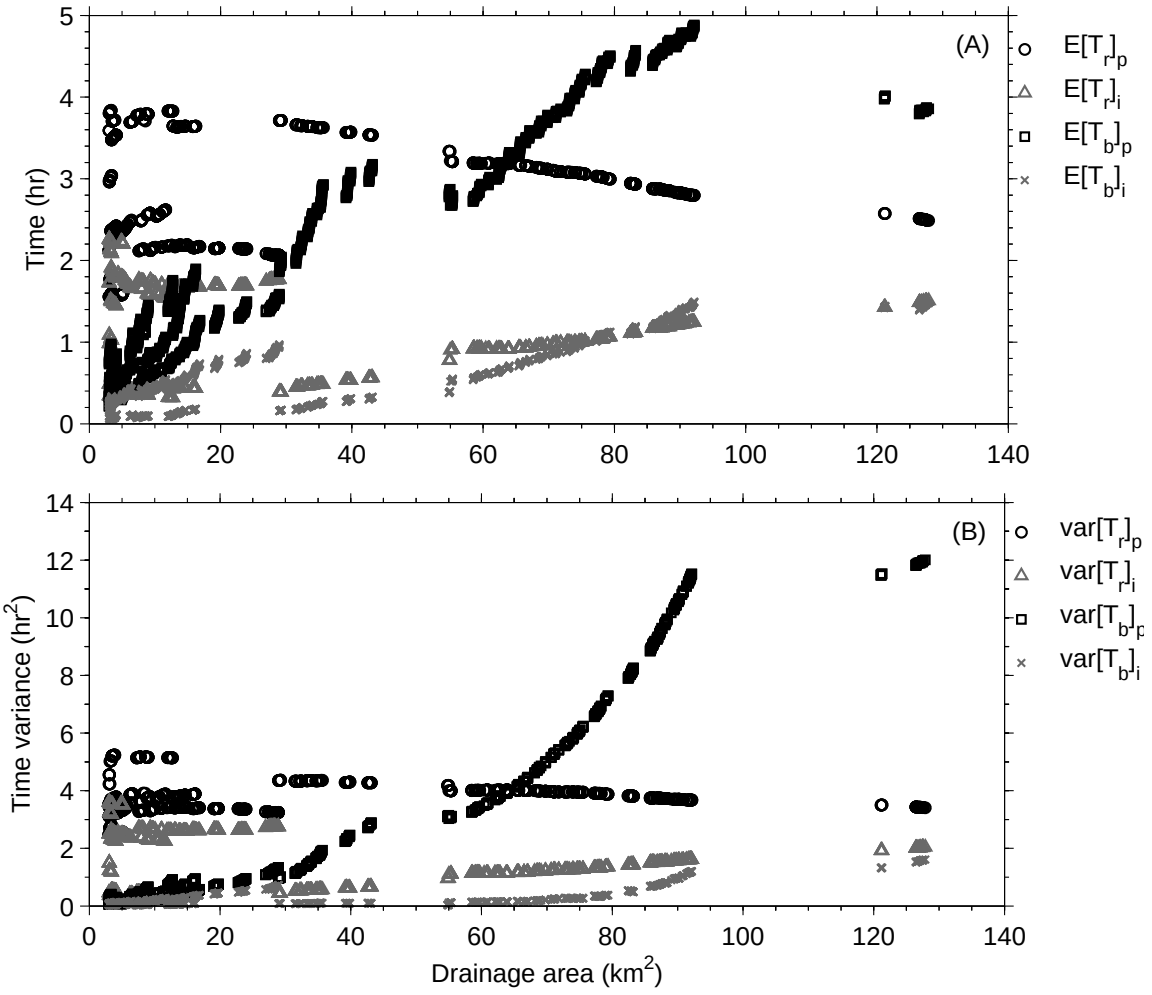

Figure 5-4. Estimation of the mean runoff time and variance for a range of watershed sizes. (a) Mean runoff time for the holding time of the rainfall excess, $E[T_r]$, and routing travel time, $E[T_b]$. (b) Variance of the runoff time induced by the rainfall excess, $Var(T_r)$, and routing, $Var(T_b)$. The estimates of the mean and variance of the runoff time are separated into pervious and impervious contributions.

5.6 Application of Space-Time Relationships for Pervious and Impervious Areas

The relationships obtained in Sections 5-4 and 5-5 can be used to examine the impacts from different rainfall and imperviousness scenarios in a straightforward manner because of their analytical nature and their explicit consideration of the rainfall and imperviousness pattern. In particular, the relationships are used to investigate two scenarios. First, the relation between the rainfall pattern and imperviousness is investigated. Then, different imperviousness scenarios are used to study how these might affect runoff and routing processes. The scenarios are determined based on the results obtained in Chapter 3.

5.6.1 Imperviousness and the Space-Time Rainfall Pattern

Since the spatial pattern of rainfall is an important source of space-time variability in urbanized watersheds [*Segond et al.*, 2007], it is important to understand its effects on the proposed relationships. For this comparison three different patterns of rainfall were selected. One of the patterns used is the observed pattern shown in Figure 5-1a which is referred to as the actual pattern. The actual pattern has the salient characteristic that most of the rainfall falls on the upstream portion of the watershed which is also the most pervious section. The pattern in Figure 5-1a was then inverted to have most of the rain fall on the downstream portion of the watershed where imperviousness is concentrated, this pattern is referred to as inverted pattern. The inversion was simply done by flipping the actual data along the horizontal and vertical axis passing through the geometric centroid of the watershed. The third pattern was assumed to be constant in space and this

pattern is referred to as uniform. The uniform pattern was set equal to the areal average of the actual spatial rainfall pattern.

The three rainfall patterns examined indicated that the spatial covariance terms can vary with watershed size and with the form of the spatial rainfall pattern. For example, the term $cov[P_t(x,y),I_t(x,y)]$ was found to vary considerably as a function of watershed scale. The changes in $cov[P_t(x,y),I_t(x,y)]$ are illustrated in Figure 5-5. In Figure 5a the actual rainfall pattern produces a $cov[P_t(x,y),I_t(x,y)]$ that changes with watershed size and can reach a minimum value of approximately -0.08. Figure 5b shows that when the rainfall is inverted, the $cov[P_t(x,y),I_t(x,y)]$ varies with watershed size and has instead a positive value, the largest value being approximately 0.05. The importance of these magnitudes can be understood by their role in equation (5-25). In essence, the values of -0.08 and 0.05 mean the runoff from impervious areas is decreased by 8% or increased by 5% depending on whether the space pattern of rain coincides with the imperviousness pattern. Obviously when rain is assumed uniform this covariance becomes essentially 0. The term $cov[P_t(x,y), W_t^*(x,y)]$ was found to be negligible for the rainfall patterns examined and across the entire range of watershed sizes within the NW Branch. This means the rainfall and runoff generation pattern are not acting together in this case to increase or decrease the amount of rainfall excess. A similar finding was reported by *Woods and Sivapalan* [1999] for a non-urbanized watershed.

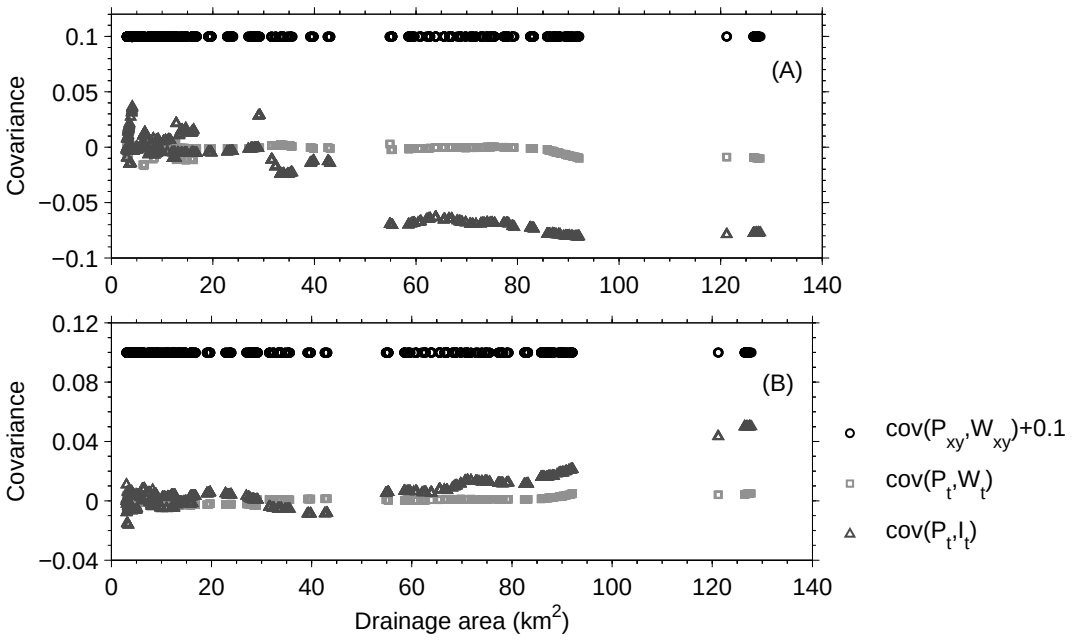

Figure 5-5. Illustration of the values of $cov[P_{x,y}(t), W^{*}_{x,y}(t)]$, $cov[P_t(x,y), W^{*}_{t}(x,y)]$, and $cov[P_t(x,y), I_t(x,y)]$ for a range of watershed sizes, and (a) the actual rainfall and (b) inverted pattern. The values of $cov[P_t(x,y), W^{*}_{t}(x,y)]$ have been offset by 0.1 for clarity.

5.6.2 Imperviousness Scenarios

The imperviousness pattern was varied to examine its effect on the relationships in Sections 5-4 and 5-5. To obtain different imperviousness patterns the approach developed in Chapter 3 was used. The approach allows the simulation of distinct imperviousness scenarios. These scenarios are illustrated in Figure 5-6 and they represent extreme ways of organizing imperviousness within the watershed. The patterns in Figure 5-6a, b, c, and d are referred to as current, channel clustering, source clustering, and uniform pattern, respectively. The current pattern represents actual land use

conditions. In the channel clustering pattern, imperviousness is organized along the main channel and this tends to reduce peak flows along the entire stream network as shown in Chapter 3. The source clustering pattern clusters development around source streams which tends to increase peak flows along the entire network. This was also shown in Chapter 3. The uniform pattern can be interpreted as an extreme case of sprawl where development is uniformly distributed across the overall watershed area. These simulated patterns mimic some of the regularities observed in impervious cover within urbanized watersheds in the United States [*Poff et al.*, 2006]. *Poff et al.* [2006] found, for example, that in the southwest States of the U.S. urbanization tends to be more prevalent on the valley floors and floodplains, while in the southeast urbanization is more common on headwater watersheds and around low order streams.

An important effect of the imperviousness scenarios examined was to change the magnitude and sign of $cov[P_t(x,y),I_t(x,y)]$ across watershed sizes, suggesting a dependence between the form of the imperviousness pattern and the spatial distribution of rainfall. These changes are illustrated in Figure 5-7. In Figure 5-7, the current scenario produced the largest changes in the magnitude of $cov[P_t(x,y),I_t(x,y)]$. The sign of $cov[P_t(x,y),I_t(x,y)]$ for the current and channel clustering scenarios tended to be negative for the larger watershed sizes while for the source clustering was positive. As expected, in the uniform scenario $cov[P_t(x,y),I_t(x,y)]$ is approximately 0 for all watershed sizes. Thus, the results in Figure 5-7 show how the importance of the rainfall space pattern can vary depending on the overall imperviousness pattern. This may be useful for deciding in suburban watersheds when spatially distributed rainfall is most needed for hydrologic modeling.

The relationships in Section 5-4 were also used to estimate the peakedness of the hydrograph. The peakedness in this case is expressed as the ratio of $R_{x,y,t}$ and $Var(T_o)$. A lower value of this ratio will indicate low peakedness and the opposite for a higher value because a lower value of $R_{x,y,t}$, the storm runoff, and a larger variance, as a surrogate for the hydrograph duration, would suggest a wider and flatter hydrograph shape. Figure 5-8 shows the peakedness estimates for the 4 imperviousness scenarios in Figure 5-6. The peakedness in Figure 5-8 was separated into pervious and impervious contributions as a way to quantify the relative importance of the mixed land use conditions on the hydrologic response. The separation was done by using $(R_{x,y,t})_p$, equation (5-29), and $(R_{x,y,t})_i$, equation (5-30), divided by the total variance, $Var(T_o)$. The total peakedness, i.e. the sum of the pervious and impervious peakedness, is also plotted in Figure 5-8. In Figure 5-8, the main difference in the peakedness of the scenarios across the range of watershed sizes considered appears to be the magnitude of the peakedness. For example, the source clustering scenario, Figure 5-8c, tends to have higher total peakedness than the channel clustering scenario, Figure 5-8b. This observation is more accentuated for the smaller watershed sizes. Also notice the pervious areas contribute the most to the peakedness across the range of watershed sizes and for all 4 patterns. Normally in urbanized watersheds peak flows are understood as being dominated by the urban runoff [*Andrieu and Chocat*, 2004], but in the mixed pervious-impervious land use conditions of suburban watersheds this might not be the case. This result agrees with findings from Chapter 4. However, here the dominance of pervious areas over impervious ones is more apparent across the range of watershed scales considered.

If the peakedness is instead estimated relative to the pervious and impervious values of both $R_{x,y,t}$ and $Var(T_o)$, $(R_{x,y,t})_p/Var(T_o)_p$ or $(R_{x,y,t})_i/Var(T_o)_i$, other distinctions between the peakedness of the scenarios emerge. These distinctions are illustrated in Figure 5-9. The main distinction to notice is that now the pervious and impervious contribution for the uniform and source clustering scenarios seem to be equally strong, but in the current and channel clustering scenarios the peakedness from impervious areas is more dominant despite the fact that over the entire watershed the pervious areas are contributing 44% more storm runoff than impervious areas. Interestingly, also recall that the current scenario had lower total peakedness in Figure 5-8, but now the peakedness due to imperviousness, as shown in Figure 5-9, is clearly larger than the pervious one. The reason for the dominance of the imperviousness peakedness for the current and channel clustering scenarios in Figure 5-9 is because these scenarios place imperviousness in locations that are, in this case, prone to soil saturation near the stream channels. This seems to cause a switching of runoff production to impervious areas rather than pervious ones, which has the beneficial consequence of limiting the total amount of runoff but at the same time can cause imperviousness to play a larger role on hydrograph variability. The increased role of imperviousness on the peakedness and the proximity to the stream channels can indicate larger disturbances to the flow regime, or greater efficiency in transporting pollutants [*Zhu et al.*, 2008]. Thus the estimated peakedness can be used to distinguish some of the impacts from imperviousness on streamflows that could be difficult to quantify otherwise.

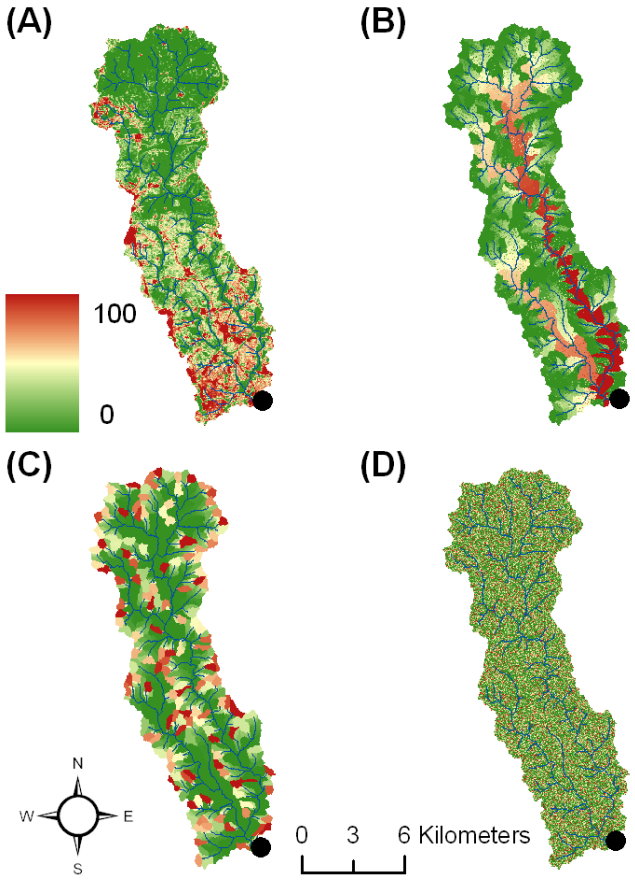

Figure 5-6. Imperviousness scenarios: (a) actual, (b) channel clustering, (c) source clustering, and (d) uniform pattern.

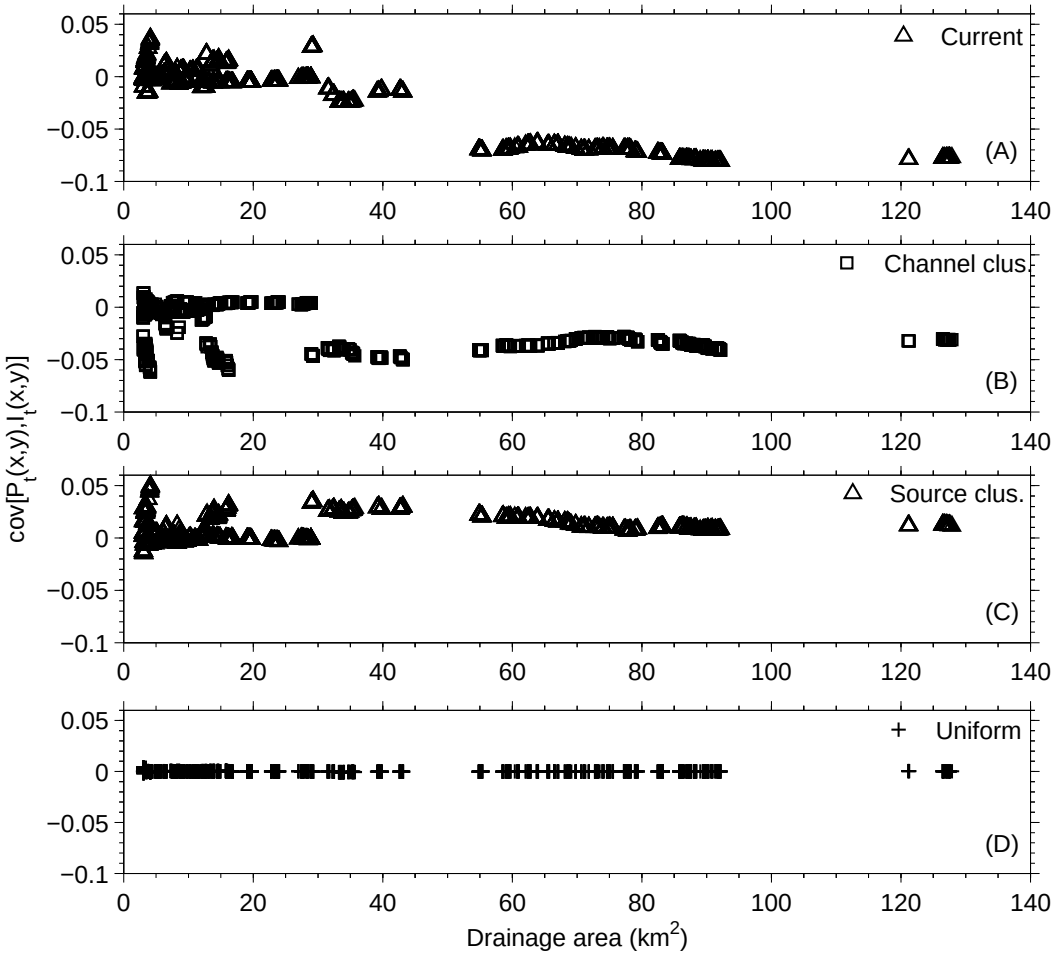

Figure 5-7. Illustration of the changes in $cov[P_t(x,y),I_t(x,y)]$ for a range of watershed sizes, and the (a) actual, (b) channel clustering, (c) source clustering, and (d) uniform imperviousness scenario.

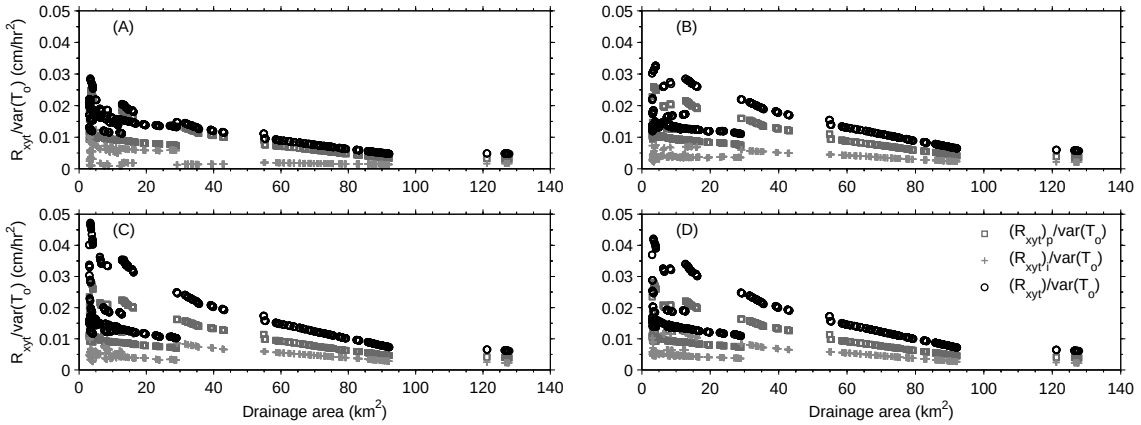

Figure 5-8. Peakedness for the (a) actual, (b) channel clustering, (c) source clustering, and (d) uniform imperviousness scenarios. The total peakedness was determined as the ratio of $R_{x,y,t}$ to the total $Var(T_o)$. The pervious and impervious contributions were estimated using $(R_{x,y,t})_p/Var(T_o)$ and $(R_{x,y,t})_i/Var(T_o)$, respectively.

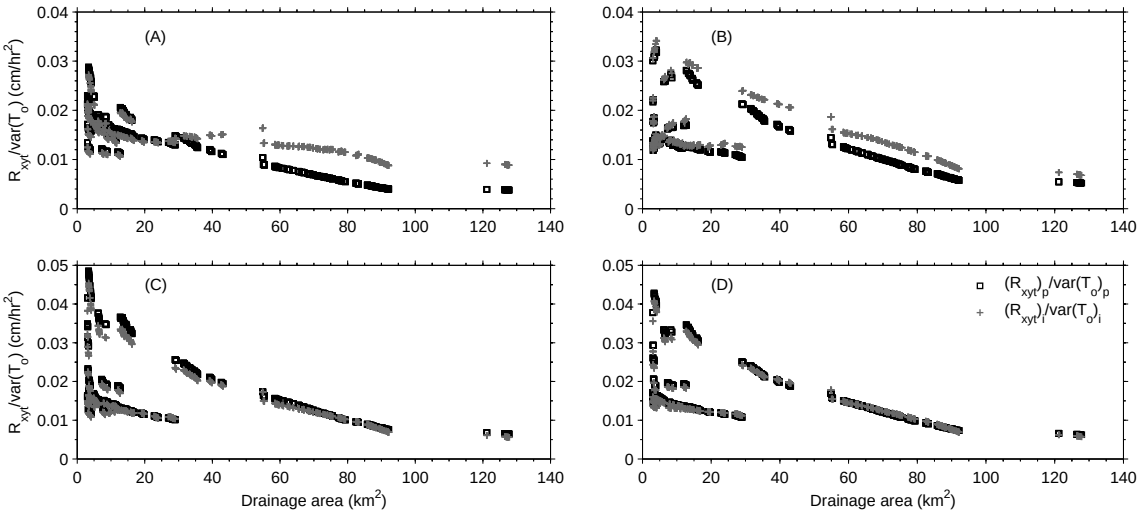

Figure 5-9. Peakedness for the (a) actual, (b) channel clustering, (c) source clustering, and (d) uniform imperviousness scenarios. The peakedness of pervious and impervious contributions were estimated using $(R_{x,y,t})_p/Var(T_o)_p$ and $(R_{x,y,t})_i/Var(T_o)_i$, respectively.

5.7 Conclusions

An analytical method was proposed that relates the spatial distribution of imperviousness in a suburban watershed to the space-time variability of rainfall, runoff generation, and routing. The objective was to separate the pervious and impervious contributions to the different processes and at the same time account for the various space-time variability. The method built on an earlier theoretical framework proposed by *Woods and Sivapalan* [1999]. The separation into pervious and impervious contributions was achieved by accounting explicitly for the location of pervious and impervious areas within the watershed. The method was used to obtain various hydrologic relationships and the estimation of the relationships was illustrated with data and conditions for a suburban watershed in the Maryland Piedmont province. Furthermore, the method and derived relationships were used to investigate several scenarios with emphasis placed on the imperviousness pattern.

The application of the proposed method in the Maryland Piedmont province indicated the space pattern of runoff generation and rainfall have a negligible relation during wet conditions, when the runoff pattern from excess saturation is most prevalent. The relation between rainfall and the imperviousness pattern was found more important and it can vary depending on the spatial pattern of both rainfall and imperviousness. The relation was quantified using the spatial covariance between the rainfall and imperviousness pattern. This covariance suggested that when most of the rain falls on a highly urbanized section of the watershed the imperviousness becomes more important. The variance of the hydrologic response and the amount of runoff were used to quantify the pervious and impervious contributions to the peakedness of the hydrograph. This

analysis indicated that in suburban watersheds with mixed land use conditions the peakedness due to pervious areas can be greater than that of impervious areas for a range of watershed sizes. It also suggested that even if the amount of runoff from pervious areas is larger, the impervious contribution can have a larger impact than the pervious ones on the peakedness depending on the overall distribution of imperviousness and the relation chosen to quantify the peakedness.

The proposed method can be used as an assessment of the importance of various hydrologic processes and sources of space-time variation in a suburban watershed. This could be useful when deciding the level of model complexity or the model components needed to simulate the response of a suburban watershed. The method can also be useful to study how changing climatic or watershed conditions, e.g. rainfall or land use, may impact runoff or the hydrologic response. Because the method allows the determination of analytical relations in terms of the different space-time variations in rainfall, runoff, and routing, it can be implemented in a straightforward manner without the necessity of detailed modeling.

5.8 Summary

The analytical method proposed in this chapter complements the modeling effort performed in Chapter 4. It provides a way for studying and analyzing some of the hydrologic complexities characteristic of a suburban watershed. The next chapter outlines the main conclusions from the three methods proposed in this dissertation, and proposes some recommendations for future work.

CHAPTER 6 - CONCLUSIONS AND RECOMMENDATIONS

6.1 Overview

The research performed in this dissertation studied the relationship between the spatial distribution of imperviousness and watershed hydrology using three approaches. The first approach, which was described in Chapter 3, relied on an optimization technique and the minimization of peak flows along the stream network to explore where in the watershed to locate imperviousness. The second approach was presented in Chapter 4. This approach used spatially distributed hydrologic modeling concepts to study the impacts of the imperviousness pattern on the hydrologic response. The third approach proposed and developed an analytical framework to relate the imperviousness pattern to the space-time pattern of rainfall, runoff, and routing. This latter approach was discussed in Chapter 5. The main conclusions from these three approaches are outlined in the next section. Recommendations for future work based on the research performed are discussed in Section 6.3.

6.2 Conclusions

The main conclusions from the research performed in this dissertation are as follows:

6.2.1 Optimization Approach for Studying the Spatial Distribution of Imperviousness

- Distinct patterns of imperviousness were derived from the optimization of water resources objectives. Three objectives were tried, each representing a separate objective function. The objectives were (1) to reduce peak flows along the entire stream network, (2) to maintain increases in peak flows uniform throughout the watershed, and (3) to include the effects of an imperviousness threshold when minimizing peak flows. The imperviousness threshold was used to represent the concept of having a limiting value of total imperviousness in the watershed after which stream degradation becomes important. The patterns were derived to account for the nested structure of watersheds and their drainage network by making use of topographic data, i.e. Digital Elevation Models (DEMs), and spatial techniques for the analysis of watersheds. The nested structure of watersheds was considered because evidence suggests this structure is intimately related to the way watersheds function [*Rodríguez-Iturbe and Rinaldo*, 1997].
- The imperviousness patterns obtained represent predictable spatial forms. This is convenient and needed because an arbitrary form cannot be reproduced in a systematic manner. Normally patterns that are disconnected from any interpretation are generated in, at best, an ad hoc manner based on the analyst's sense of personal aesthetics. The development of a method to produce different imperviousness patterns facilitates the use of the patterns as future development scenarios in other applications and contexts, and provides a starting point in forming of a more general understanding about imperviousness at the watershed scale.

- The optimization approach offers a way of explaining how urbanization may be placed in the entire watershed to produce benefits to water resources, where the benefit in this case is the minimization of peak flows. Also, the proposed approach is useful because the spatial distribution of imperviousness has been studied little at the watershed scale despite the fact that its importance as a predictor of many environmental impacts at the watershed scale has increased.
- The optimization approach was also used to study the impact of imperviousness threshold-based policies on the spatial distribution of imperviousness. The imperviousness threshold-based policies recommend a 10% total imperviousness limit after which stream degradation becomes significant [*Schueler*, 1994]. The approach showed that imperviousness threshold-based policies can have unintended consequences [*Mejía and Moglen*, 2009]. For example, they can promote sprawl-type development in some areas of the watershed as long as these areas do not surpass the threshold. This is important because threshold-based policies may be promoted without recognition of this potential consequence.

6.2.2 Hydrologic Response under Spatially Distributed Imperviousness

- The main contribution from the development and application of a simple event-based model to existing suburban watershed conditions was to demonstrate that the spatial distribution of imperviousness can have an important effect on the hydrologic response at the watershed scale. This demonstration was done under conditions of spatially distributed rainfall and runoff generation processes, i.e. infiltration and saturation excess, which are conditions not typically included when studying impacts

from urbanization. Effort was made to account for the variability associated with parameters and the initial condition of the model when comparing different land use scenarios. It is useful to account for this variability or uncertainty because it can support greater understanding of the importance of the change induced on the response by the different scenarios. The common approach is to assume instead that the change produced by the scenarios is completely due to the land use, where in reality part of the simulated change could be attributed to imperfections in the model.

- The application of the event-based model also demonstrated the increasing importance of channel flows in suburban watersheds. This is relevant because hillslopes have a slow response relative to the channels, and because hillslopes can ultimately have an equal or larger effect on the hydrologic response than channels [*Saco and Kumar*, 2004]. The process of a slow hillslope response having an important contribution to the overall watershed response appears to be highly disrupted by urbanization, an issue that has receive little attention. It points to the need for accurate and reliable field estimates of channel velocity to improve predictions in urbanized watersheds. Additionally, it suggests a need to understand the interactions between subsurface processes and imperviousness in urbanized hillslopes because subsurface processes can be an important source of hillslope runoff and can affect the overall response time.
- This research found that assuming rainfall to be spatially uniform (a common assumption) can lead to erroneous conclusions. For instance, it was found using rainfall radar data that the rainfall space-time variability can lead to the condition where more rain falls on the most pervious portion of the watershed than in the

impervious portion. This in turn can produce higher peak flows in sub-watersheds that have lesser imperviousness than sub-watersheds with the same drainage area and greater imperviousness. This can have the consequence of misrepresenting the magnitude and location of impacts, i.e. increases in peak flows, along the stream network which could influence the effectiveness of mitigation measures.

- The application of the event-based model indicated the widespread presence of saturation excess in the Maryland Piedmont province. The practical implications of this finding can be quite useful. It suggests previous modeling efforts developed for the Maryland Piedmont province have missed (at least conceptually if not in the actual modeling approach) the dominant processes that produce runoff. Assuming the improvement upon process representation is valued, this finding could provide some guidance to future modeling efforts.
- The application of the event-based model also highlighted the potential usefulness of certain simplifying assumptions about imperviousness and their relation to watershed hydrology. These assumptions include the treatment of impervious areas as extensions to the stream channel and the possibility of using digital topographic data, to estimate the drainage patterns of suburban areas. Additionally, the explicit incorporation of topography, land use, and soil data by the event-based model indicates the possibility of relaxing assumptions made about the way in which topography, soils, and land use relate to each other implied by more common approaches to land use change such as curve number-based methods. Thus, the event-based model provides a simple way to account for physical watershed heterogeneities without the need to average or aggregate these heterogeneities. The

averaging of these heterogeneities could potentially mask their effect as sources of variability on the hydrologic response.

- The application of the event-based model also demonstrated the usefulness of incorporating information about specific hydrologic processes (e.g. runoff generation processes) and theories about the hydrology of natural watersheds (i.e. the geomorphic instantaneous unit hydrograph and topographic index) to study urbanized watersheds. This is important because these methods are used widely for watersheds in natural conditions but their applicability to urbanized conditions is limited to relatively few studies.

6.2.3 Relating the Imperviousness Pattern to the Space-Time Variation in Rainfall, Runoff, and Routing

- A method was proposed and developed to represent the relation between the imperviousness pattern and the space-time pattern of rainfall, runoff, and routing. The development of the method involved the analytical expression of the space-time pattern of rainfall, runoff, and routing in order to account for the complex variability characteristic of hydrologic data and processes. The method aimed at capturing this complexity in simple relationships. The proposed method can synthesize a wealth of space and time data (i.e. DEMs, SSURGO soils, NEXRAD Stage-III precipitation, and NLCD land use data) and information that otherwise will remain disaggregated within the different components of a hydrologic model or disconnected from each other making the understanding of their inter-relations difficult. The method built on research previously performed by *Woods and Sivapalan* [1999].

The main difference with respect to the method proposed by *Woods and Sivapalan* [1999] is the consideration of imperviousness which changes the derivation of all of the relationships and makes the method more general. Also, new relationships were derived for the case of urbanized watersheds such as the instantaneous ratio of rainfall excess and the storm-averaged ratio of rainfall excess. In addition, the runoff generation and routing processes were defined differently than in *Woods and Sivapalan* [1999]. The runoff generation was defined to account for both infiltration and saturation excess. *Woods and Sivapalan* [1999] only accounted for saturation excess. The routing process in this case was defined using a GIUH that uses an IG distribution for the travel times and has path probabilities based on the runoff produced at every cell. *Woods and Sivapalan* [1999] used an unit hydrograph approach defined in terms of the area function and the distribution of flow distances.

- An advantage of this method is the separation of the variations (i.e. rainfall, runoff, and routing) in terms of pervious and impervious contributions which allows for the quantification of the relative importance of pervious and impervious areas to runoff generation and routing. This method can be highly useful to hydrologic modelers using spatial data sets that are interested in understanding which components of the rainfall, runoff, and routing processes are the most relevant in a suburban watershed. It can be useful to assess the importance or influence of different data sets, assumptions, and the role of watershed scale before more detailed modeling is performed. The approach can also be helpful in comparing various land use scenarios or examining different input conditions, as it provides a direct analytical framework for making such a comparison.

- The application of the approach to the NW Brach Anacostia River watershed in the Maryland Piedmont province, for the March 21, 2000, storm event, indicates there is little relation between the spatial pattern of rainfall and runoff. The main contribution to runoff variation was found to be, in this case, the time component of the rainfall field. However, the spatial relationship between rainfall and the imperviousness pattern was found to be important and to vary depending on how imperviousness is distributed. For instance, it was shown how the covariance between the imperviousness and rainfall pattern tends to increase when more rainfall falls on the most impervious areas of the watershed than the pervious ones, which means, within the proposed method, that rainfall excess will tend to be larger in this case than expected from assuming spatially uniform rainfall.

6.3 Recommendations for Future Research

Some recommendations for future research motivated by the work performed in this dissertation are as follows:

- The efficiency of the optimization algorithm used to derive the imperviousness patterns could be improved. For instance, a set of conditions could be defined to help direct the optimization search. The conditions could be specified based on the objective functions and results obtained in this research. The goal here is simply to speed up the optimization runs. While such an improvement would only decrease the computer time needed for the optimizations, it will not give rise to new or different scenarios.

- In order to obtain different scenarios, the optimization algorithm used could be coupled with an urban growth model. Some of the urban growth models available operate under a very simple set of rules that can be easily combined with the optimizations performed [*Claggett et al.*, 2005]. This could allow for the formulation of scenarios based on other conditions such as socio-economic or policy constraints. The competition between hydrologic and other conditions, e.g. socio-economic decisions, could be explored. This will only be useful, in terms of hydrology, for maximum annual floods of a given return period, unless a more comprehensive modeling scheme (e.g. a conceptual rainfall-runoff model) is implemented.

  A foreseeable difficulty with using an urban growth model and a more comprehensive hydrologic model are the need to calibrate both of these simultaneously. This will likely add additional complexity to the problem of parameter estimation and uncertainty in conceptual hydrologic modeling. Thus it seems beneficial to first assess the ability of the hydrologic model to adapt to changing land use or urban growth conditions before doing the coupling with the urban growth model.

- For the event-based hydrologic model a number of improvements could be proposed. One improvement that I consider valuable and interesting is the conceptualization and simulation of subsurface and groundwater contributions to the hydrologic response. I would recommend to first test a conceptualization for natural watershed conditions and, after a proper modeling structure has been achieved, to apply the model to urbanized conditions. A more useful test of model structure will likely necessitate a more complete data set. For example, the data set could include subsurface,

groundwater, and soil moisture data. These data sets could help the modeling effort by facilitating the direct evaluation of state variables in the model and of specific model components (e.g. a subsurface storage).

- The extension of the event-model to include subsurface processes could be done simultaneously at both the hillslope and watershed scales. This in turn could be used to study the performance of the model at both of these scales. The information gained from this comparison could be helpful for developing a simple aggregation or up-scaling scheme to simplify the heterogeneities in a hillslope. This simplification could be used to make the model more efficient for distributed predictions and other tasks such as model calibration or uncertainty estimation. Currently the spatial resolution of the event model makes these tasks extremely computer intensive at the watershed scale. This recommendation goes beyond the event model used here and it could be used, in general, with other conceptualizations of hydrologic response modeling.
- The parameterization of wave celerity in the GIUH could be improved by studying the space-time variation of velocity in real watersheds. Of particular interest would be the estimation of velocities in time at selected stream cross-sections during storm events. Although this is a known limitation and problem with the GIUH, it seems little data collection and analysis has been done to overcome this situation.
- The representation of the path probabilities in the GIUH as varying in space and time could be explored further. For example, the method used by *Rinaldo et al.* [1991] to determine the moments of the GIUH could be tried for obtaining moments that

include path probabilities that change in time during an event. The current moments are derived only for path probabilities that vary in space.

- Another approach for the space-time modeling effort could be to try to relate the event model to a simple stochastic rainfall model using a derived distribution approach [*Eagleson*, 1972]. However this could be a difficult analytical problem, unless the space pattern of rainfall and imperviousness is accounted for in some simplified manner. Perhaps the covariance between the spatial pattern of rainfall and imperviousness could be used for this simplification. In addition, changes in imperviousness cover with time, i.e. urban growth, will need to be described analytically and it is not clear at this point how this can be done. The goal with this approach would be to obtain expressions for the pdf of runoff volume and peak flows, for example, in terms of the long term climatic inputs and the impervious cover. This in turn could be used to explore the role of the imperviousness pattern and urban growth on frequency analysis.
- An interesting research direction is to expand the simple event-model or the space-time approach to larger scales for more global hydrologic modeling. The insight and understanding gained from the event-model and the space-time approach could be used to propose a land surface parameterization scheme for suburban watershed conditions. This will need to account for additional processes, such as evapotranspiration and subsurface flows, and for water and energy balances. The existing TOPLATS parameterization could be used as a starting point [*Famiglietti and Wood*, 1994]. The suburban watershed condition could be particularly interesting because of the importance of both pervious and impervious areas. This type of

References

Aarts, E., and J. Kost (1990), *Simulated Annealing and Boltzmann Machines*, 114 pp., Wiley, Hoboken, New Jersey.

Allan, J. D. (2004), Landscapes and riverscapes: the influence of land use on stream ecosystems, *Annual Review of Ecology, Evolution, and Systematics*, *35*, 257-284.

Ambroise, B., K. J. Beven, and J. Freer (1996), Toward a generalization of the TOPMODEL concepts: Topographic indices of hydrological similarity, *Water Resources Research*, *32*(7), 2135-2145.

Anderson, D. G. (1970), Effects of urban development on floods in Northern Virginia, *Professional Paper 2001-C*, C1-C22, U.S. Geological Survey, Washington, D.C.

Andrieu, H., and B. Chocat (2004), Introduction to the special issue on urban hydrology, *Journal of Hydrology*, *299*(3-4), 163-165.

Arnold, C., and C. Gibbons (1996), Impervious surface coverage: the emergence of a key environmental indicator, *Journal of the American Planning Association*, *62*(2), 243-258.

Beven, K. J. (2000), *Rainfall-Runoff Modelling, The Primer*, 360 pp., John Wiley, Chichester.

Beven, K. J. (2008), On doing better hydrological science, *Hydrological Processes*, *22*(17), 3549-3553, doi:10.1002/hyp.7108.

Beven, K. J., and A. Binley (1992), The future of distributed models: model calibration and uncertainty prediction, *Hydrological Processes*, *6*(3), 279-298.

Beven, K. J., and M. J. Kirkby (1979), A physically based variable contributing area model of basin hydrology, *Hydrological Science Bulletin*, *24*(1), 43-69.

Blöschl G. (2006), Hydrologic synthesis: across processes, places, and scales, *Water Resources Research*, *42*, W03S02, doi:10.1029/2005WR004319.

Booth, D. B., J. R. Karr, S. Schauman, C. P. Konrad, S. A. Morley, M. G. Larson, and S. J. Burges (2004), Reviving urban streams: land use, hydrology, biology, and human behavior, *Journal of the American Water Resources Association*, 40(5), 1351-1364.

Brutsaert, W., and J. L. Nieber (1977), Regionalized drought flow hydrographs from a mature glaciated plateau, *Water Resources Research*, *13*(3), 637-643.

Burges, S. J., M. S. Wigmosta, and J. M. Meena (1998), Hydrological effects of land-use change in a zero-order catchment, *Journal of Hydrologic Engineering*, *3*(2), 86-97, doi:10.1061/(ASCE)1084-0699(1998)3:2(86).

Buytaert, W., D. Reusser, S. Krause, and J.-P. Renaud (2008), Why can't we do better than TOPMODEL?, *Hydrological Processes*, *22*(20), 4175-4179, doi:10.1002/hyp.7125.

Clark, M. P., A. G. Slater, D. E. Rupp, R. A. Woods, J. A. Vrugt, H. V. Gupta, T. Wagener, and L. E. Hay (2008), Framework for Understanding Structural Errors (FUSE): a modular framework to diagnose differences between hydrological models, *Water Resources Research*, *44*, W00B02, doi:10.1029/2007WR006735.

Carter, R. W. (1961), Magnitude and frequency of floods in suburban areas, *Professional Paper 424-B*, B9-B11, U.S. Geological Survey, Washington, D.C.

Center for Watershed Protection (2003), Impacts of impervious cover on aquatic systems, *Watershed Protection Research Monograph No. 1*, 135 pp., Ellicot City, Maryland.

Claggett, P. R, C. A. Jantz, S. J. Goetz, and C. Bisland (2004), Assessing development pressure in the Chesapeake Bay watershed: an evaluation of two land use change models, *Environmental Monitoring and Assessment*, *94*(1-3), 129-146.

Cuo, L., D. P. Lettenmaier, B. V. Mattheussen, P. Storck, and M. Wiley (2008), Hydrologic prediction for urban watersheds with the Distributed Hydrology-Soil-Vegetation Model, *Hydrological Processes*, *22*(21), 4205-4213.

Dawdy, D. R. (2007), Prediction versus understanding (The 2006 Ven Te Chow Lecture), *Journal of Hydrologic Engineering*, *12*(1), doi:10.1061/(ASCE)1084-0699(2007)12:1(1).

DeFries, R., and K. N. Eshleman (2004), Land-use change and hydrologic processes: a major focus for the future, *Hydrological Processes*, *18*(11), 2183-2186.

Delleur, J. W. (2003), The evolution of urban hydrology: past, present, and future, *Journal of Hydrologic Engineering*, *129*(563), doi:10.1061/(ASCE)0733-9429(2003)129:8(563).

DeWalle, D. R., B. R. Swistock, T. E. Johnson, and K. J. McGuire (2000), Potential effects of climate change and urbanization on mean annual streamflow in the United States, *Water Resources Research*, *36*(9), 2655-2664.

Dingman, S. L. (1994), *Physical Hydrology*, 575 pp., Macmillian, New York.

D'Odorico P., and R. Rigon (2003), Hillslope and channel contributions to the hydrologic response, *Water Resources Research*, *39*(5), 1113, doi:10.1029/2002WR001708.

Dooge, J. (1986), Looking for hydrologic laws, *Water Resources Research*, *22*(09S), 46S-58S.

Duan, J., and N. Miller (1997), A generalized power function for the subsurface transmissivity profile in TOPMODEL, *Water Resources Research*, *33*(11), 2559-2562.

Duan, Q., S. Sorooshian, and V. Gupta (1992), Effective and efficient global optimization for conceptual rainfall-runoff models, *Water Resources Research*, *28*(4), 1015-1031.

Dunne, T., and L. B. Leopold (1978), *Water in Environmental Planning*, 818 pp., W. H. Freeman and Company, New York, Sixteenth printing, 2002.

Eagleson, P. S. (1967), A distributed linear model for peak catchment discharge, paper presented at the International Hydrology Symposium, Colorado State University, Fort Collins, Colorado.

Eagleson, P. S. (1972), Dynamics of flood frequency, *Water Resources Research*, *8*(4), 878-898.

Easton, Z. M., P. Gérard-Marchant, M. T. Walter, A. M. Petrovic, and T. S. Steenhuis (2007), Hydrologic assessment of an urban variable source watershed in the northeast United States, *Water Resources Research*, *43*, W03413, doi:10.1029/2006WR005076.

Ebel, B. A., and K. Loague (2006), Physics-based hydrologic-response simulation: Seeing through the fog of equifinality, *Hydrological Processes*, *20*(13), 2887-2900.

Elliot, T. S., Four quartets, in *Complete Poems and Plays: 1909-1950*, 400 pp., Harcourt Brace & Company, New York, New York, 1967.

Ewen, J., and G. Parkin (1996), Validation of catchment models for predicting land-use and climate change impacts. 1. Method, *Journal of Hydrology*, *175*(1-4), 583-594.

Famiglietti, J., and E. Wood (1994), Multiscale modeling of spatially variable water and energy balance processes, *Water Resources Research*, *30*(11), 3061-3078.

Fohrer, N., S. Haverkamp, and H.-G. Frede (2005), Assessment of the effects of land use patterns on hydrologic landscape functions: development of sustainable land use concepts for low mountain range areas, *Hydrological Processes*, *19*(3), 659-672.

Franchini, M., J. Wendling, C. Obled, and E. Todini (1996), Physical interpretation and sensitivity analysis of the TOPMODEL, *Journal of Hydrology*, *175*(1-4), 293-338.

Gabriel, S. A., J. Faria, and G. E. Moglen (2006), A multiobjective optimization approach to smart growth in land development, *Socio-Economic Planning Sciences*, *40*(3), 212-248.

Galster, J. C., F. J. Pazzaglia, B. R. Hargreaves, D. P. Morris, S. C. Peters, and R. N. Weisman (2006), Effects of urbanization on watershed hydrology: the scaling of discharge with drainage area, *Geology*, *34*(9), 713-716.

Grayson, R. B., and G. Blöschl (2000), *Spatial patterns in catchment hydrology - Observations and modeling*, 404 pp., Cambridge University Press, Cambridge.

Grayson, R. B., I. Moore, and T. McMahon (1992), Physically based hydrologic modeling 2. Is the concept realistic?, *Water Resources Research*, *28*(10), 2659-2666.

Grimmond, C., T. Oke, and D. Steyn (1986), Urban water balance 1. A model for daily totals, *Water Resources Research*, *22*(10), 1397-1403.

Guo, Y., and B. Adams (1998), Hydrologic analysis of urban catchments with event-based probabilistic models 1. Runoff volume, *Water Resources Research*, *34*(12), 3421-3431.

Gupta, V., E. Waymire, and C. Wang (1980), A representation of an instantaneous unit hydrograph from geomorphology, *Water Resources Research*, *16*(5), 855-862.

Hammer, T. R. (1972), Stream channel enlargement due to urbanization, *Water Resources Research*, *8*(6), 1530-1540.

Hatt, B. E., T. D. Fletcher, C. J. Walsh, and S. L. Taylor (2004), The influence of urban density and drainage infrastructure on the concentrations and loads of pollutants in small streams, *Environmental Management*, *34*(1), 112-124.

Hollis, G. (1975), The effect of urbanization on floods of different recurrence intervals, *Water Resources Research*, *11*(3), 431-435.

Homer, C., J. Dewitz, J. Fry, M. Coan, N. Hossain, C. Larson, N. Herold, A. McKerrow, J. N. VanDriel, and J. Wickham (2007), Completion of the 2001 National Land Cover Database for the conterminous United States, *Photogrammetric Engineering and Remote Sensing*, *73*(4), 337-341.

Horton, R. E. (1931), The field, scope, and status of the science of hydrology, *Eos Trans. AGU*, *12*, 189-202.

Hundecha, Y., and A. Bárdossy (2004), Modeling of the effect of land use changes on the runoff generation of a river basin through parameter regionalization of a watershed model, *Journal of Hydrology*, *292*(1-4), 281-295.

Kirchner, J. W. (2006), Getting the right answers for the right reasons: Linking measurements, analyses, and models to advance the science of hydrology, *Water Resources Research*, *42*, W03S04, doi:10.1029/2005WR004362.

Kirkpatrick, S., Jr., C. D. Gellat, and M. P. Vecchi (1983), Optimization by simulated annealing, *Science*, *220*(13), 671–680.

Klein, R. D. (1979), Urbanization and stream quality impairment, *Journal of the American Water Resources Association*, *15*(4), 948-963, doi:10.1111/j.1752-1688.1979.tb01074.x.

Kuczera, G., and E. Parent (1998), Monte Carlo assessment of parameter uncertainty in conceptual catchment models: The Metropolis algorithm, *Journal of Hydrology*, *211*(1-4), 69-85.

Kuczera, G., D. Kavetski, S. Franks, and M. Thyer (2006), Towards a Bayesian total error analysis of conceptual rainfall-runoff models: characterising model error using storm-dependent parameters, *Journal of Hydrology*, *331*(1-2), 161-177.

Kuichling, E. (1889), The relationship between the rainfall and the discharge of sewers in populous districts, *Transactions of the American Society of Civil Engineers*, *20*, 1-56.

Leopold, L. B. (1968), Hydrology for urban land planning: A guidebook on the hydrologic effects of urban land use, *U.S. Geological Survey Circular 554*, 18 pp., U.S. Geological Survey, Reston, Virginia.

Leopold, L. B., and T. Maddock (1953), The hydraulic geometry of stream channels and some physiographic implications, *Professional Paper 252*, 57 pp., U.S. Geological Survey, Washington D.C.

Lee, J. G., and J. P. Heaney (2003), Estimation of urban imperviousness and its impacts on storm water systems, *Journal of Water Resources Planning and Management*, *129*(5), 419-426.

Lin, S. (1965), Computer solutions for the traveling salesman problem, *Bell Systems Technology Journal*, *44*(5), 2245-2269.

McCuen, R. H. (1998), *Hydrologic Analysis and Design*, 814 pp., Prentice Hall, New Jersey.

McCuen, R. H. (2003), Smart growth: hydrologic perspective, *Journal of Professional Issues in Engineering Education and Practice*, *129*(151), doi:10.1061/(ASCE)1052-3928(2003)129:3(151).

McCuen, R. H., and W. Snyder (1975), A proposed index for comparing hydrographs, *Water Resources Research*, *11*(6), 1021-1024.

McDonnell, J. J., et al. (2007), Moving beyond heterogeneity and process complexity: A new vision for watershed hydrology, *Water Resources Research*, *43*, W07301, doi:10.1029/2006WR005467.

Mejía, A. I., and G. E. Moglen (2009), Spatial patterns of urban development from optimization of flood peaks and imperviousness-based measures, *Journal of Hydrologic Engineering*, *14*(4), 416-424.

Mesa, O. J., and E. R. Mifflin (1986), On the relative role of hillslope and network geometry in hydrologic response, in *Scale Problems in Hydrology*, edited by V. K. Gupta et al., pp. 1-17, D. Reidel, Norwell, Massachusetts.

Miller, C. V., A. L. Gutiérrez-Magness, B. L. Feit Majedi, and G. D. Foster (2007), Water quality in the Upper Anacostia River, Maryland: Continuous and discrete monitoring with simulations to estimate concentrations and yields, 2003-05, *Scientific Investigation Report 2007-5142*, 43 pp., U.S. Geological Survey, Reston, Virginia.

Milly, P. (1986), An event-based simulation model of moisture and energy fluxes at a bare soil surface, *Water Resources Research*, *22*(12), 1680-1692.

Moglen, G. E. (2009), Hydrology and impervious areas, *Journal of Hydrologic Engineering*, *14*(4), 303-304, doi:10.1061/(ASCE)1084-0699(2009)14:4(303).

Moglen, G. E., and R. E. Beighley (2002), Spatially explicit hydrologic modeling of land use change, *Journal of the American Water Resources Association*, *38*(1), 241-253.

Moglen, G. E., and S. Kim (2007), Limiting imperviousness: Are threshold-based policies a good idea?, *Journal of the American Planning Association*, *73*(2), 161-171.

Moglen, G. E., S. A. Gabriel, and J. A. Faria (2003), A framework for quantitative smart growth in land development, *Journal of the American Water Resources Association*, *39*(4), 947-959.

Moglen, G., W. O. Thomas, and C. G. Cuneo (2006), Evaluation of alternative statistical methods for estimating frequency of peak flows in Maryland, *Final report (SP907C4B)*, 78 pp., Maryland Department of Transportation, Hanover, Maryland.

Montgomery, D. R., and W. E. Dietrich (1988), Where do channels begin?, *Nature*, *336*(232), 232-234.

Moramarco, T., F. Melone, and V. P. Singh (2005), Assessment of flooding in urbanized ungauged basins: a case study in the Upper Tiber area, Italy, *Hydrological Processes*, *10*(19), 1909-1924.

Naef, F., S. Scherrer, and M. Weiler (2002), A process based assessment of the potential to reduce flood runoff by land use change, *Journal of Hydrology*, *267*(1-2), 74-79.

Nash, J. E., and J. V. Sutcliffe (1970), River flow forecasting through conceptual models part I - A discussion of principles, *Journal of Hydrology*, *10*(3), 282-290, doi:10.1016/0022-1694(70)90255-6.

National Oceanic and Atmospheric Administration (NOAA) (2008a), MARFC Operational NEXRAD Stage III Data, http://dipper.nws.noaa.gov/hdsb/data/nexrad/marfc_stageiii.php, Silver Spring, Maryland.

National Oceanic and Atmospheric Administration (NOAA) (2008b), NCDC Storm Event database, http://www4.ncdc.noaa.gov/cgi-win/wwcgi.dll?wwEvent~Storms, Silver Spring, Maryland.

National Oceanic and Atmospheric Administration (NOAA) (2008c), Point Precipitation Frequency Estimates from NOAA Atlas 14 for Maryland, http://www.nws.noaa.gov/oh/hdsc/index.html, Silver Spring, Maryland.

National Resources Conservation Service (NRCS) (1986), Urban hydrology for small watersheds TR-55, *Technical Release 55*, Washington D.C.

Natural Resources Conservation Service (NRCS) (2008a), Soil Survey Geographic Database (SSURGO), http://soils.usda.gov/survey/geography/ssurgo/, Washington D.C.

Natural Resources Conservation Service (NRCS) (2008b), State Soil Geographic (STATSGO) Database for Maryland, http://soildatamart.nrcs.usda.gov, Washington D.C.

National Weather Service (NWS) (1961), Rainfall Frequency Atlas of the United States, *Technical Paper #40*, U.S. Department of Commerce, Washington D.C.

Nicótina L., E. Alessi Celegon, A. Rinaldo, and M. Marani (2008), On the impact of rainfall patterns on the hydrologic response, *Water Resources Research*, *44*, W12401, doi:10.1029/2007WR006654.

Niehoff, D., U. Fritsch, and A. Bronstert (2002), Land-use impacts on storm-runoff generation: scenarios of land-use change and simulation of hydrological response in a meso-scale catchment in SW-Germany, *Journal of Hydrology*, *267*(1-2), 80-93.

Nunes, L. M., E. Paralta, M. C. Cunha, and L. Ribeiro (2004), Groundwater nitrate monitoring network optimization with missing data, *Water Resources Research*, *40*(2), 1-18.

O'Callaghan, J. F., and D. M. Mark (1984), The extraction of drainage networks from digital elevation data, Computer Vision, *Graphics and Image Processing*, 328-344.

Ogden, F. L., and D. R. Dawdy (2003), Peak discharge scaling in a small hortonian watershed, *Journal of Hydrologic Engineering*, *8*(2), 64-73.

Olivera, F., and D. Maidment (1999), Geographic Information Systems (GIS)-based spatially distributed model for runoff routing, *Water Resources Research*, *35*(4), 1155-1164.

Oleson, K. W., G. B. Bonan, J. Feddema, M. Vertenstein, and C. S. B. Grimmond (2008), An urban parameterization for a global climate model: 1. Formulation and evaluation, *Journal of Applied Meteorology and Climatology*, *47*(4), 1038-1060. doi:10.1175/2007JAMC1597.1.

Pham, D. T., and D. Karaboga (2000), *Intelligent Optimisation Techniques: genetic algorithms, tabu search, simulated annealing, and neural networks*, 302 pp., Springer, London.

Philip, J. R., (1960), The theory of infiltration, in *Advances in Hydroscience*, edited by V. T. Chow, vol. 5, pp. 215-296, Academic, Orlando, Florida.

Pielke, R. A. (2005), Land use and climate change, *Science*, *310*(5754), 1625-1626.

Poff, N. L., J. D. Allan, M. B. Bain, J. R. Karr, K. L. Prestegaard, B. D. Richter, R. E. Sparks, and J. C. Stromberg (1997), The natural flow regime: a paradigm for river conservation and restoration, *BioScience*, *47*(11), 769-784.

Poff, N. L., B. P. Bledsoe, and C. O. Cuhaciyan (2006), Hydrologic variation with land use across the contiguous United States: geomorphic and ecological consequences for stream ecosystems, *Geomorphology*, *79*(3-4), 264-285.

Reed, P. M., R. P. Brooks, K. J. Davis, D. R. DeWalle, K. A. Dressler, C. J. Duffy, H. Lin, D. A. Miller, R. G. Najjar, K. M. Salvage, T. Wagener, and B. Yarnal (2006), Bridging river basin scales and processes to assess human-climate impacts and the terrestrial hydrologic system, *Water Resources Research*, *42*, W07418, doi:10.1029/2005WR004153.

Reeves, C. R. (1993), *Modern Heuristic Techniques for Combinatorial Problems*, 320 pp., John Wiley & Sons, Inc., New York, New York.

Rinaldo, A., and I. Rodríguez-Iturbe (1996), Geomorphological theory of the hydrological response, *Hydrological Processes*, *10*(6), 803-829.

Rinaldo, A., A. Marani, and R. Rigon (1991), Geomorphological dispersion, *Water Resources Research*, *27*(4), 513-525.

Robinson, J., M. Sivapalan, and J. Snell (1995), On the relative roles of hillslope processes, channel routing, and network geomorphology in the hydrologic response of natural catchments, *Water Resources Research*, *31*(12), 3089-3101.

Rodriguez, F., C. Cudennec, and H. Andrieu (2005), Application of morphological approaches to determine unit hydrographs of urban catchments, *Hydrological Processes*, *19*(5), 1021-1035.

Rodríguez-Iturbe, I., and A. Rinaldo (1997), *Fractal River Basins: Chance and Self-Organization*, 564 pp., Cambridge Univ. Press, New York.

Rodríguez-Iturbe, I., and J. B. Valdés (1979), The geomorphologic structure of the hydrologic response, *Water Resources Research*, *15*(6), 1409-1420.

Rodríguez-Iturbe, I., A. Rinaldo, R. Rigon, R. L. Bras, A. Marani, and E. Ijjász-Vásquez (1992), Energy dissipation, runoff production, and the three-dimensional structure of river basins, *Water Resources Research*, *28*(4), 1095-1103.

Romanowicz, R. J. (1997), A MATLAB implementation of TOPMODEL, *Hydrological Processes*, *11*(9), 1115-1129.

Rosso, R. (1984), Nash model relation to Horton order ratios, *Water Resources Research*, *20*(7), 914-920.

Saco, P. M., and P. Kumar (2002), Kinematic dispersion in stream networks, 1. Coupling hydraulic and network geometry, *Water Resources Research*, *38*(11), 1244, doi:10.1029/2001WR000695.

Saco, P. M., and P. Kumar (2004), Kinematic dispersion effects of hillslope velocities, *Water Resources Research*, *40*, W01301, doi:10.1029/2003WR002024.

Sauer, V. B., W. O Thomas, Jr., V. A. Stricker, and K. V. Wilson (1983), Flood characteristics of urban watersheds in the United States, *Water-Supply Paper 2207*, 63 pp., U.S. Geological Survey, Reston, Virginia.

Scanlon, T., J. Raffensperger, G. Hornberger, and R. Clapp (2000), Shallow subsurface storm flow in a forested headwater catchment: observations and modeling using a modified TOPMODEL, *Water Resources Research*, *36*(9), 2575-2586.

Schueler, T. (1994), The importance of imperviousness, *Watershed Protection Techniques*, *1*(3), 100-111.

Segond, M. L., H. S. Wheater, and C. Onof (2007), The significance of spatial rainfall representation for flood runoff estimation: A numerical evaluation based on the Lee catchment, UK, *Journal of Hydrology*, *347*(1-2), 116-131, doi:10.1016/j.jhydrol.2007.09.040.

Shuster, W. D., J. Bonta, H. Thurston, E. Warnemuendes, and D. R. Smith (2005), Impacts of impervious surface on watershed hydrology: a review, *Urban Water Journal*, *2*(4), 263-275.

Singh, V. P., and D. A. Woolhiser (2002), Mathematical modeling of watershed hydrology, *Journal of Hydrologic Engineering*, *7*(4), 270-292.

Sivapalan, M. (2003), Prediction in ungauged basins: a grand challenge for theoretical hydrology, *Hydrological Processes*, *17*(15), 3163-3170.

Sivapalan, M. (2009), The secret to 'doing better hydrological science': change the question!, *Hydrological Processes*, *23*(9), 1391-1396.

Sivapalan, M., and E. F. Wood (1987), A multidimensional model of nonstationary space-time rainfall at the catchment scale, *Water Resources Research*, *23*(7), 1289-1299.

Sivapalan, M., K. Beven, and E. Wood (1987), On hydrologic similarity 2. A scaled model of storm runoff production, *Water Resources Research*, *23*(12), 2266-2278.

Sivapalan, M., E. Wood, and K. Beven (1990), On hydrologic similarity 3. A dimensionless flood frequency model using a generalized geomorphologic unit hydrograph and partial area runoff generation, *Water Resources Research*, *26*(1), 43-58.

Smith, J. A., M. L. Baeck, K. L. Meierdiercks, P. A. Nelson, A. J. Miller, and E. J. Holland (2005), Field studies of the storm event hydrologic response in an urbanizing watershed, *Water Resources Research*, *41*, W10413, doi:10.1029/2004WR003712.

Smith, M. B. (1993), A GIS-based distributed parameter hydrologic model for urban areas, *Hydrological Processes*, *7*(1), 45-61.

Spear, R. C., and G. M. Hornberger (1980), Eutrophication in Peel Inlet. II. Identification of critical uncertainties via generalized sensitivity analysis, *Water Research*, *14*(1), 43-49, doi:10.1016/0043-1354(80)90040-8.

Stern, J. E. (1990), State Plane Coordinate System of 1983, *NOAA Manual NOS NGS 5*, U.S. Department of Commerce, Rockville, Maryland.

Szilagyi, J., and M. B. Parlange (1998), Baseflow separation based on analytical solutions of the Boussinesq equation, *Journal of Hydrology*, *204*(1-4), 251-260.

Tang, Z., B. A. Engel, K. J. Lim, B. C. Pijanowski, and J. Harbor (2005), Minimizing the impact of urbanization on long term runoff, *Journal of the American Water Resources Association*, *41*(6), 1347-1359.

Tarboton, D. (1997), A new method for the determination of flow directions and upslope areas in grid digital elevation models, *Water Resources Research*, *33*(2), 309-319.

Tarboton, D. G., R. L. Bras, and I. Rodríguez-Iturbe (1991), On the extraction of channel networks from digital elevation data, *Hydrological Processes*, *5*(1), 81-100.

Tenenbaum, D. E., L. E. Band, S. T. Kenworthy, and C. L. Tague (2006), Analysis of soil moisture patterns in forested and suburban catchments in Baltimore, Maryland, using high-resolution photogrammetric and LIDAR digital elevation datasets, *Hydrological Processes*, *20*(2), 219-240.

Toprak, Z. F., and H. Kerem Cigizoglu (2008), Predicting longitudinal dispersion coefficient in natural streams by artificial intelligence methods, *Hydrological Processes*, *22*(20), 4106-4129.

Troch, P. A., F. De Troch, and W. Brutsaert (1993), Effective water table depth to describe initial conditions prior to storm rainfall in humid regions, *Water Resources Research*, *29*(2), 427-434.

Troch, P. A., J. A. Smith, E. F. Wood, and F. P. de Troch (1994), Hydrologic controls of large floods in a small basin, *Journal of Hydrology*, *156*(1-4), 285-309.

Turner, E. R. (2006), Comparison of infiltration equations and their field validation with rainfall simulation, M.S. thesis, 202 pp., University of Maryland at College Park.

U.S. Environmental Protection Agency (2004), Protecting water resources with smart growth, *EPA 231-R-04-002*, 120 pp., Washington, D.C.

U.S. Environmental Protection Agency and U.S. Geological Survey (2006), National hydrography dataset plus, http://www.horizon-systems.com/nhdplus/index.php,, Herndon, Virginia.

U.S. Geological Survey (USGS) (2007), National Elevation Dataset, http://gisdata.usgs.net/ned/, Reston, Virginia.

U.S. Geological Survey (USGS) (2008a). Instantaneous Data Archive - IDA, http://ida.water.usgs.gov/ida/, Reston, Virginia.

U.S. Geological Survey (USGS), (2008b), National Land Cover Database 2001, http://www.mrlc.gov/index.asp, Reston, Virginia.

Valdés, J. B, M. Díaz-Granados, and R. L. Bras (1990), A derived PDF for the initial soil moisture in a catchment, *Journal of Hydrology*, *113*(1-4), 163-176.

Valeo, C., and S. Moin (2001), Hortonian and variable source area modeling in urbanizing basins, *Journal of Hydrologic Engineering*, *6*(328), doi:10.1061/(ASCE)1084-0699(2001)6:4(328).

Vörösmarty, C. J., P. Green, J. Salisbury, and R. B. Lammers (2000), Global water resources: vulnerability from climate change and population growth, *Science*, *289*(5477), 284, doi:10.1126/science.289.5477.284.

Vrugt, J. A., H. V. Gupta, W. Bouten, and S. Sorooshian (2003), A shuffled complex evolution metropolis algorithm for optimization and uncertainty assessment of hydrologic model parameters, *Water Resources Research*, *39*(8), 1201, doi:10.1029/2002WR001642.

Vrugt, J. A., C. J. F. ter Braak, M. P. Clark, J. M. Hyman, and B. A. Robinson (2008a), Treatment of input uncertainty in hydrologic modeling: Doing hydrology backward with Markov chain Monte Carlo simulation, *Water Resources Research*, *44*, W00B09, doi:10.1029/2007WR006720.

Vrugt, J. A., C. J. F. ter Baak, H. V. Gupta, and B. A. Robinson (2008b), Equifinality of formal (DREAM) and informal (GLUE) Bayesian approaches in hydrologic modeling?, *Stochastic Environmental Research and Risk Assessment*, 1-16, doi:10.1007/s00477-008-0274-y.

Wagener, T. (2007), Can we model the hydrological impacts of environmental change?, *Hydrological Processes*, *21*(23), 3233-3236, doi:10.1002/hyp.6873.

Wagener, T., H. S. Wheater, and M. J. Lees (2004), Monte-Carlo Analysis Toolbox User Manual, Pennsylvania State University, University Park, Pennsylvania.

Walsh, C. J., A. H. Roy, J. W. Feminella, P. D. Cottingham, P. M. Groffman, and R. P. Morgan II (2005), The urban stream syndrome: current knowledge and the search for a cure, *Journal of the North American Benthological Society*, *24*(3), 706-723.

Weiler, M., B. L. McGlynn, K. J. McGuire, and J. J. McDonnell (2003), How does rainfall become runoff? A combined tracer and runoff transfer function approach, *Water Resources Research*, *39*(11), 1315, doi:10.1029/2003WR002331.

Wigmosta, M. S., and S. J. Burges (1990), Proposed model for evaluating urban hydrologic change, *Journal of Water Resources Planning and Management*, *116*(6), 742-763, doi:10.1061/(ASCE)0733-9496(1990)116:6(742).

Wohl, E., P. L. Angermeier, B. Bledsoe, G. M. Kondolf, L. MacDonnell, D. M. Merritt, M. A. Palmer, N. L. Poff, and D. Tarboton (2005), River restoration, *Water Resources Research*, *41*, W10301, doi:10.1029/2005WR003985.

Wong, T. S. (2006), Physically based approach in hydrology - What is the benefit?, *Journal of Hydrologic Engineering*, *11*(4), 293-295, doi:10.1061/(ASCE)1084-0699(2006)11:4(293).

Woods, R., and M. Sivapalan (1999), A synthesis of space-time variability in storm response: rainfall, runoff generation, and routing, *Water Resources Research*, *35*(8), 2469-2485.

Yeo, I.-Y., S. I. Gordon, and J.-M. Guldman (2004), Optimizing patterns of land use to reduce peak runoff flow and nonpoint source pollution with an integrated hydrological and land-use model, *Earth Interactions*, *8*(6), 1-20.

Yeo, I.-Y., J.-M. Guldmann, and S. I. Gordon (2007), A hierarchical optimization approach to watershed land use planning, *Water Resources Research*, *43*, W11416, doi:10.1020/2006WR005315.

Young, C. B., A. A. Bradley, W. F. Krajewski, A. Kruger, and M. L. Morrissey (2000), Evaluating NEXRAD multisensor precipitation estimates for operational hydrologic forecasting, *Journal of Hydrometeorology*, *1*(3), 241–254.

Zheng, P. Q., and B. W. Baetz (1999), GIS-Based analysis of development options from a hydrology perspective, *Journal of Urban Planning and Development*, *125*(4), 164-180.

Zhu, W., J. G., Graney, and K. Salvage (2008), Land-use impact on water pollution: elevated pollutant input and reduced pollutant retention, *Journal of Contemporary Water Research and Education*, *138*, 15-21.